NASA Contractor Report 3512

Terminal Area Automatic Navigation, Guidance, and Control Research Using the Microwave Landing System (MLS)

Part 3 – A Comparison of Waypoint Guidance Algorithms for RNAV/MLS Transition

Samuel Pines

CONTRACT NAS1-15116
JANUARY 1982

NASA

NASA Contractor Report 3512

Terminal Area Automatic Navigation, Guidance, and Control Research Using the Microwave Landing System (MLS)

Part 3 – A Comparison of Waypoint Guidance Algorithms for RNAV/MLS Transition

Samuel Pines
Analytical Mechanics Associates, Inc.
Hampton, Virginia

Prepared for
Langley Research Center
under Contract NAS1-15116

NASA
National Aeronautics
and Space Administration

Scientific and Technical
Information Branch

1982

CONTENTS

LIST OF FIGURES

LIST OF FIGURES (CONTINUED)

LIST OF TABLES

SUMMARY

This report contains the results of an investigation carried out for the Langley Research Center Terminal Configured Vehicle (TCV) Program. The investigation generated and compared three path update algorithms designed to provide smooth transition for an aircraft guidance system from DME, VORTAC, and barometric navaids to the more precise MLS by modifying the desired 3-D flight path. The first, called the Zero Cross Track, eliminates the discontinuity in cross track and altitude error by designating the first valid MLS aircraft position as the desired first waypoint, while retaining all subsequent waypoints. The discontinuity in track angle is left unaltered. The second, called the Tangent Path also eliminates the discontinuity in cross track and altitude and chooses a new desired heading to be tangent to the next oncoming circular arc turn. No attempt is made to eliminate the track angle error. The third, called the Continued Track, eliminates the discontinuity in cross track, altitude and track angle by accepting the current MLS position and track angle as the desired ones and recomputes the location of the next waypoint. The Zero Cross Track and Tangent Path schemes may only be used while flying along a straight line segment while the Continued Track scheme will reconstruct the path while on a circular turn segment.

A method is presented for providing a waypoint guidance path construction which treats turns of less than, and greater than, 180^{o} in a uniform manner to construct the desired path. This method, when used in conjunction with the Continued Track method, may be used to reconstruct a smooth transition path to landing at every position in the terminal area including during turns.

INTRODUCTION

The use of MLS precision navaids in the terminal area generate transition problems in automated navigation and guidance for aircraft for systems which track RNAV paths defined by preset waypoints. These problems are described in Refs. 1* and 2** along with suggested fixes and simulation studies of typical aircraft terminal approach patterns. This report develops the equations for three competitive Path Reconstruction Algorithms, using typical waypoint techniques in use on the TCV B-737 aircraft and similar commercial and military airplanes.

A simulation study of the performance of these comparative algorithms is carried out and the resulting data are displayed. A separate appendix derives a Path Construction Method which treats turns of less than 180^{o} and greater than 180^{o} in a uniform and precise manner. The method makes possible a solution of the transition problems at every position in the terminal area, including during turns, and provides for a smooth landing approach with minimal redesign of the original path by eliminating the cross track, track angle, and altitude errors at the acquisition of the first complete valid MLS position.

---

1. * Pines, S.; Schmidt, S. F.; and Mann, F.: Automated Landing, Rollout, and Turnoff Using MLS and Magnetic Cable Sensors. NASA CR-2907, Oct. 1977.

2. ** Pines, S.: Terminal Area Automatic Navigation, Guidance, and Control Research Using the Microwave Landing System (MLS). Part 2 - RNAV/MLS Transition Problems for Aircraft. NASA CR-3511, 1982.

I. PATH RECONSTRUCTION ALGORITHMS

A. General Comments

The method for constructing a path for RNAV guidance is given in Reference 1. The path is completely defined given the following data:

1) N, the integer number of waypoints designating the start, termination, and all interior corners at which turns are required.

2) λ (I) , the longitude, and δ (I) , the latitude of each waypoint.

3) h (I) , the height above the earth reference sphere, and v_D(I) , the desired airspeed at each waypoint.

4) R_T(I) , the turn radius, at each interior waypoint.

These data, following the logic in Reference 1, yield a series of path segments, consisting of straight lines and turns, which completely define the desired position and velocity of the aircraft.

In developing a path reconstruction algorithm at RNAV/MLS transition, the competing methods each redefine a small number of waypoints, altitudes and desired velocities , and utilize the existing navigation structure to redefine the desired path. The objective is to minimize the aircraft maneuvers in the lateral and vertical directions at transition without unduly invading the originally designated airspace of the initial flight plan in the terminal area.

Three algorithms will be developed here. They are:

1) Zero Cross Track
2) Tangent Path
3) Continued Track

All three eliminate the transition error in altitude and desired airspeed. The first also eliminates the cross track error. The second eliminates the cross track error but retains the location of the center and the radius of the next turn. The third eliminates both the cross track and the track angle error. The algorithms for the three competing methods are given below.

In addition to the above, in order to accommodate turns greater than 180^{o} it is necessary to alter the structure of the path construction routine in order to allow the alternative of designating the center of the turn as an interior waypoint in place of the interior corner. The equations for these changes are contained in Appendix I.

B. Zero Cross Track (ZCT)

The algorithm for this transition path reconstruction is contained in Reference 1 and is included here only for the purpose of convenience of comparison. (See Figure 1).

To begin, we note that the algorithm cannot be implemented in a turn nor can it be used if the MLS position lies within the turn circle. Furthermore, even if we are outside the turn radius, but too close to the incoming turn circle, large errors in track angle result and the advantage of a smooth transition is lost. In order to avoid these adverse effects we include a test for the minimum allowable distance from the initial turn circle center to execute the ZTC algorithm.

Let RE be the position vector of the aircraft in the Fixed Earth Inertial Coordinate System, obtained from the valid MLS update at transition. Let N be the number of waypoints in the initial flight plan. Let P be the number of the last interior waypoint passed in the flight. For example, on the initial leg of the aircraft trajectory, P = 1; after passing the middle of the first turn, P = 2, etc.

Let $\hat{CR}(P)$ be the unit vector to the center of the oncoming turn. The distance from the aircraft to the center of the turn is given by

$$DTEST = r_E \left(\sin^{-1} \left| \hat{RE} \times \hat{CR}(P) \right| \right) \qquad (1)$$

where

$$\hat{RE} = RE \Big/ |RE|$$

and

r_E = the radius of the earth.

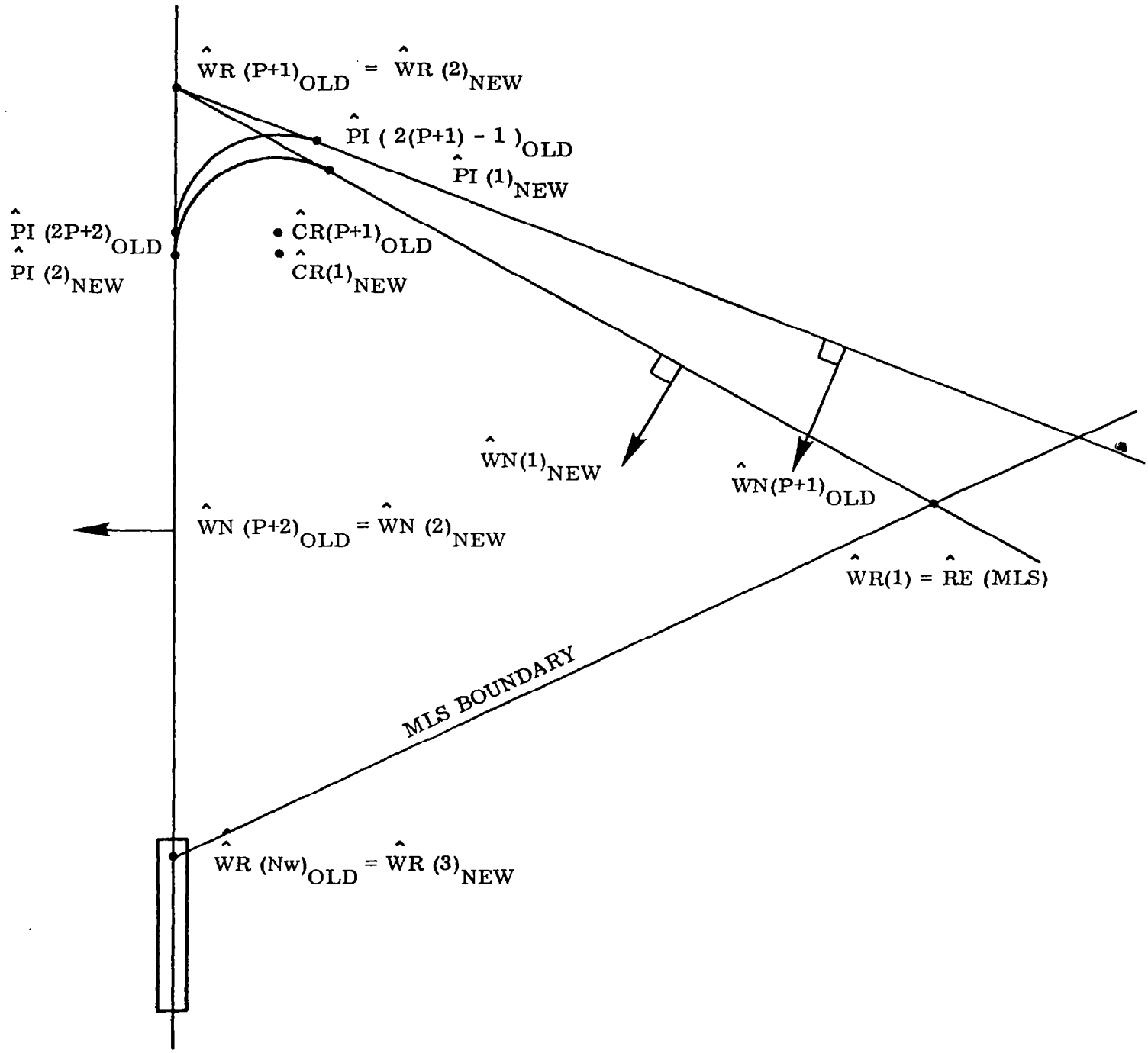

Figure 1. Zero Cross Track Construction

If DTEST > $R_T(P)$ + D (ZTC) we execute the ZTC algorithm below. The value of D (ZTC) is preset in bulk storage and is usually taken to be $\frac{1}{2} R_T(P)$. If the test fails we execute the continued track algorithm (CT) with a message that the ZTC test has failed.

We set

$$\lambda(1) = \tan^{-1}\left(-\hat{R}_E(2) / \hat{R}_E(3)\right) \pi/180$$

$$\delta(1) = \sin^{-1}\left(\hat{R}_E(1)\right) \pi/180 \qquad (2a)$$

$$h(1) = \left|R_E\right| - r_E$$

$v_D(1)$ = current desired airspeed in knots

To fill out the remainder of the path input block data, we set

$$\begin{aligned} \lambda(I) &= \lambda(P+I) \\ \delta(I) &= \delta(P+I) \\ h(I) &= h(P+I) \\ v_D(I) &= v_D(P+I) \end{aligned} \qquad I = 1, N-P \qquad (2b)$$

and if $N - P + 1 \geq 3$

$$R_T(I) = R_T(P+I-1) \quad I = 1, N-P-1 \qquad (2c)$$

We note that while the oncoming interior waypoint, $\hat{WR}(P+1)$, is retained, the unit vector to the center of the oncoming turn, $\hat{CR}(P)$, is moved. Figure 1 illustrates a typical ZCT path construction. The logic for constructing the altered path, and the guidance parameter computation is identical to that used in generating the original path and is contained in Reference 1. The total number of waypoints in the reconstructed path is $J = N - P + 1$.

C. Tangent Path (TP)

The algorithm for the tangent path construction assigns the initial waypoint, $\hat{WR}(1)$, to the unit position vector of the aircraft, $\hat{WE}$, and chooses the second waypoint, $\hat{WR}(2)$ so that the great circle determined by the plane containing $\hat{WE}$ and $\hat{WR}(2)$ shall be tangent to the existing oncoming turn circle with the unit center vector, $\hat{CR}(P)$, and turn radius, $R_T(P)$. We proceed to determine the new first interior waypoint, $\hat{WR}(2)$.

Let $\hat{M}$ be the unit normal to the great circle plane containing the present position, $\hat{WE}$, and the center of the circle, $\hat{CR}(P)$.

$$\hat{M} = \frac{\hat{RE} \times \hat{CR}(P)}{\left|\hat{RE} \times \hat{CR}(P)\right|} \tag{3}$$

The unit normal, $\hat{WN}(1)$, to the great circle plane containing $\hat{RE}$ and the oncoming unit tangent vector, $\hat{PI}(1)$, may be obtained by rotating, $\hat{M}$, about $\hat{RE}$ through an unknown angle, σ. We have

$$\hat{WN}(1) = \cos\sigma\, \hat{M} + \text{sign}(\Delta\psi) \sin\sigma\, \hat{RE} \times \hat{M} \tag{4}$$

To determine the angle σ we resort to spherical trigonometry (see Fig. 2)

$$\sin\sigma = \frac{\sin(R_T(P)/r_E)}{\left|\hat{RE} \times \hat{CR}(P)\right|}$$

$$\cos\sigma = \sqrt{1 - \sin^2\sigma} \tag{5}$$

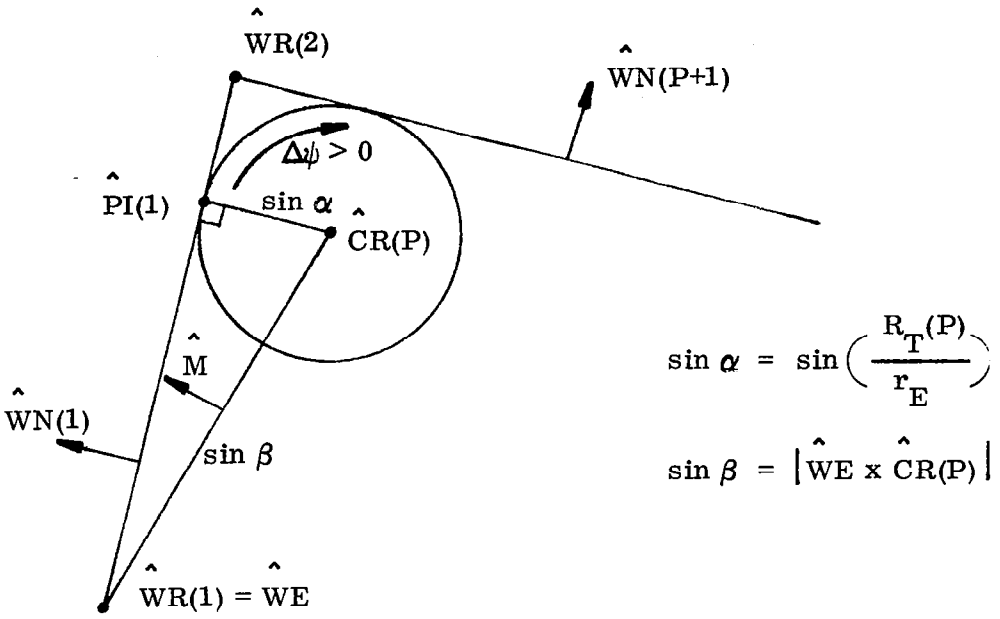

Positive $\Delta\psi$

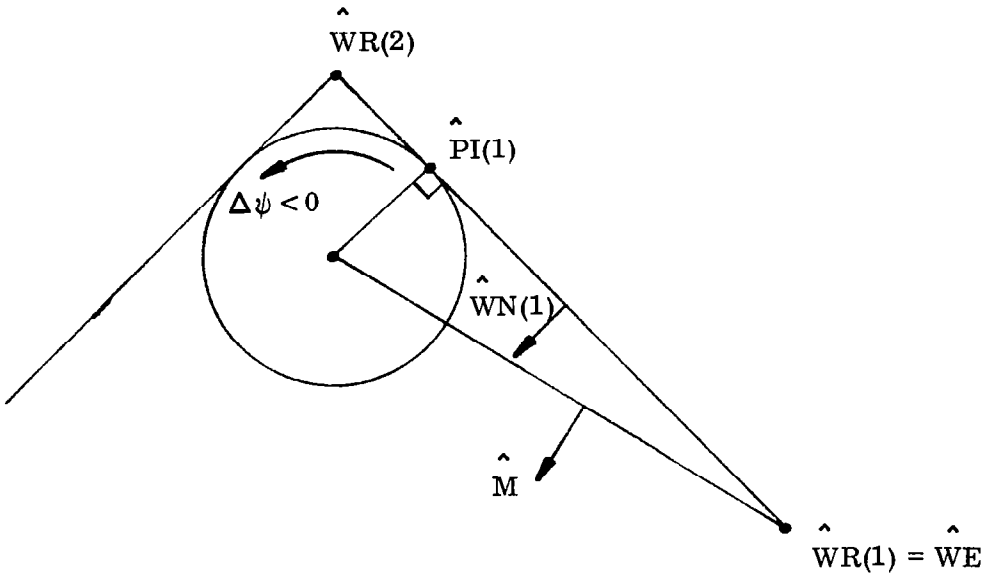

Negative $\Delta\psi$

Figure 2. Tangent Path Construction

To determine the new first interior waypoint, $\hat{WR}(2)$, we note that it is determined by the cross product of the incoming and outgoing normals. Since the remainder of the path past the oncoming turn is left unaltered, we have

$$\hat{WN}(2) = \hat{WN}(P+1) \tag{6}$$

and

$$WR(2) = -\text{sign}(\Delta\psi)\,\frac{\hat{WN}(1) \times \hat{WN}(2)}{\left|\hat{WN}(1) \times \hat{WN}(2)\right|} \tag{7}$$

To obtain the block data information for the tangent path we set

$$\lambda(1) = \tan^{-1}\left(-\hat{RE}(2) / \hat{RE}(3)\right)\ \pi/180$$

$$\delta(1) = \sin^{-1}\left(\hat{RE}(1)\right)\ \pi/180 \tag{8a}$$

$$h(1) = \left|R_E\right| - r_E$$

$$v_D(1) = \text{current desired airspeed in knots}$$

Let

$$\hat{A} = \hat{WR}(2)$$

then, for the second waypoint, we have

$$\begin{aligned} \lambda(2) &= \tan^{-1}\left(-\hat{A}(2) / \hat{A}(3)\right) \\ \delta(2) &= \sin^{-1}\left(\hat{A}(1)\right) \\ h(2) &= h(P+1) \\ v_D(2) &= v_D(P+1) \end{aligned} \tag{8b}$$

For the remainder of the block data we set

$$\begin{aligned} \lambda(I) &= \lambda(P+I) \\ \delta(I) &= \delta(P+I) \\ h(I) &= h(P+I) \qquad I = 2, N-P \\ v_D(I) &= v_D(P+I) \end{aligned} \tag{8c}$$

and if $N - P + 1 \geq 3$

$$R_T(I) = R_T(P+I-1) \qquad I = 1, N-P-1 \tag{8d}$$

As in the case of the Zero Cross Track method, the Tangent Path Transition Technique eliminates the cross track error and the command altitude error, but does not eliminate the track angle error. Consequently, if the transition takes place too close to the oncoming turn circle, a large track angle error is produced along the new path and large turn commands may result. Here again, it is recommended to defer using the TP method if the distance to the center of the oncoming turn is too close.

Let PTEST be computed as

$$PTEST = r_E \left(\sin^{-1} \left| \hat{RE} \times \hat{CR}(P) \right| \right) \tag{8e}$$

If DTEST $>$ $R_T(P) + D(TP)$ we execute the TP procedure. Otherwise, we call for the continued track method (CT) and display a message to that effect to the pilot.

D. Continued Track (CT)

The Continued Track transition method accepts the MLS position and velocity vectors, thus eliminating the need for corrections at transition. Moreover it is capable of being executed along a great circle (straight line path) or in a turn and thus provides a truly smooth transition.

Let RE be the aircraft position vector in the earth fixed inertial coordinate system, and $\dot{RE}$ be the aircraft velocity vector in the same system. Then, the unit normal to the first aircraft reconstructed path is given by

$$\hat{WN}\ (1) = \frac{RE \times \dot{RE}}{\left|RE \times \dot{RE}\right|} \tag{9}$$

At this juncture it is necessary to introduce the ability of utilizing either an interior corner or a center of turn as an input waypoint in the initial block data. This is done in order to accommodate turns of greater than 180 degrees. The addition is introduced in Appendix I of this report. An array, IC (I) , is created in block data. For each waypoint we choose either IC (I) = 0, or IC (I) = 1.

$$\text{If IC (I)} = 0\,, \tag{10a}$$

then λ (I) , δ (I) correspond to a regular interior waypoint.

$$\text{If IC (I)} = 1\,, \tag{10b}$$

then λ (I) , δ (I) correspond to a center of turn waypoint.

In addition, we must assign to each turn a SIGN (I), indicating whether the turn is in the direction of increasing azimuth with respect to north, SIGN (I) = 1., or decreasing, SIGN (I) = -1.

For the first waypoint, following a valid MLS update, we set

$$
\begin{aligned}
IC\ (1) &= 0 \\
\lambda\ (1) &= \tan^{-1}\ (-\hat{RE}\ (2)/\ \hat{RE}\ (3))\ \pi/180 \\
\delta\ (1) &= \sin^{-1}\ (\hat{RE}\ (1)\ )\ \pi/180 \\
h\ (1) &= |RE| - r_E \\
v_D(1) &= \text{current desired airspeed in knots} \\
SIGN\ (1) &= SIGN\ (P)
\end{aligned}
\tag{11}
$$

1. CT on a straight line segment

If the aircraft is not in a turn, we determine the second interior way point using Eq. (2),

$$
\hat{WR}\ (2) = -\ SIGN\ (P)\ \frac{\hat{WN}\ (1) \times \hat{WN}\ (P+1)}{|\hat{WN}\ (1) \times \hat{WN}\ (P+1)|} \tag{12}
$$

Let σ be the sign of the vector dot product of $\hat{WR}\ (2)$ and $\hat{CR}\ (P)$, the turn center of the original oncoming turn.

$$
\sigma = sign\ (\hat{WR}\ (2) \cdot \hat{CR}\ (P)\ ) \tag{13}
$$

Then, the new unit vector to the center of the first oncoming turn, $\hat{CR}\ (1)$, is given by

$$
\hat{CR}\ (1) = \sigma \sqrt{1 - \frac{2 \sin^2 A}{1 + \hat{WN}(1) \cdot \hat{WN}\ (P+1)}}\ \hat{WR}\ (2) - \frac{\sin A}{1 + \hat{WN}(1) \cdot \hat{WN}(P+1)}\ (\hat{WN}(1) + \hat{WN}(P+1)) \tag{14a}
$$

where $\sin A = \sin\ (R_T(P) / r_E\ )$ (14b)

In addition, set

$$h(2) = h(P) \tag{15a}$$

$$R_T(1) = R_T(P) \tag{15b}$$

$$IL = P \tag{15c}$$

2. CT in turn

If transition takes place during a turn we must set the trigger, ITURN , to inform block data that the first straight line segment should be eliminated in generating the new path.

The second item to be determined is whether we are in the first half of the turn or the second. If we are in the first half of the turn, it is a relatively short distance to the middle of the turn. Since we have accepted the existing aircraft altitude as the desired altitude, we must alter the desired altitude at the middle of the turn to avoid an abrupt change in glide slope over the short distance remaining. This is accomplished in the path generation logic (see Appendix I). If we are in the second half of the turn there is little danger of an abrupt change in desired glide slope since the next altitude is defined at the middle of the next turn, which is usually some distance away.

The third item to be determined is whether we are in the final turn prior to landing. It is necessary to know this for the following reason. If we are in a turn we know that the unit position vector, $\hat{RE}$, lies on the turn circle and we know the unit normal, $\hat{WN}(1)$. Together with the radius of the turn, $R_T(1)$, and the SIGN (P), these items completely determine the unit vector to the center of the turn, $\hat{CR}(1)$. The location of the center, $\hat{CR}(1)$, and the unit vector to the center of the next turn $\hat{CR}(2)$, together with their radii, $R_T(1)$ and $R_T(2)$, and their SIGN's, completely determine the outgoing unit normal vector, WN(2). However, on the last leg, leading to touchdown, we are not free to choose the outgoing unit normal, $\hat{WN}(2)$, since this is determined by the heading of the runway, ψR , and the final waypoint , $\hat{WR}(N)$. Consequently we must surrender

a degree-of-freedom to accommodate the final straight line leg. We choose to give up the radius of the turn, $R_T(1)$.

The sequence of the choices proceeds as follows:

If we are in a turn, we set,

$$\text{ITURN} = 1 \tag{16a}$$

Otherwise, ITURN is defaulted to 0.

If we are in the turn and it is the first half of the turn, then we set

$$\text{IMOD} = 2 \tag{16b}$$

$$\text{GRX} = \text{GRAD (P)} \tag{16c}$$

Otherwise, these are defaulted to be IMOD = 1 and GRX = 0.

The path generation logic will use these triggers to eliminate the first straight line segment, and to determine the altitude at the middle of the turn to provide for a continuous glide slope.

In addition we set

$$M = N - P + 1 \tag{16d}$$

$$IL = P \tag{16e}$$

If we are in a turn and in the second half of the turn, then we set

$$\text{IMOD} = 0 \tag{16f}$$

$$M = N - P + 2 \tag{16g}$$

$$IL = P - 1 \tag{16h}$$

Now we check if we are on the last turn. If M = 3, we must determine the radius of the turn.

For this case we have

$$A1 = \hat{WN}(N-1) \cdot \hat{RE} \tag{17a}$$

$$A2 = 1. - \hat{WN}(1) \cdot \hat{WN}(N-1) \tag{17b}$$

$$\sin A = \frac{|A1|}{\sqrt{(A1)^2 + (A2)^2}} \tag{17c}$$

$$R_T(1) = r_E \sin^{-1}(\sin A) \tag{17d}$$

If $M > 3$ we set

$$R_T(1) = R_T(IL) \tag{17e}$$

For all the above cases we proceed to determine the unit center of the new turn. Let

$$\sin A = r_E \sin^{-1}\left(R_T(1)/r_E\right) \tag{18a}$$

$$\cos A = (1. - (\sin A)^2)^{\frac{1}{2}} \tag{18b}$$

$$\hat{CR}(1) = \cos A \, \hat{RE} - \text{sign}(\Delta\psi) \sin A \, \hat{WN}(1) \tag{19}$$

3. CT Block Data for all cases

Having determined the unit center of the turn for all three CT cases, we set

$$\hat{A} = \hat{CR}(1) \tag{20}$$

$$IC(2) = 1 \tag{21a}$$

$$\lambda(2) = \tan^{-1}(-\hat{A}(2) / \hat{A}(3)) \, \pi/180 \tag{21b}$$

$$\delta\ (2) = \sin^{-1}\ (\hat{A}\ (1)\ )\ \pi/180 \tag{21c}$$

$$h\ (2) = h\ (P+1) \tag{21d}$$

$$v_D = v_D\ (P+1) \tag{21e}$$

II. SIMULATION STUDY OF THE COMPARATIVE PATH RECONSTRUCTION METHODS

A. Description of the Simulation Test Data

This section contains the plots of computer runs carried out using the FILCOMP program. Each run consists of 3 sets of plots.

The first in each series contains a plot of the aircraft ground track illustrating the original and reconstructed paths. The original waypoint data point is indicated by a point enclosed by a diamond. The reconstructed waypoint is marked by a point contained in a circle. The boundary limits of the MLS azimuth antenna are illustrated by a dashed line emanating from the azimuth antenna. The boundary limits of the elevation antenna are illustrated by a dashed line emanating from the antenna site to the right of the start of the runway. The initial waypoint at the start of each trajectory is shown by a point enclosed in a diamond. Transition occurs immediately after entering the elevation coverage. If the center of a turn is relocated during path reconstruction, both the original and new center are shown. If the tangent path method is used, the center of the turn is not altered, but the vertex corner may be altered, and both the original and the reconstructed vertex are shown. Pertinent data requiring winds, Path Construction Algorithm used, navigation filter type, etc., are printed on this page. Finally, to illustrate the remaining distance to touchdown, each plot contains either the original path design approach distance in nautical units, or the reconstructed final distance.

The second page in each series contains 7 plots of pertinent data as a function of time. These consist of the following:

1) Glide path deviation in meters for both the true deviation and the estimated deviation for the particular navigation filter in use in the guidance loop for aircraft control.

2) Aircraft pitch angle in degrees for the true pitch, the measured pitch output of the IMU (used by the complementary filter) and the estimated pitch corrected for the estimated gyro drift bias (used in the Kalman filters).

3) Aircraft altitude rate, measured in meters per second, for both the true rate of climb and the estimated rate obtained by the particular navigation filter supplying the control equations.

4), 5), 6) Errors in the estimate of the forward, lateral and vertical coordinates of the aircraft measured in the flat earth runway coordinates of the aircraft measured in the flat earth runway coordinate system for both the complementary and Kalman filters, measured in meters.

7) Error in the estimate of the forward velocity component $\hat{\dot{x}}_{1R}$ in the runway coordinate system, measured in meters per second for both the complementary and the Kalman filters.

The last of the figures in each series of three contain 8 plots of data as function of time. These consist of the following:

1) Cross track error, measured in meters, for both the true CRTE and the estimated CRTE obtained by the navigation filter used to supply the guidance equations.

2) Track angle error, converted from degrees to the time rate of change of cross track error by multiplying by the ground speed. Both the true track angle error and the estimated track angle error supplying the guidance equations are shown, measured in meters per second.

3) Aircraft roll angle, measured in degrees, for the true roll angle, the measured roll angle supplying the complementary filter, and the measured roll angle corrected for the gyro drift bias (used in the Kalman filter estimate of the aircraft roll angle).

4) Error in the estimate of the north component of the wind, in meters per second, for both the Kalman and complementary filters.

5) Error in the estimate of the west component of the wind, in meters per second, for both the Kalman and complementary filters.

6) Difference between the true desired airspeed and the true airspeed. A second plot also shows the difference between the true ground speed and the true airspeed. The curves are mirror images of one another in the event the winds are zero, and differ in the presence of winds.

7) Error in the estimate of the lateral velocity $\hat{\dot{x}}_{2R}$, in the runway coordinate system, in meters per second, for both the Kalman and the complementary filter.

8) Error in the estimate of the vertical velocity, $\hat{\dot{x}}_{3R}$, in the runway coordinate system, in meters per second, for both the Kalman and the complementary filter.

B. Discussion of the Results

Case 1 illustrates a successful application of the tangent path technique. In this case transition occurs sufficiently far away from the oncoming turn circle so that the uncorrected error in track angle does not cause an excessive roll. Fig. 3(a) shows the ground track for this case. Transition occurs 40 seconds after the start of the simulation immediately after the aircraft enters the elevation coverage. The large sweep of 75^{o} permits the aircraft to update the path on the straight line portion fully 15 seconds prior to the start of the turn at a distance of over 1100 meters. The maximum roll angle needed to erase the uncorrected track angle error is shown in Plot 3 of Fig. 3(c) and is seen to be approximately 3^{o}. This occurs sufficiently far away from the required turn so that the aircraft has time to level off before executing the turn.

Case 2 illustrates a less successful application of the tangent path reconstruction technique. In this case (Fig. 4(a)), transition occurs after the completion of the first turn and prior to the start of the second turn. The aircraft guidance is presented with a large track angle error (see Plot 2, Fig. 4(c)). A roll angle of 10^{o} is required to regain the heading alignment. (See Plot 3, Fig. 4(c)). Since this follows the exit of the previous turn, an undesirable sequence of turns result.

Case 3 illustrates the advantage of the continued track path construction over the tangent path method. In this case, the same transition geometry Fig. 5(a)) results in a smooth path without extra turns. The center of the oncoming circle is only slightly altered to accommodate the elimination of the error in cross track and track angle. Plot 1 and 3 of Fig. 5(c) shows no cross track

error or roll angle following the transition time at 110 seconds. The superiority of the continued track over the tangent path reconstruction method is clearly illustrated.

Case 4 is a further illustration of the undesirability of utilizing the tangent path when the aircraft is too close to the oncoming turn circle. In this case (see Fig. 6(a)) the elevation coverage limits are set at 35^{o}. The change in heading required to produce a path tangent to the oncoming circle produces an error in cross track rate of over 20 m/sec (see Plot 2, Fig. 6(c)) and a roll angle of 20^{o} (see Plot 3, Fig. 6(c)). This is immediately followed by the onset of the required turn, which causes an undesirable series of turns.

Case 5 shows the identical transition history with the continued track algorithm. Once again, with a slight adjustment of the center of the oncoming turn, the cross track and these track angle errors are eliminated and no extra maneuvering occurs. Fig. 7(a) shows the smooth ground track. The altered center of the second turn is indicated by the small circle in the center of the turn. It should be noted that the last outgoing tangent point, at the intersection of the second circle and the runway track, has been moved forward somewhat, but that the remaining ground distance to touchdown is still 1.80 nautical miles; long enough to permit a normal landing.

Cases 6, 7, 8, 9, and 10 illustrate the adaptability and applicability of the continued track reconstruction technique at every point along the approach flight path. By varying the boundary limits of the elevation coverage it is possible to force the transition point to occur at a straight line segment on the first half or second half of a turn, and either the first or the final approach turn. Each case is handled successfully, without requiring any extra roll to recapture the original path.

Case 6, Figs. 8(a), 8(b), and 8(c) illustrate the application of the continued path with transition occurring on the straight line segment immediately prior to the onset of the first turn. Plots 2 and 3 of Fig. 8(c), show little cross track velocity after transition and no roll angle required until the start of the reconstructed first turn.

Case 7, Figs. 9(a), 9(b), and 9(c) illustrate the application of the continued track technique when transition occurs on the first half of the first turn circle.

Once again, examination of Plots 2 and 3 of Fig. 9(c) shows the elimination of the cross track velocity in the middle of the required turn and no extra roll angle is called for whatsoever. It should be noted that a small change in the relocation of the center of the second turn is required, resulting in a small movement (.08 nautical miles) of the outgoing tangent point along the runway extension segment. (See Fig. 9(a)).

Case 8, illustrates the same smooth continued path reconstruction when transition occurs on the second half of the first turn. (See Figs. 10(a), 10(b), and 10(c)).

Case 9, Figs.11(a),11(b), and11(c) illustrate the continued path reconstruction when transition occurs on the first half of the last turn. The only significant feature here is the need to change the radius of the last turn and the movement of the tangent to the runway centerline to a point 1.79 nautical miles from touchdown.

Case 10 illustrates the most critical of all transitions. This one takes place on the second half of the final turn. A smooth transition occurs again. The only significant problem is the shortening of the final approach segment, from the tangent point to touchdown from its initial value of 2 nautical miles to 1.47 nautical miles. There appears to be no reason why a successful smooth letdown cannot be executed in this remaining distance. Plot 6, Fig. 12(b) illustrates the readjustment in the estimate of vertical height at transition. Plot 2, Fig. 12(b), illustrates the smooth pitch profile. It is interesting to examine Plot 2, Fig. 12(c). The roll angle following transition is lowered from 15^{o} to 10^{o} to accommodate the increase in the altered turn radius.

Cases 11 and 12 are illustrations of the capability of path construction for turns greater than 180^{o}, and the ability of the continued path to reconstruct a path greater than 180^{o} on the first and second half of a final turn.

Case 11, Fig.'s 13(a), 13(b), and 13(c) represent an approach path with a 220^{o} turn into the final runway segment. Transition takes place shortly before the aircraft has entered the first half of the turn. Fig. 13(a) shows the reconstruction of the turn circle, including the determination of the new turn radius. Once again, the outgoing tangency point with the final runway segment has been

altered from 2.0 nautical miles to 1.67 nautical miles. A successful landing is accomplished without undue maneuvering.

Case 12, Figs. 14(a), 14(b), and 14(c) represent the same 220^{o} turn approach with the transition occurring on the second half of the turn. Once again, the change in turn radius at transition calls for a somewhat smaller roll angle as seen in Plot 3, Fig. 14(a). Examination of Plot 3, Fig. 14(b) illustrates a slight oscillation of the vertical altitude rate following the transition time. This oscillation is inherent in the pitch channel due to coupling between the engine thrust and the error in desired airspeed.

TABLE I

VORTAC AND MLS STATION COORDINATES

VORTAC STATION COORDINATES

STATION LONGITUDE	40.40316
STATION LATITUDE	-27.164894
STATION ALTITUDE	45.72 m

MLS STATION COORDINATES

AZIMUTH & DME LONGITUDE	40.25
AZIMUTH & DME LATITUDE	-77.025
AZIMUTH & DME ALTITUDE	0.

ELEVATION DISTANCE FROM RUNWAY COORDINATE FRAME ORIGIN

XEL(1) = 1000., XEL(2) = 254.78, XEL(3) = .47

RUNWAY HEADING = 30 ^{o}

TABLE II

INPUT DATA FOR WAYPOINT CONSTRUCTION

CASES 1 THROUGH 10

N = 4

I	λ(I) DEG	δ(I) DEG	h(I) m	v_D(I) m/sec	IC
1	40.29759451	-77.14538380	994.654	74.594	0
2	40.23788553	-77.13148869	640.811	69.450	0
3	40.20574384	-77.05845224	290.748	64.305	0
4	40.25237254	-77.02320521	0.	64.305	0

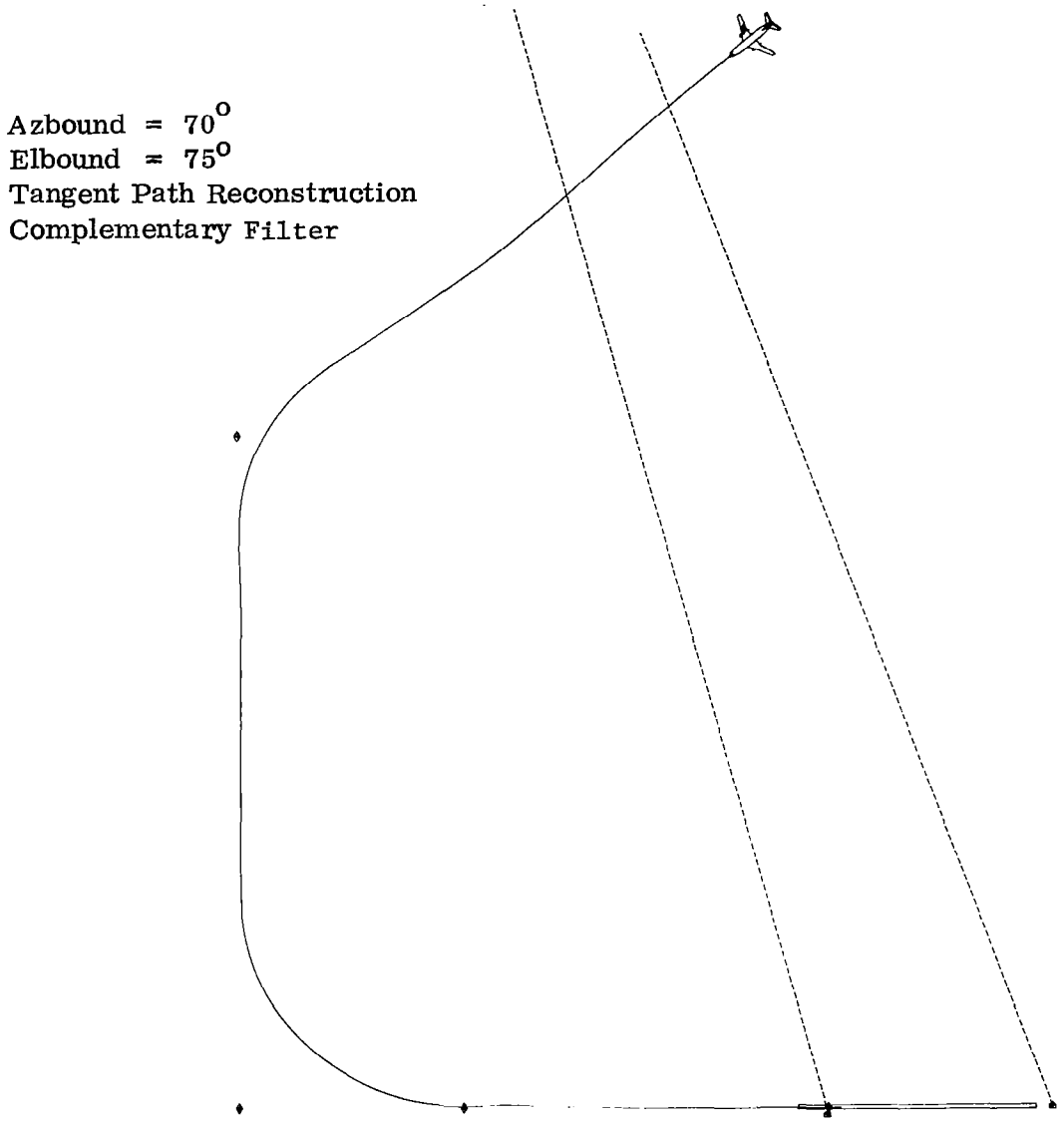
Azbound = 70°
Elbound = 75°
Tangent Path Reconstruction
Complementary Filter
Final Distance = 2.00 Nautical Miles
Aircraft Ground Track

Fig. 3(a) CASE 1

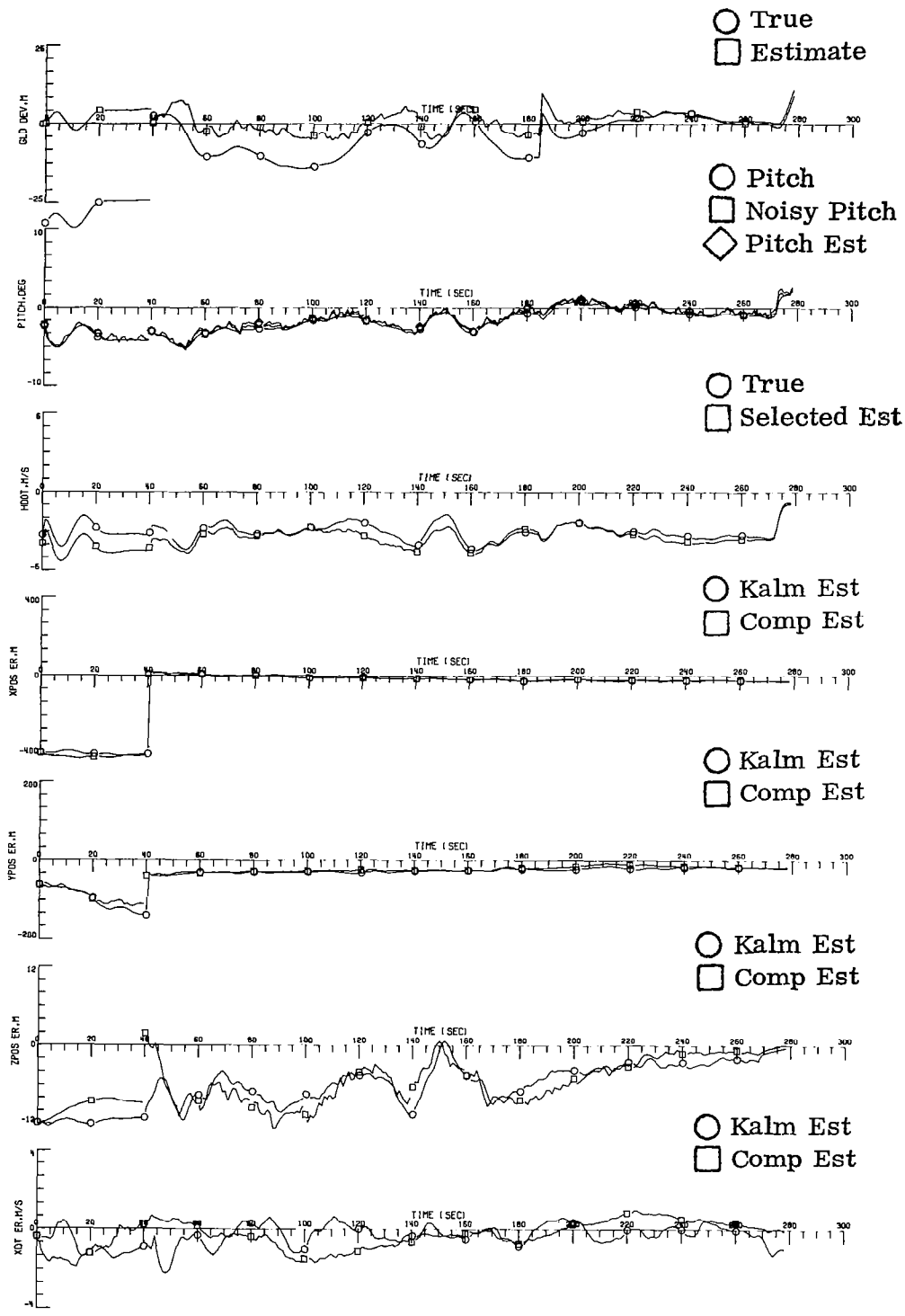
True
Estimate
GLD DEV.M
TIME (SEC)
Pitch
Noisy Pitch
Pitch Est
PITCH.DEG
TIME (SEC)
True
Selected Est
HDOT.M/S
TIME (SEC)
Kalm Est
Comp Est
XPOS ER.M
TIME (SEC)
Kalm Est
Comp Est
YPOS ER.M
TIME (SEC)
Kalm Est
Comp Est
ZPOS ER.M
TIME (SEC)
Kalm Est
Comp Est
XDT ER.M/S
TIME (SEC)

Fig. 3(b) CASE 1

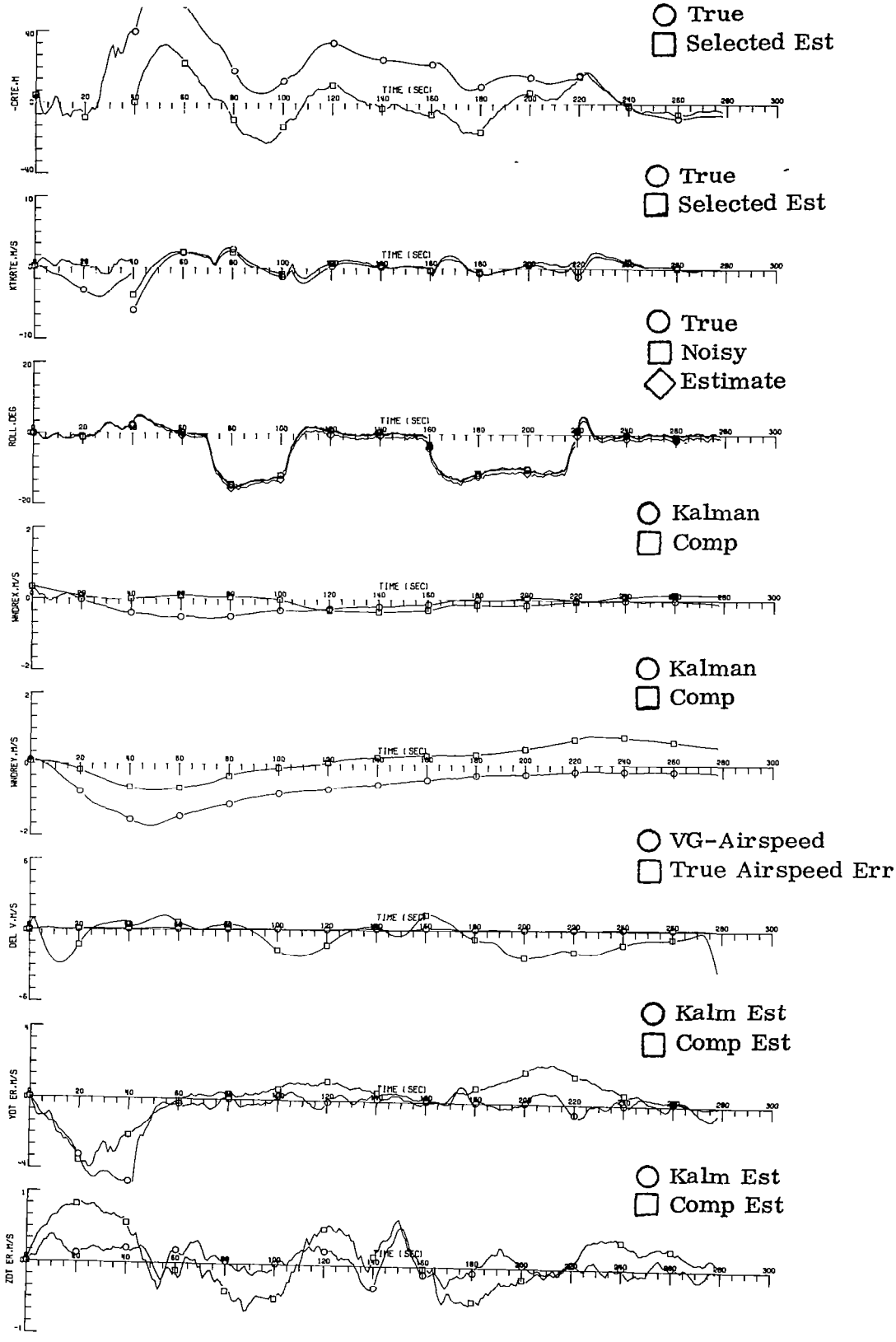
True
Selected Est
-DRTE.M
TIME (SEC)
True
Selected Est
KTKRTE.M/S
TIME (SEC)
True
Noisy
Estimate
ROLL.DEG
TIME (SEC)
Kalman
Comp
WNDREX.M/S
TIME (SEC)
Kalman
Comp
WNDREY.M/S
TIME (SEC)
VG-Airspeed
True Airspeed Err
DEL V.M/S
TIME (SEC)
Kalm Est
Comp Est
YDT ER.M/S
TIME (SEC)
Kalm Est
Comp Est
ZDT ER.M/S
TIME (SEC)

Fig. 3(c) CASE 1

Azbound = 70°
Elbound = 45°
Tangent Path Reconstruction
Complementary Filter

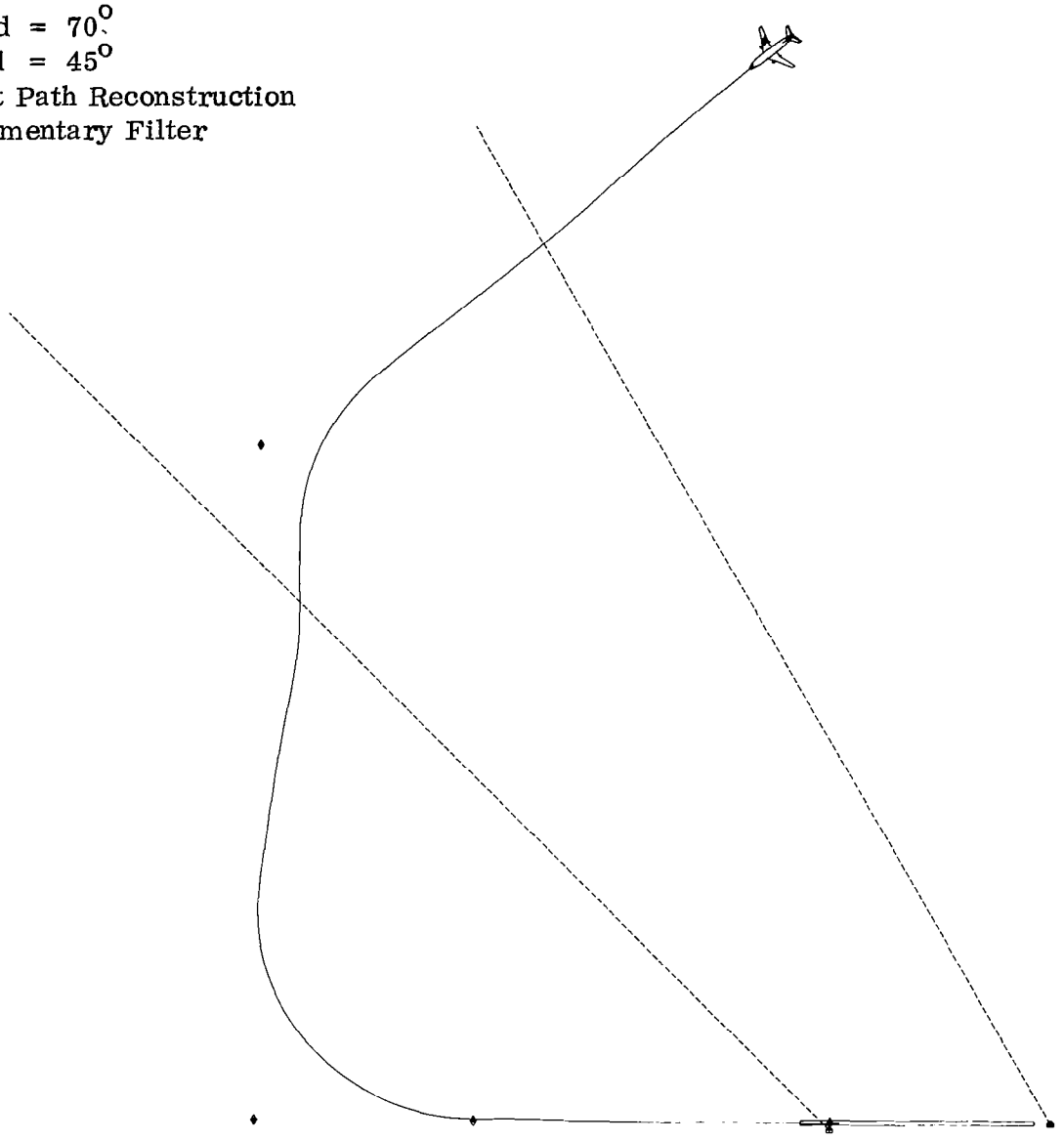

Final Distance = 2.00 Nautical Miles

Aircraft Ground Track

Fig. 4(a) CASE 2

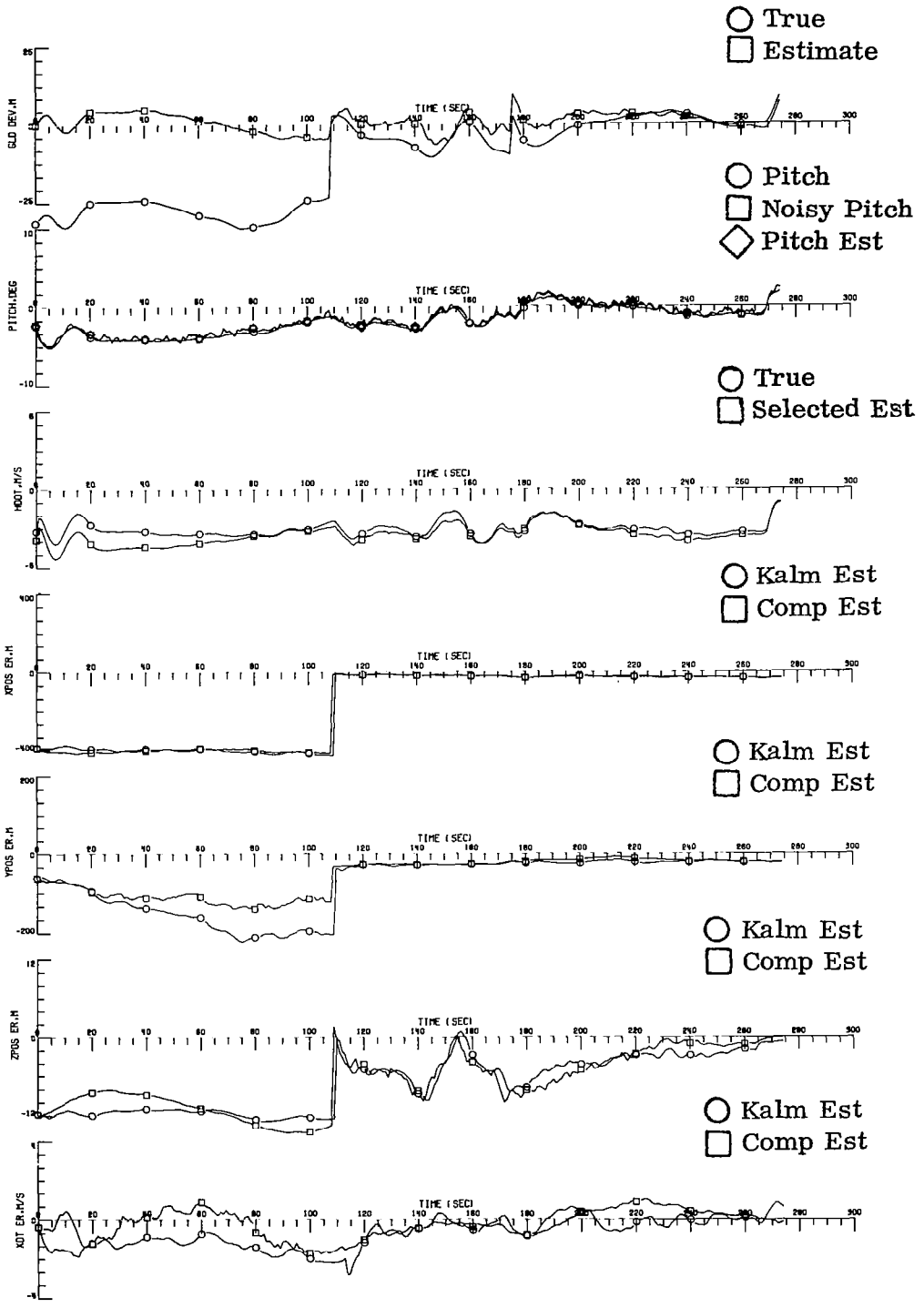
True
Estimate
GLD DEV.M
TIME (SEC)
Pitch
Noisy Pitch
Pitch Est
PITCH,DEG
TIME (SEC)
True
Selected Est
HDOT,M/S
TIME (SEC)
Kalm Est
Comp Est
XPOS ER,M
TIME (SEC)
Kalm Est
Comp Est
YPOS ER,M
TIME (SEC)
Kalm Est
Comp Est
ZPOS ER,M
TIME (SEC)
Kalm Est
Comp Est
XDT ER,M/S
TIME (SEC)

Fig. 4(b) CASE 2

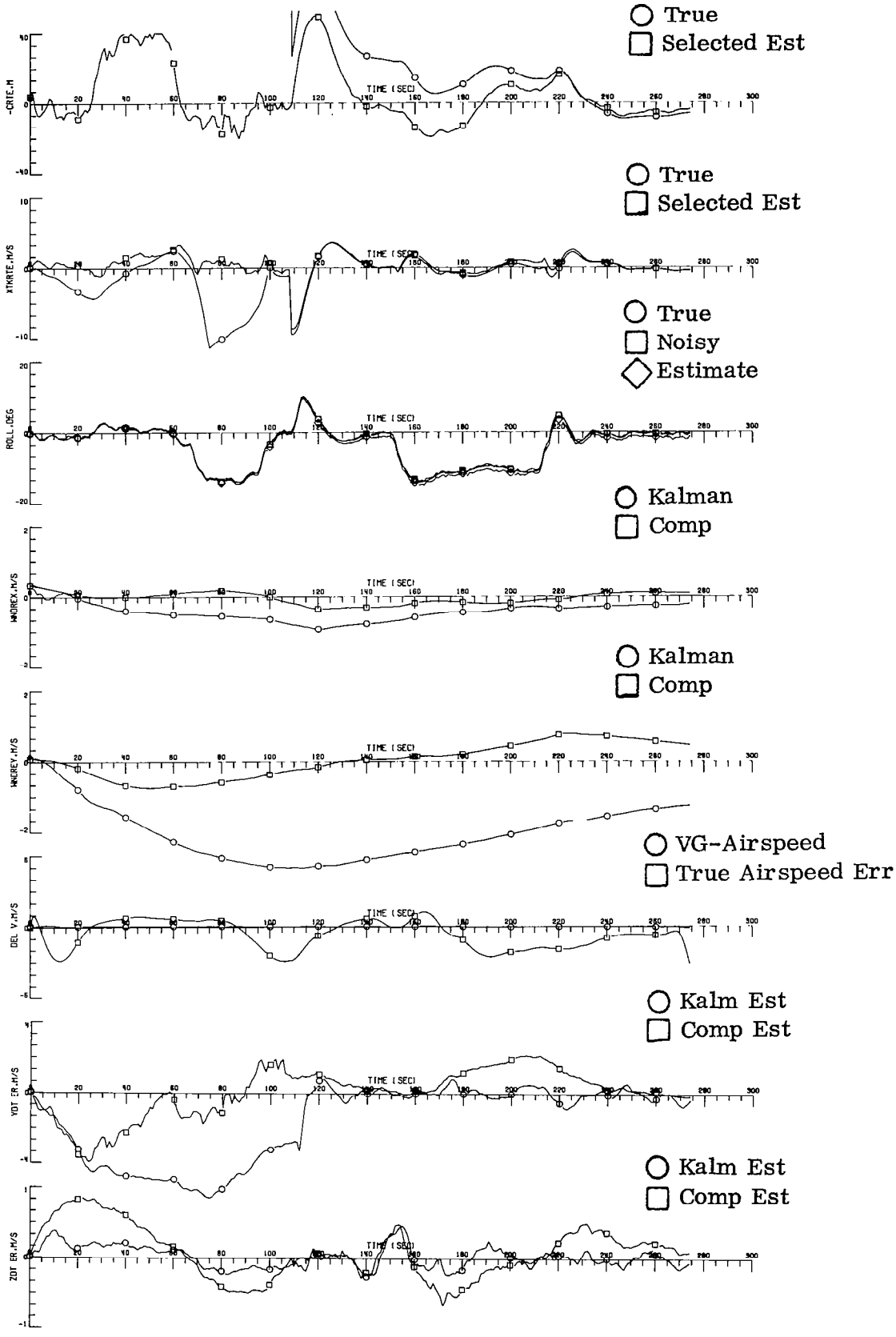
True
Selected Est
-CRTE.M
TIME (SEC)
True
Selected Est
XMRTE.M/S
TIME (SEC)
True
Noisy
Estimate
ROLL.DEG
TIME (SEC)
Kalman
Comp
WNDREX.M/S
TIME (SEC)
Kalman
Comp
WNDREY.M/S
TIME (SEC)
VG-Airspeed
True Airspeed Err
DEL V.M/S
TIME (SEC)
Kalm Est
Comp Est
VDT ER.M/S
TIME (SEC)
Kalm Est
Comp Est
ZDT ER.M/S
TIME (SEC)

Fig. 4(c) CASE 2

Azbound = 70^{o}
Elbound = 45^{o}
Continued Path Reconstruction
Complementary Filter

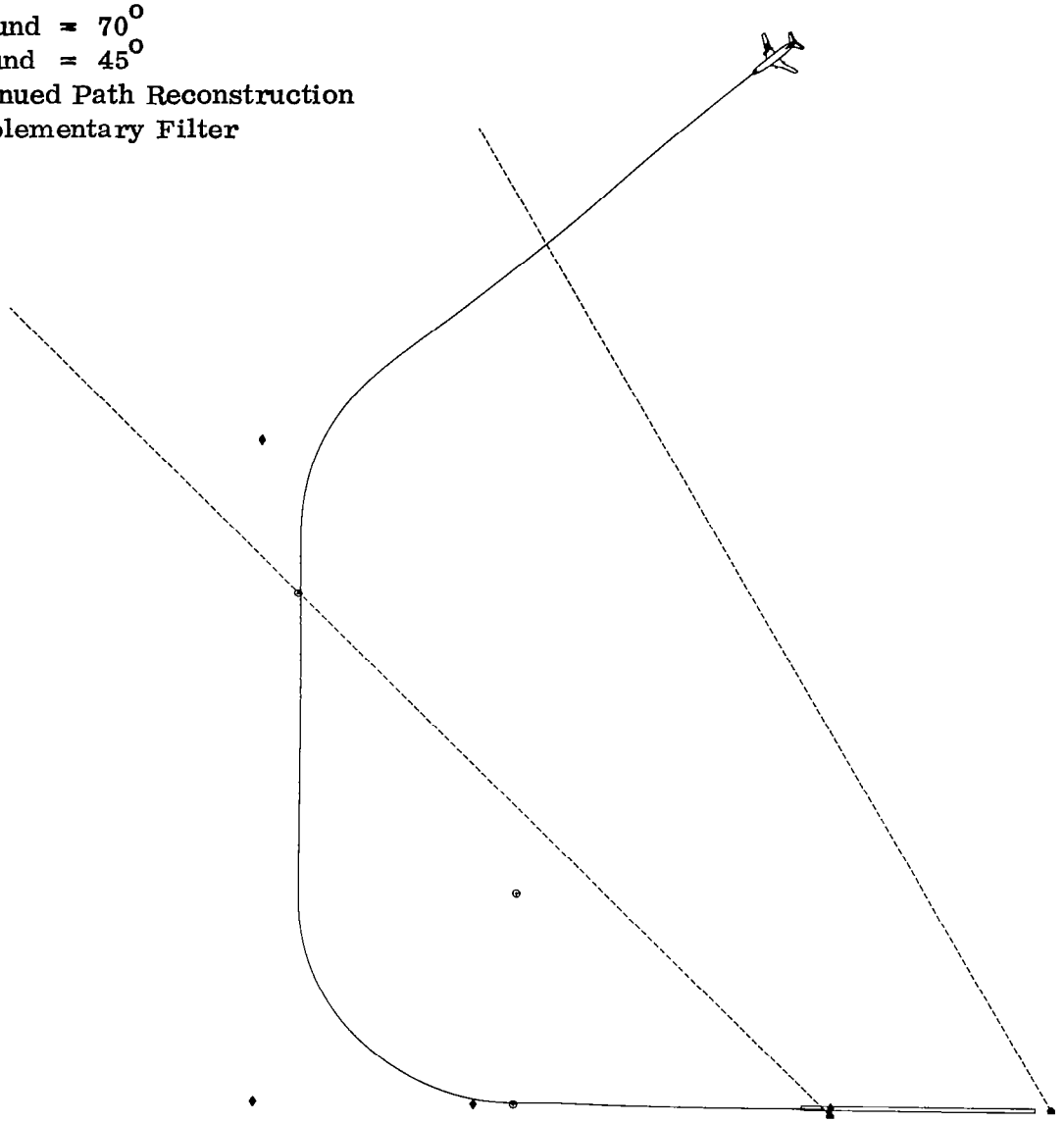

Final Distance = 1.78 Nautical Miles

Aircraft Ground Track

Fig. 5(a) CASE 3

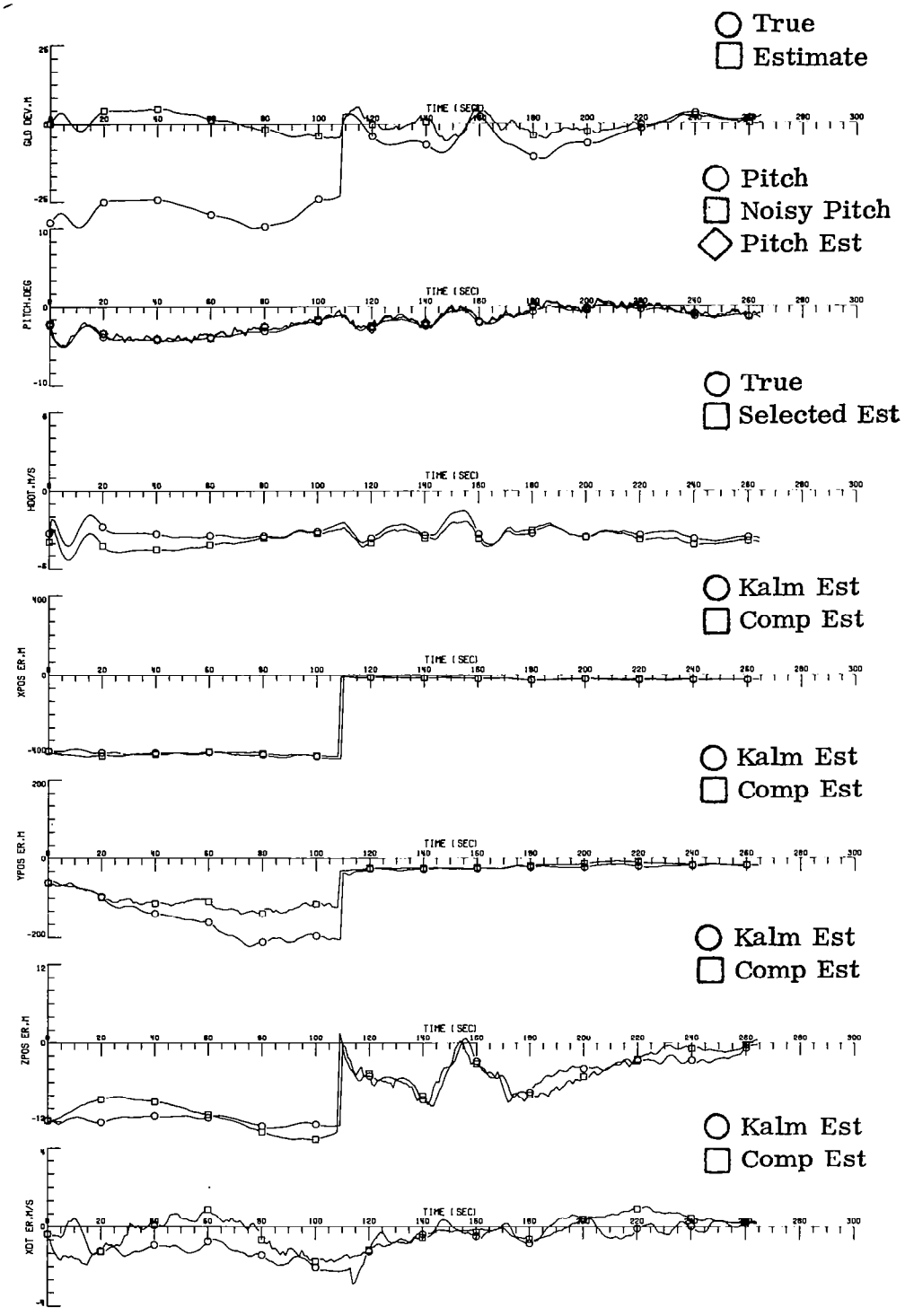
True
Estimate
GLD DEV.M
TIME (SEC)
Pitch
Noisy Pitch
Pitch Est
PITCH.DEG
TIME (SEC)
True
Selected Est
HDOT.M/S
TIME (SEC)
Kalm Est
Comp Est
XPOS ER.M
TIME (SEC)
Kalm Est
Comp Est
YPOS ER.M
TIME (SEC)
Kalm Est
Comp Est
ZPOS ER.M
TIME (SEC)
Kalm Est
Comp Est
XDT ER.M/S
TIME (SEC)

Fig. 5(b) CASE 3

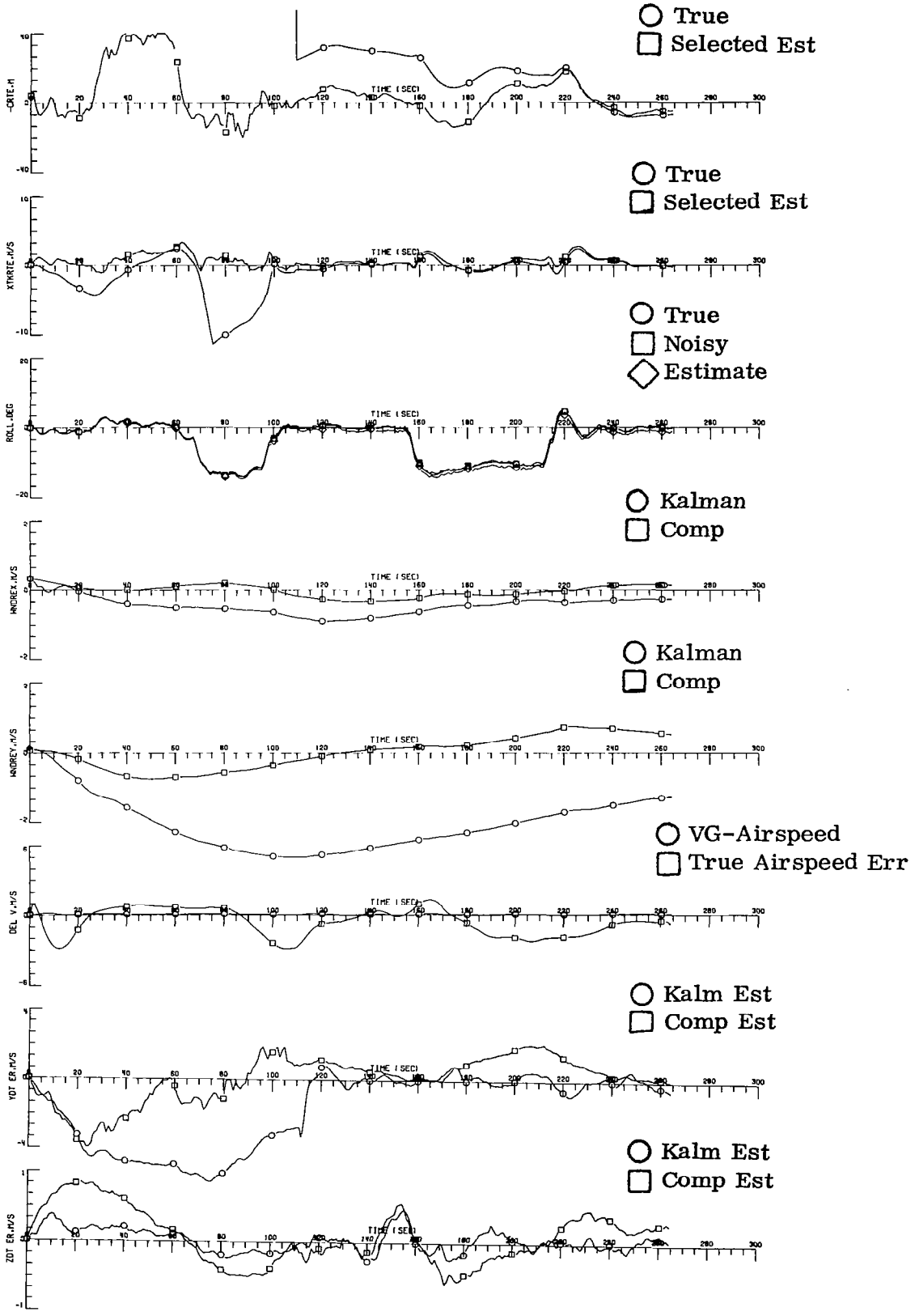
True
Selected Est
True
Selected Est
True
Noisy
Estimate
Kalman
Comp
Kalman
Comp
VG-Airspeed
True Airspeed Err
Kalm Est
Comp Est
Kalm Est
Comp Est

Fig. 5(c) CASE 3

Azbound = 20^{o}
Elbound = 35^{o}
Tangent Path Reconstruction
Complementary Filter

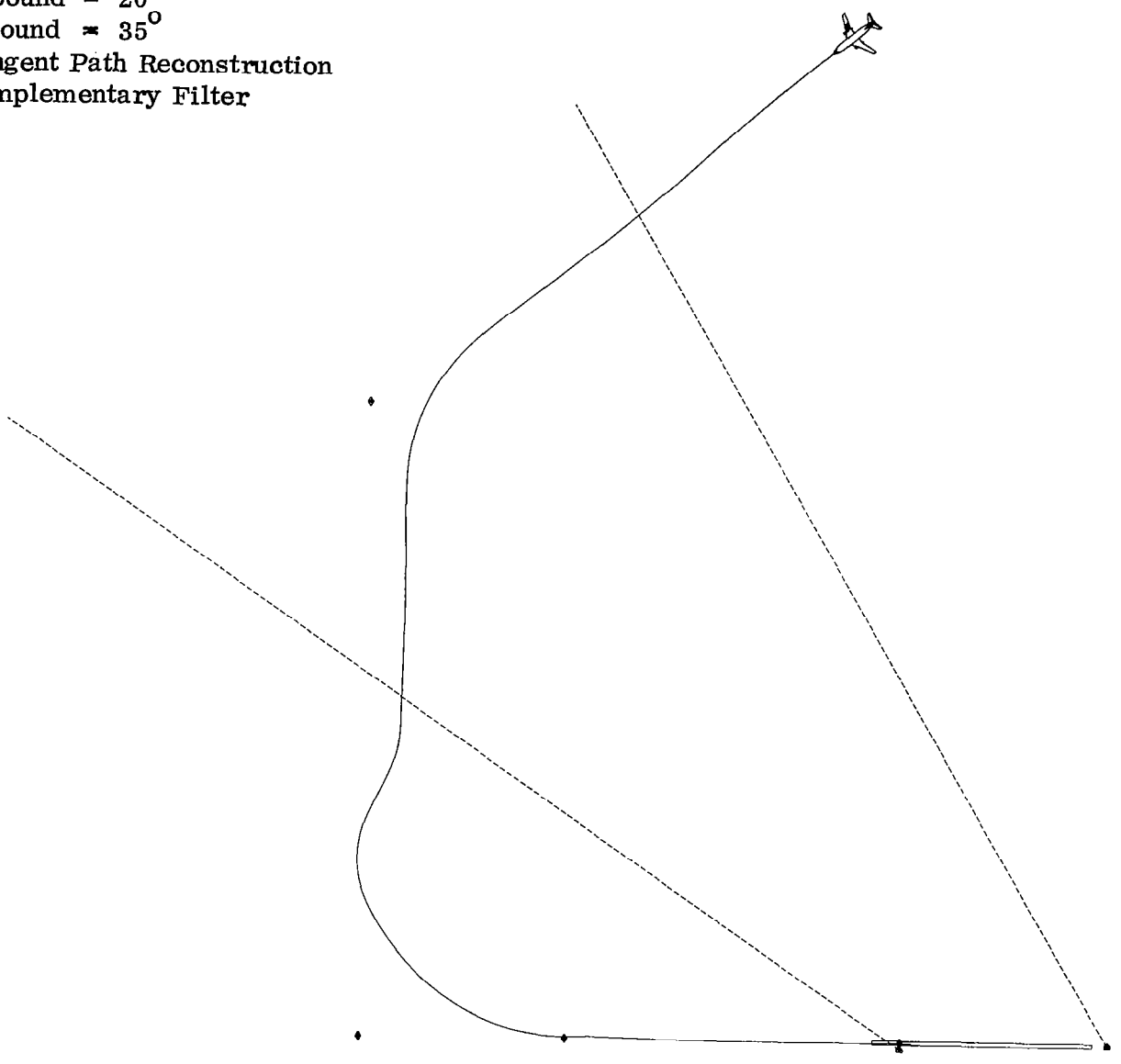

Final Distance = 2.00 Nautical Miles

Aircraft Ground Track

Fig. 6(a) CASE 4

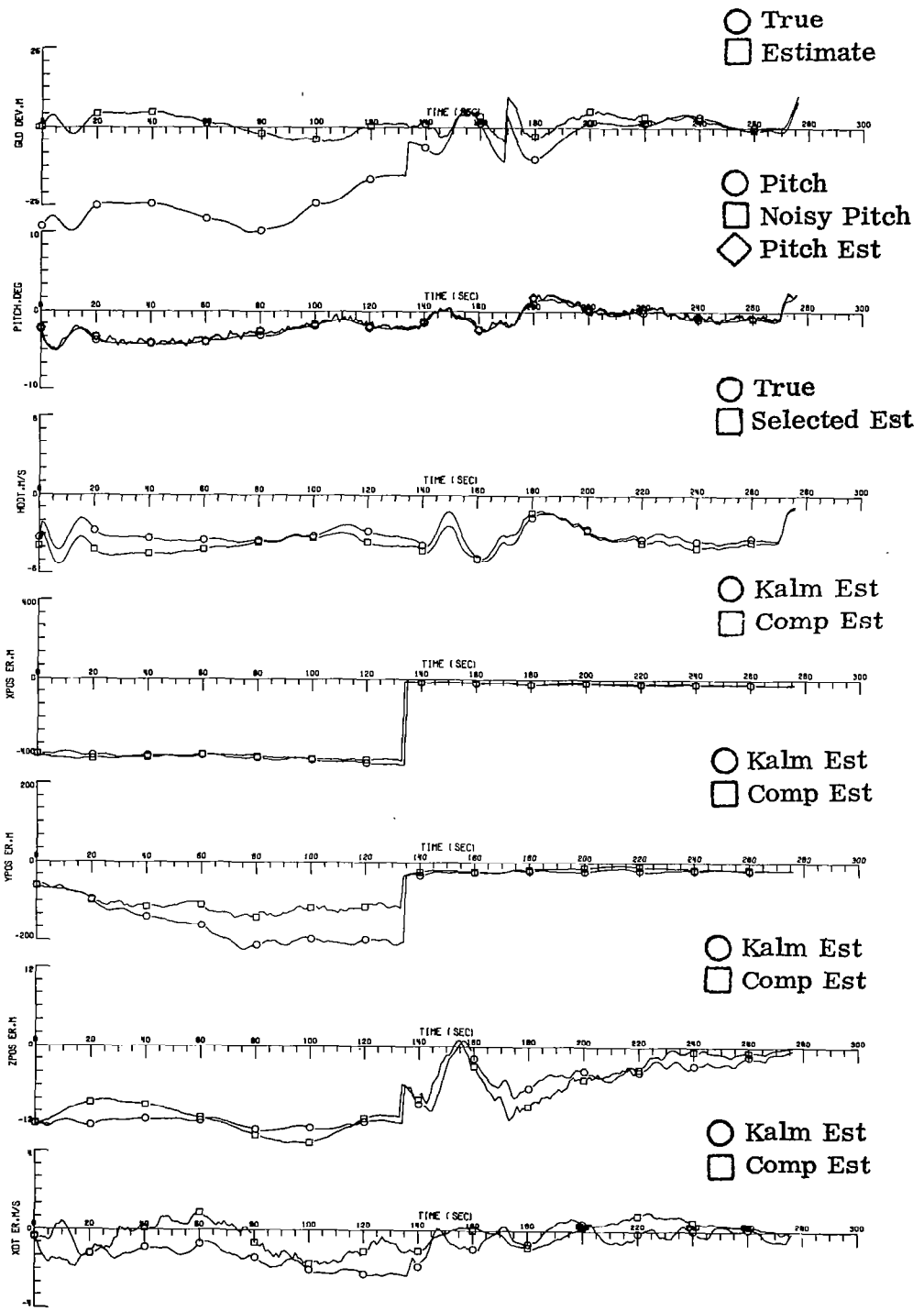
True
Estimate
TIME (SEC)
Pitch
Noisy Pitch
Pitch Est
TIME (SEC)
True
Selected Est
TIME (SEC)
Kalm Est
Comp Est
TIME (SEC)
Kalm Est
Comp Est
TIME (SEC)
Kalm Est
Comp Est
TIME (SEC)
Kalm Est
Comp Est
TIME (SEC)

Fig. 6(b) CASE 4

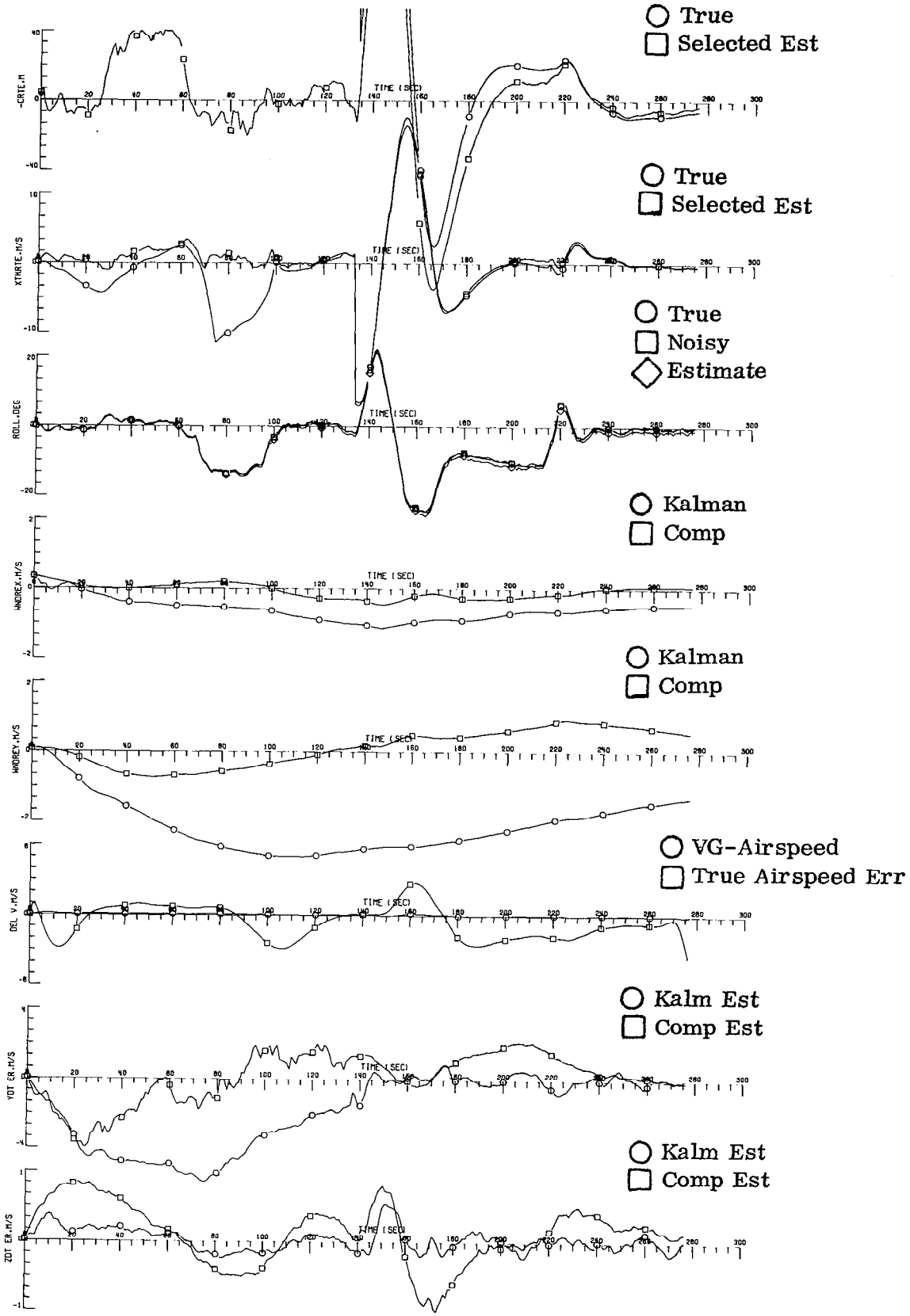
True
Selected Est
-CRTE.M
TIME (SEC)
True
Selected Est
XTRATE.M/S
TIME (SEC)
True
Noisy
Estimate
ROLL.DEG
TIME (SEC)
Kalman
Comp
WNDREX.M/S
TIME (SEC)
Kalman
Comp
WNDREY.M/S
TIME (SEC)
VG-Airspeed
True Airspeed Err
DEL V.M/S
TIME (SEC)
Kalm Est
Comp Est
YDT ER.M/S
TIME (SEC)
Kalm Est
Comp Est
ZDT ER.M/S
TIME (SEC)

Fig. 6(c) CASE 4

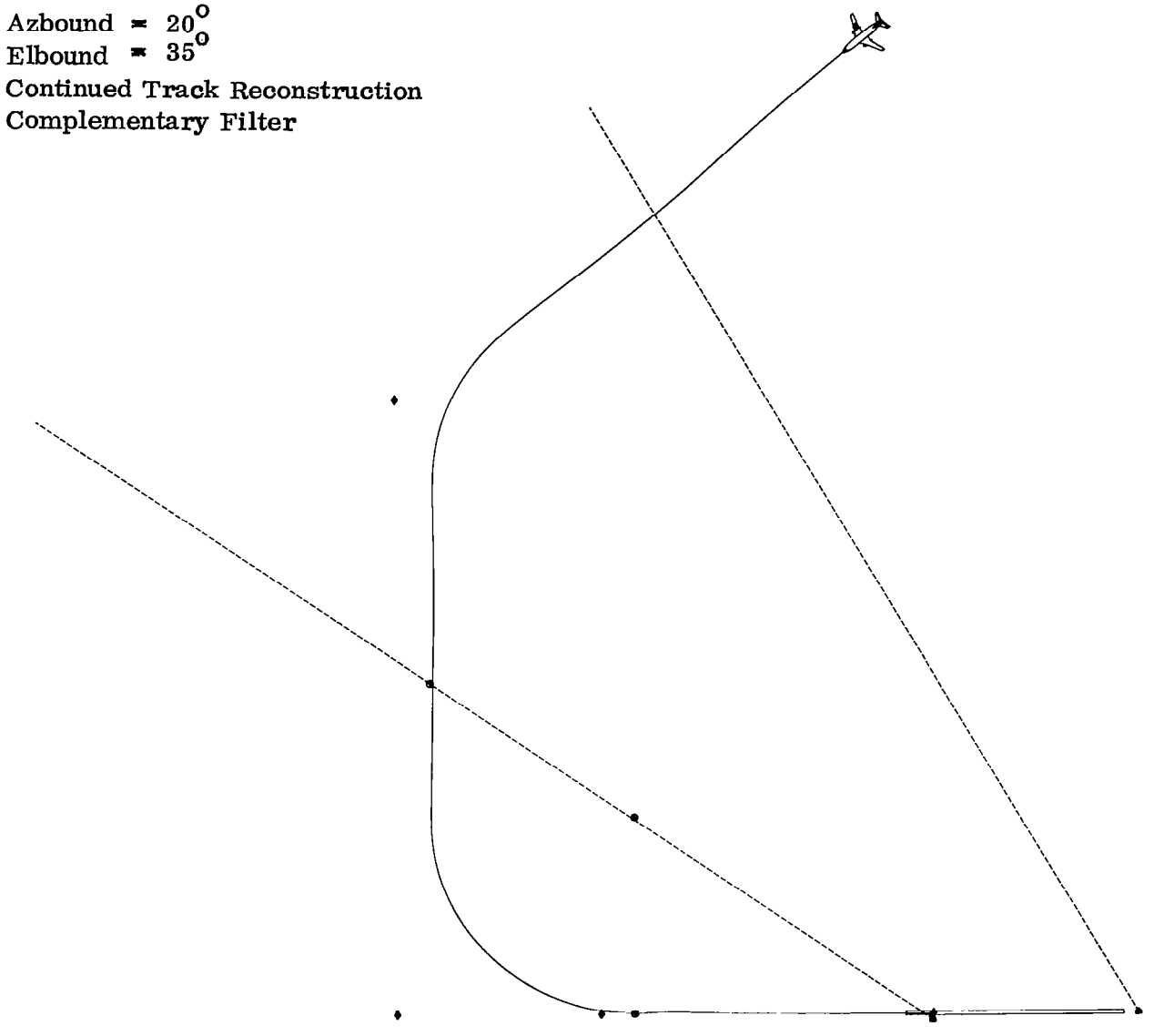
Azbound = 20°
Elbound = 35°
Continued Track Reconstruction
Complementary Filter
Final Distance = 1.80 Nautical Miles
Aircraft Ground Track

Fig. 7(a) CASE 5

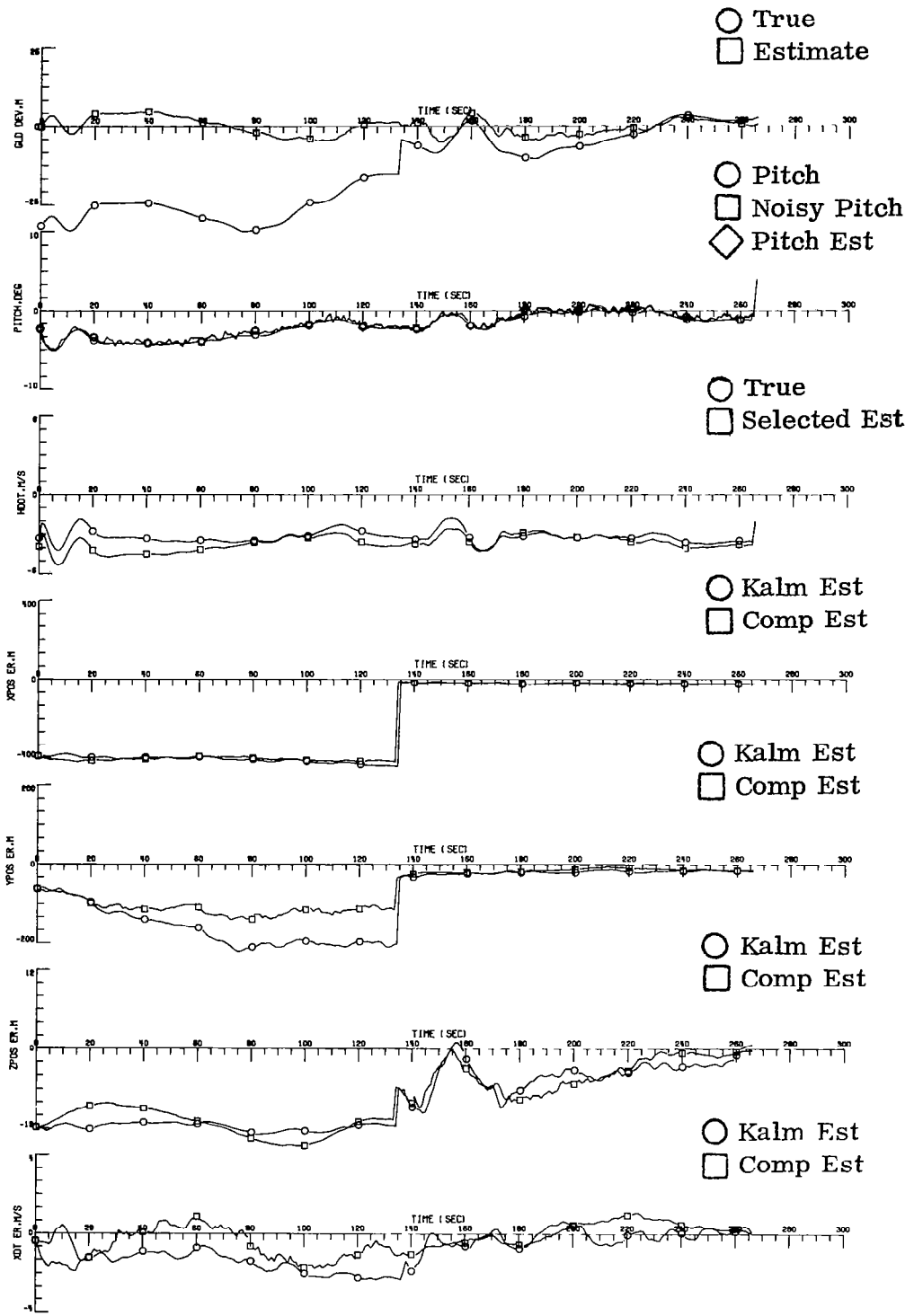
True
Estimate
GLD DEV.M
TIME (SEC)
Pitch
Noisy Pitch
Pitch Est
PITCH.DEG
TIME (SEC)
True
Selected Est
HDOT.M/S
TIME (SEC)
Kalm Est
Comp Est
XPOS ER.M
TIME (SEC)
Kalm Est
Comp Est
YPOS ER.M
TIME (SEC)
Kalm Est
Comp Est
ZPOS ER.M
TIME (SEC)
Kalm Est
Comp Est
XDT ER.M/S
TIME (SEC)

Fig. 7(b) CASE 5

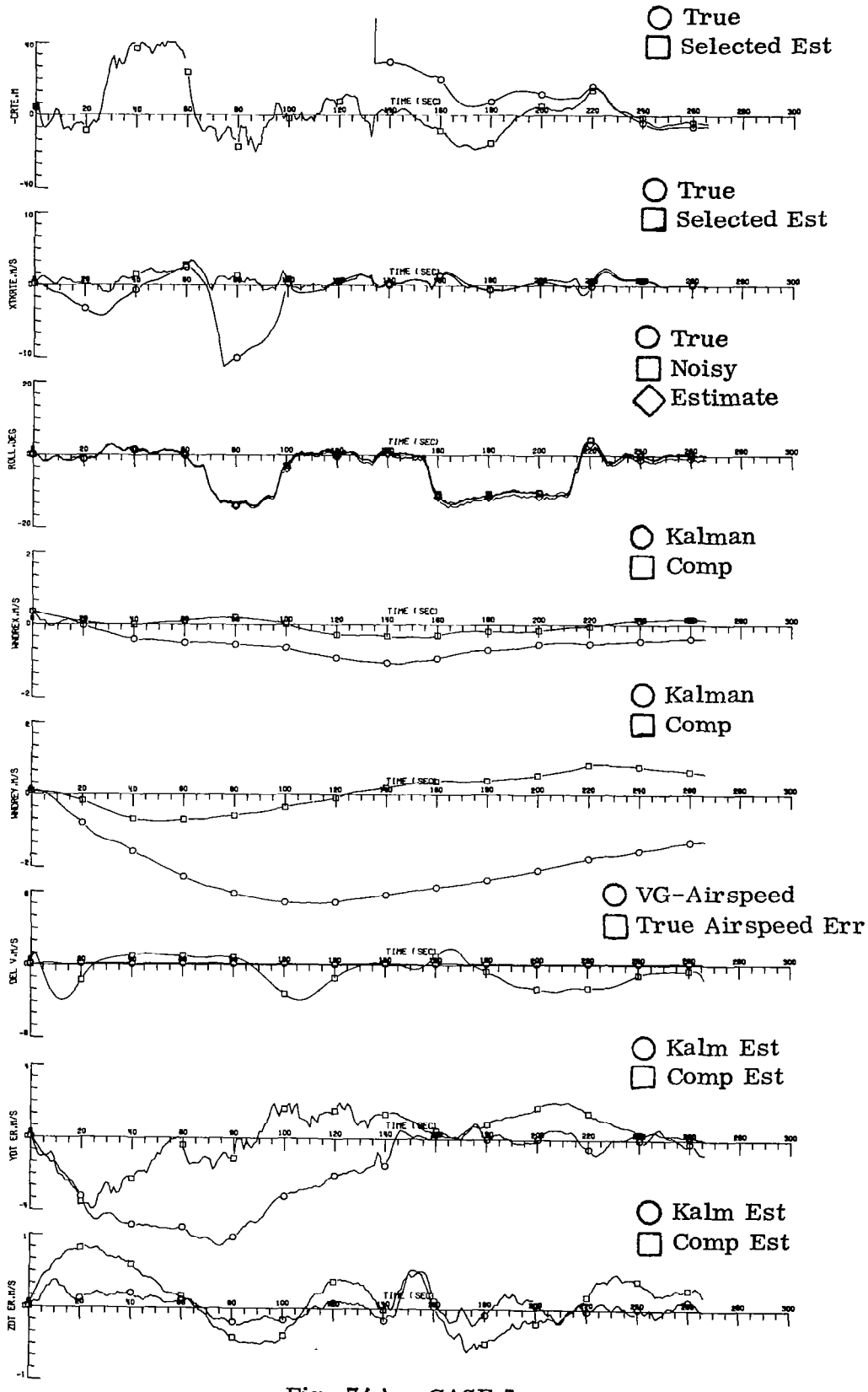
True
Selected Est
TIME (SEC)
True
Selected Est
TIME (SEC)
True
Noisy
Estimate
TIME (SEC)
Kalman
Comp
TIME (SEC)
Kalman
Comp
TIME (SEC)
VG-Airspeed
True Airspeed Err
TIME (SEC)
Kalm Est
Comp Est
TIME (SEC)
Kalm Est
Comp Est
TIME (SEC)

Fig. 7(c) CASE 5

Azbound = 70°
Elbound = 65°
Continued Track Reconstruction
Complementary Filter

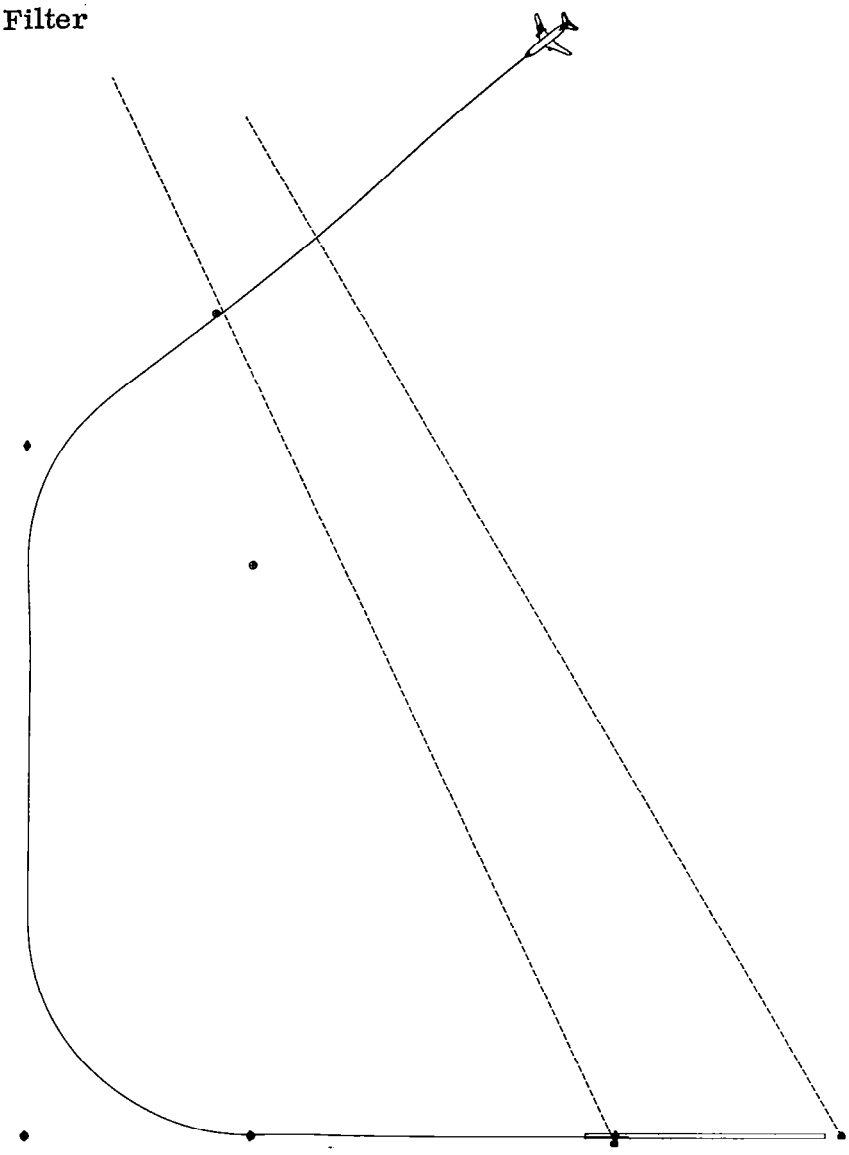

Final Distance = 2.00 Nautical Miles

Aircraft Ground Track

Fig. 8(a) CASE 6

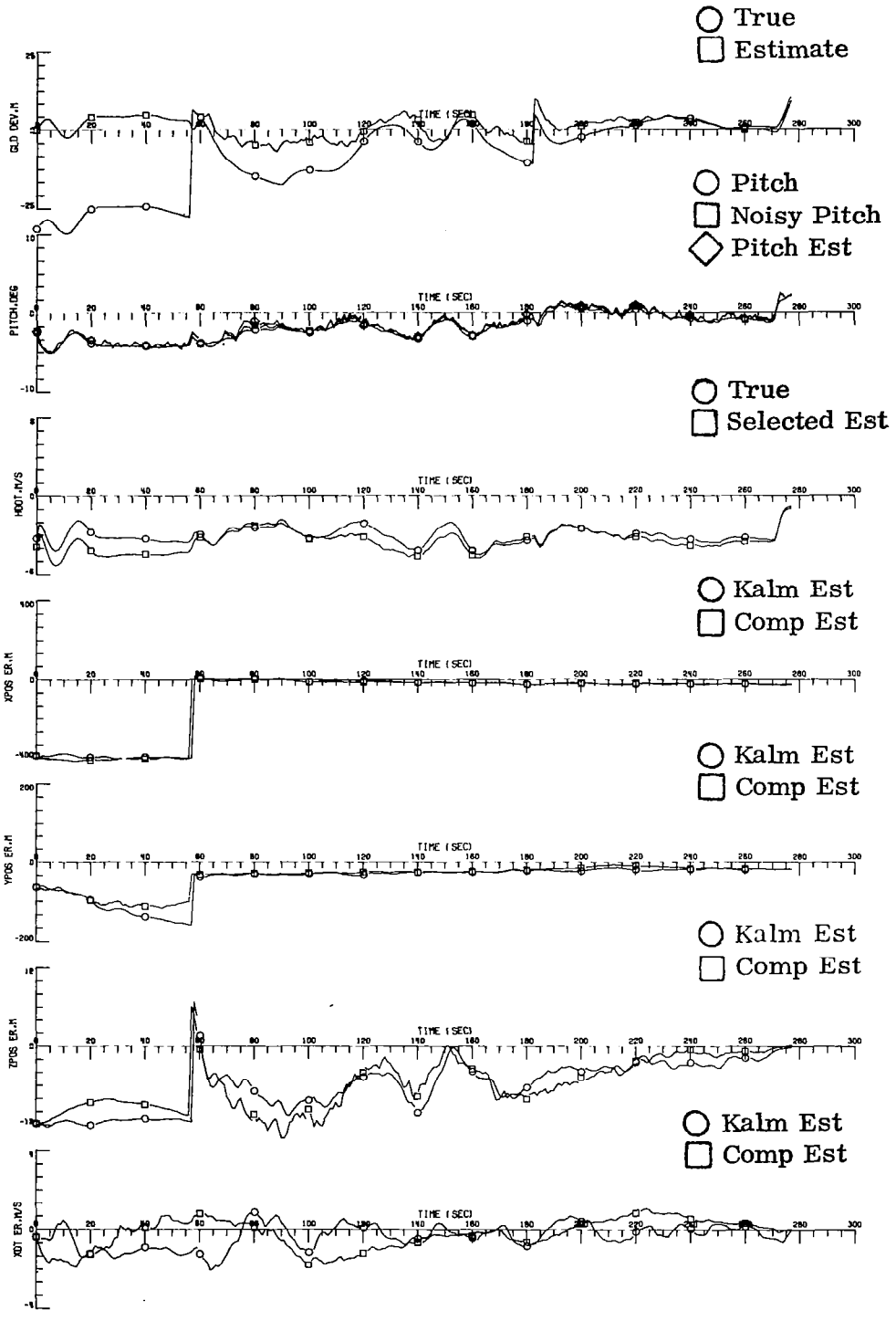
True
Estimate
GLD DEV.M
TIME (SEC)
Pitch
Noisy Pitch
Pitch Est
PITCH.DEG
TIME (SEC)
True
Selected Est
HDOT.M/S
TIME (SEC)
Kalm Est
Comp Est
XPOS ER.M
TIME (SEC)
Kalm Est
Comp Est
YPOS ER.M
TIME (SEC)
Kalm Est
Comp Est
ZPOS ER.M
TIME (SEC)
Kalm Est
Comp Est
XDT ER.M/S
TIME (SEC)

Fig. 8(b) CASE 6

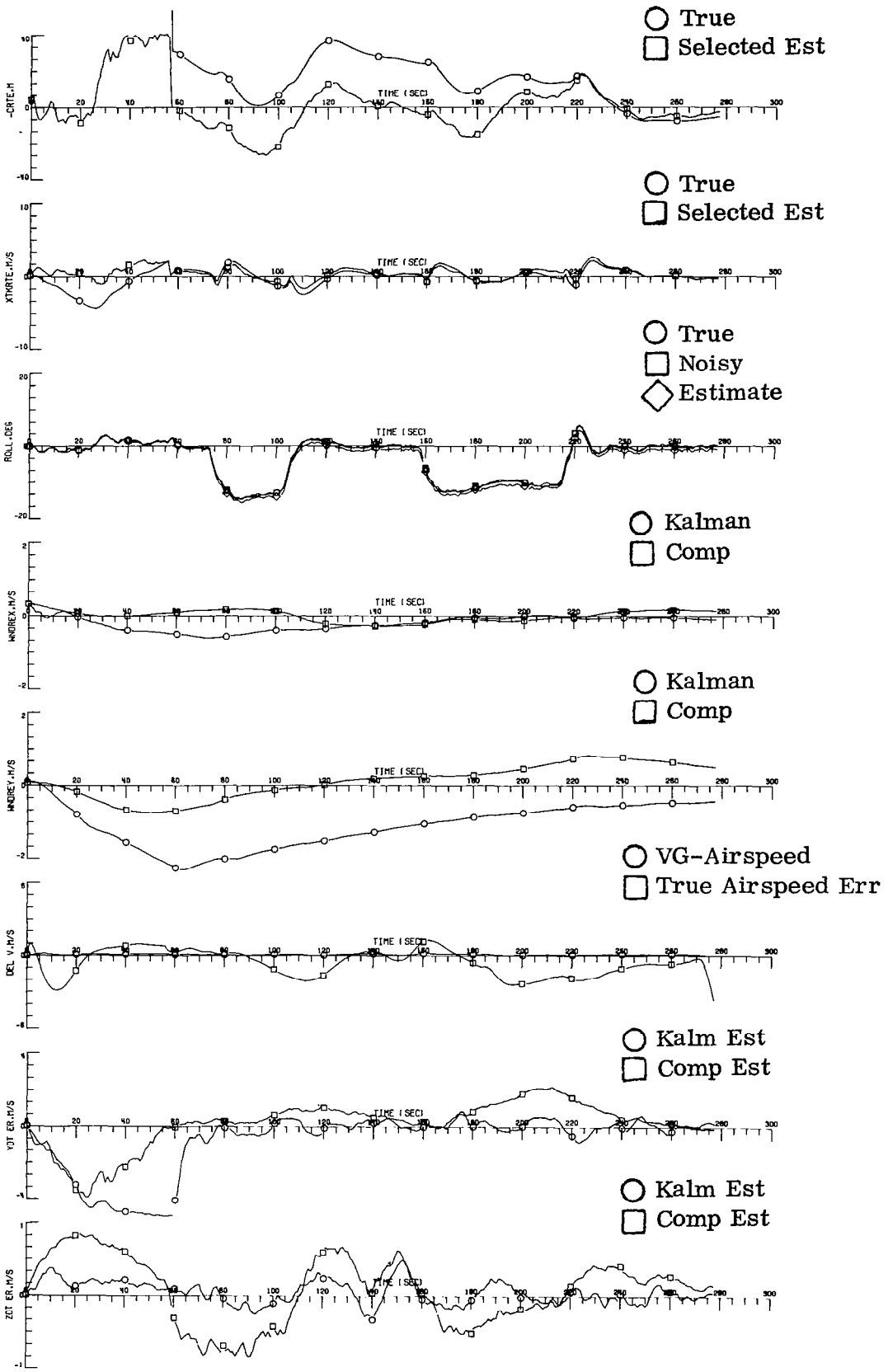
True
Selected Est
TIME (SEC)
-CRTE.M
True
Selected Est
TIME (SEC)
XTKRTE.M/S
True
Noisy
Estimate
TIME (SEC)
ROLL.DEG
Kalman
Comp
TIME (SEC)
WNDREX.M/S
Kalman
Comp
TIME (SEC)
WNDREY.M/S
VG-Airspeed
True Airspeed Err
TIME (SEC)
DEL V.M/S
Kalm Est
Comp Est
TIME (SEC)
VDT ER.M/S
Kalm Est
Comp Est
TIME (SEC)
ZDT ER.M/S

Fig. 8(c) CASE 6

Azbound = 70°
Elbound = 55°
Continued Track Reconstruction
Complementary Filter

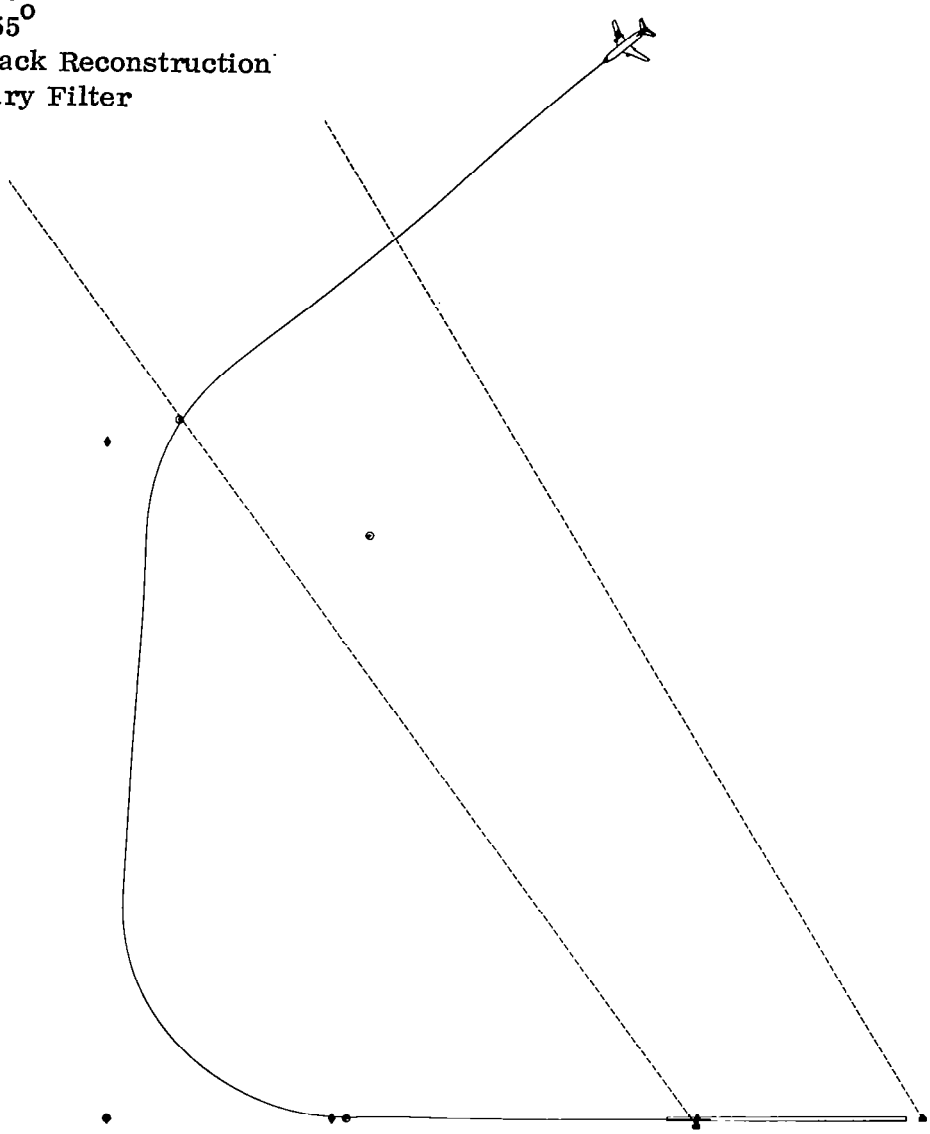

Final Distance = 1.92 Nautical Miles

Aircraft Ground Track

Fig. 9(a) CASE 7

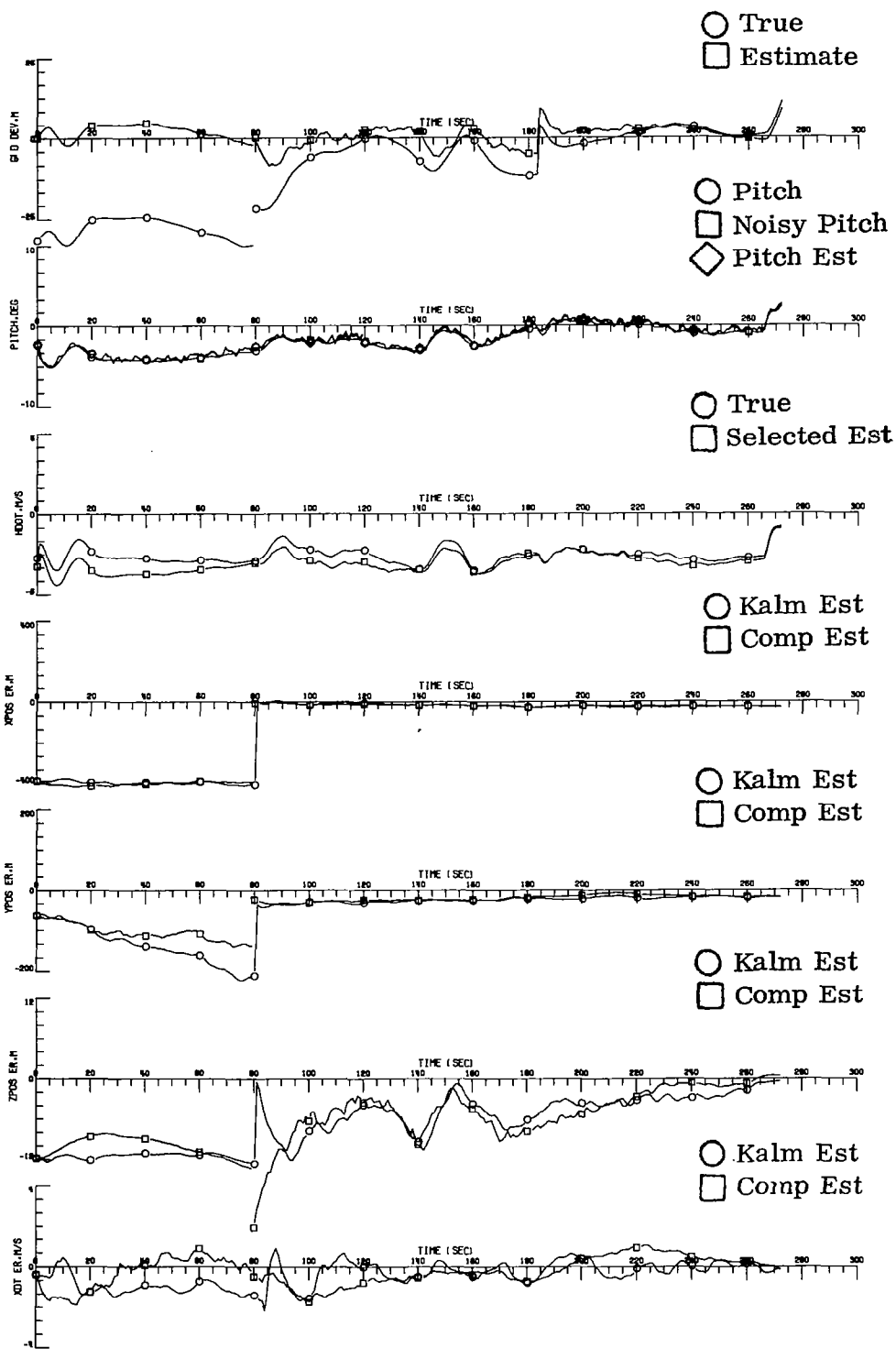
True
Estimate
Pitch
Noisy Pitch
Pitch Est
True
Selected Est
Kalm Est
Comp Est
Kalm Est
Comp Est
Kalm Est
Comp Est
Kalm Est
Comp Est
TIME (SEC)

Fig. 9(b) CASE 7

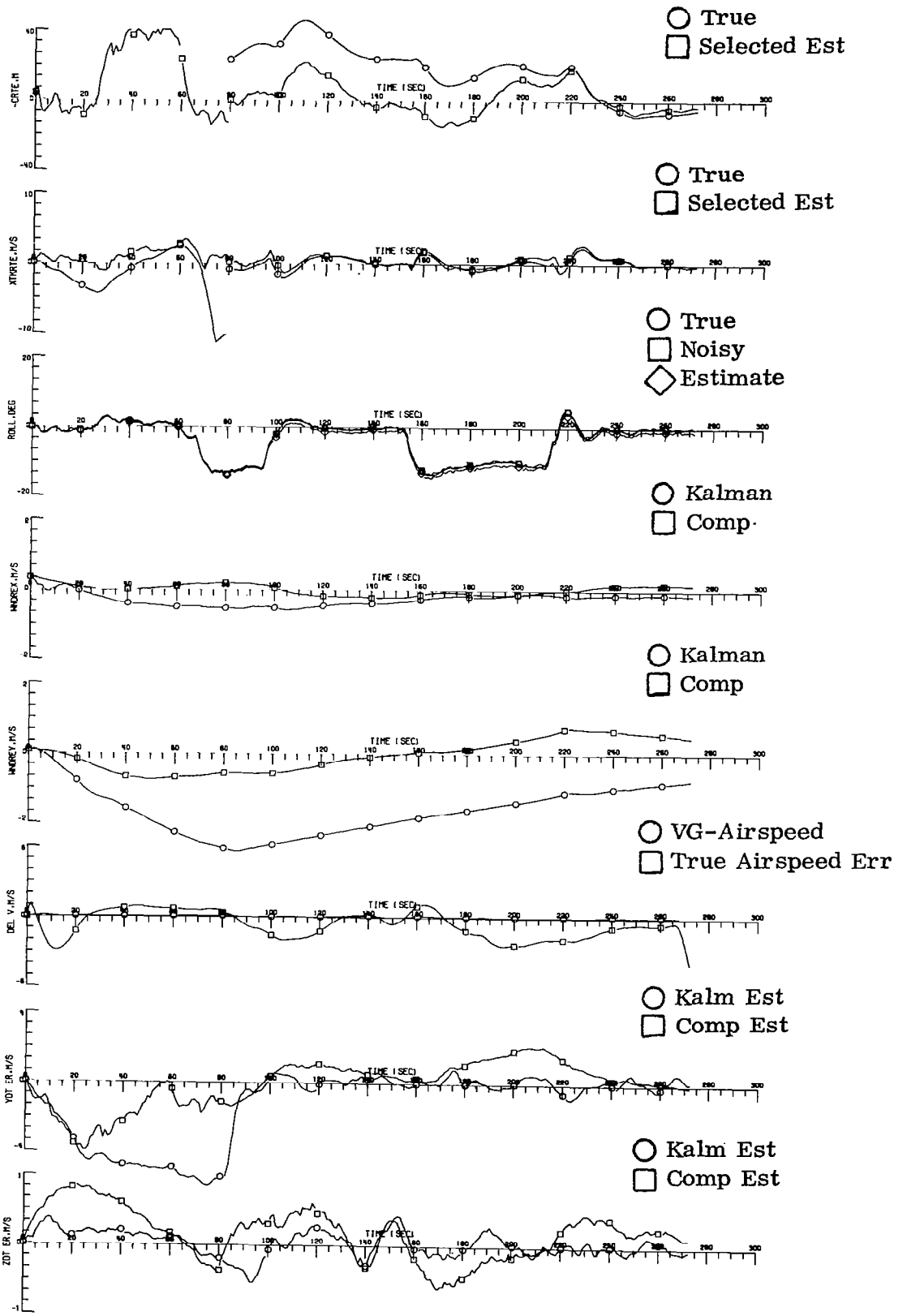
True
Selected Est
TIME (SEC)
True
Selected Est
TIME (SEC)
True
Noisy
Estimate
TIME (SEC)
Kalman
Comp
TIME (SEC)
Kalman
Comp
TIME (SEC)
VG-Airspeed
True Airspeed Err
TIME (SEC)
Kalm Est
Comp Est
TIME (SEC)
Kalm Est
Comp Est
TIME (SEC)

Fig. 9(c) CASE 7

Azbound = 70°
Elbound = 50°
Continued Track Reconstruction
Complementary Filter

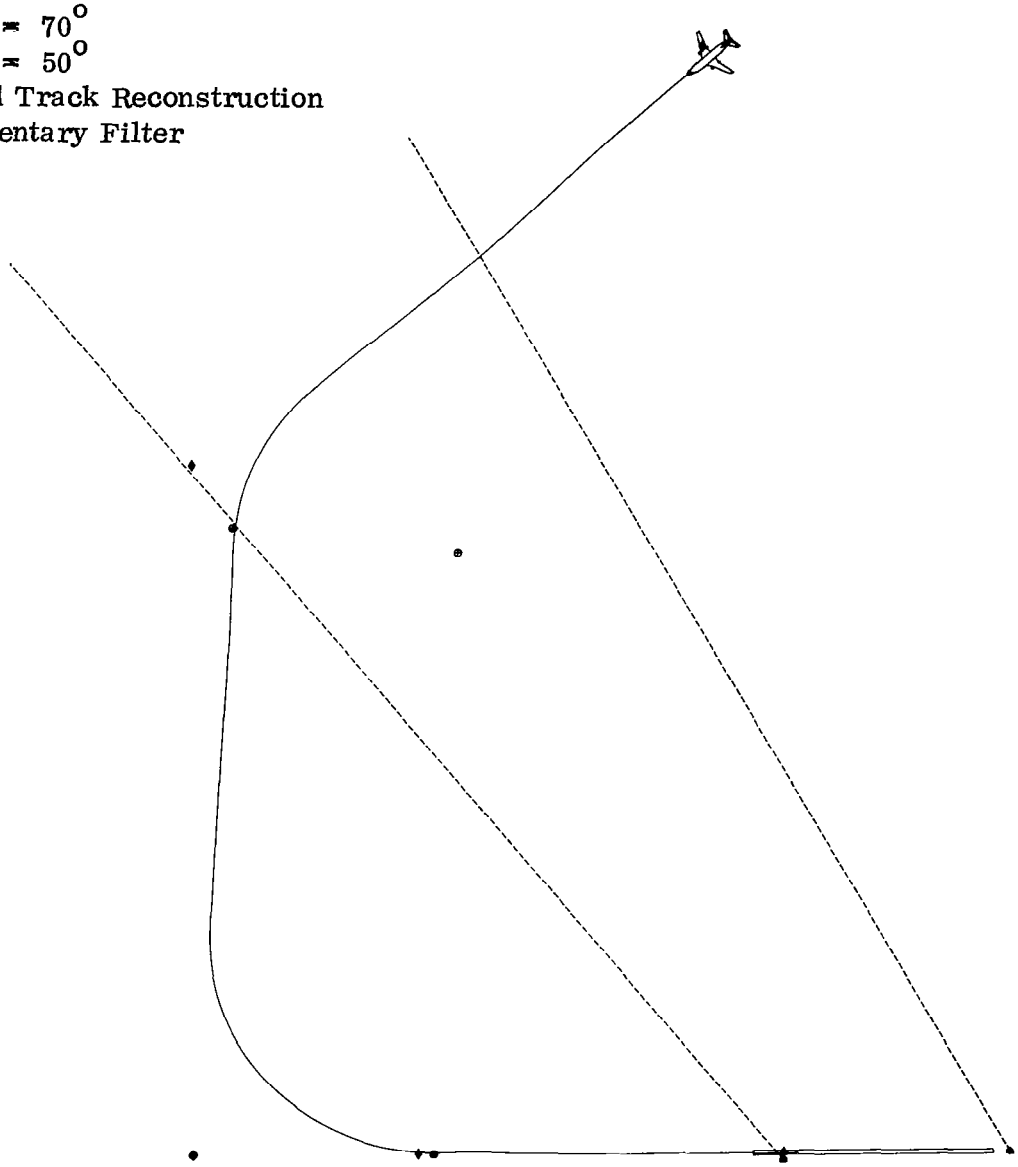

Final Distance = 1.92 Nautical Miles

Aircraft Ground Track

Fig. 10(a) CASE 8

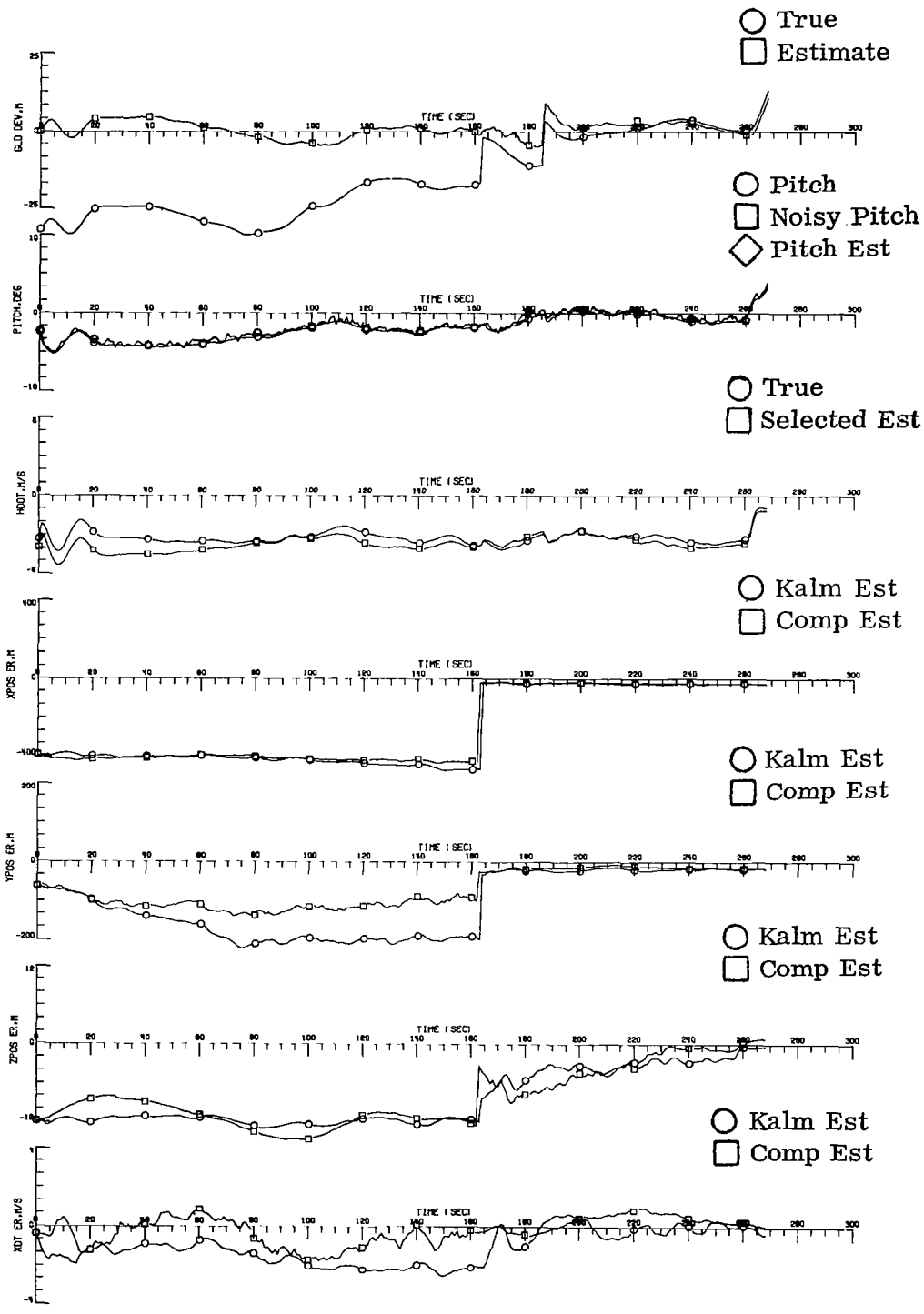

Fig. 10(b) CASE 8

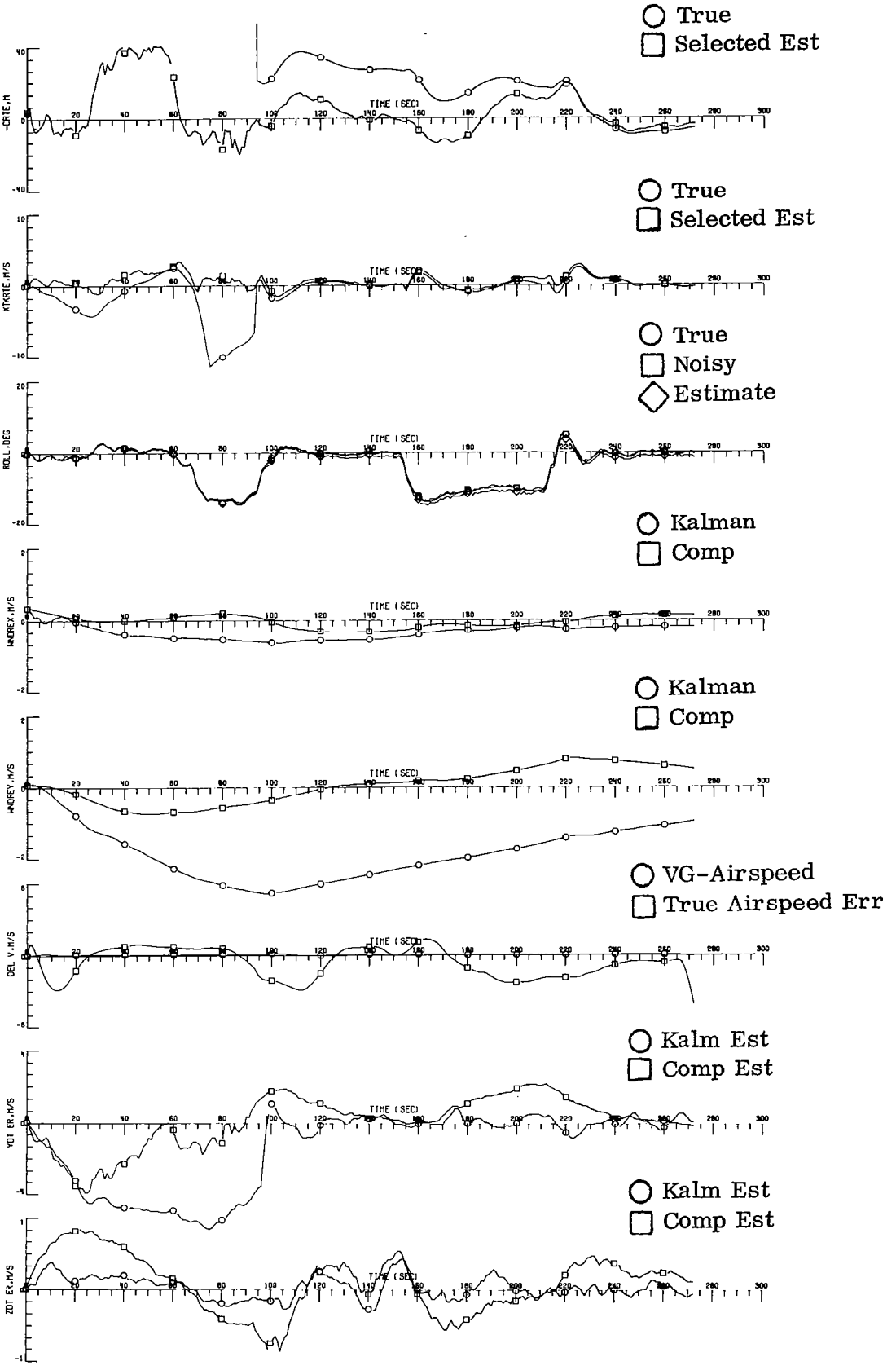

Fig. 10(c) CASE 8

Azbound = 70°
Elbound = 20°
Continued Track Reconstruction
Complementary Filter

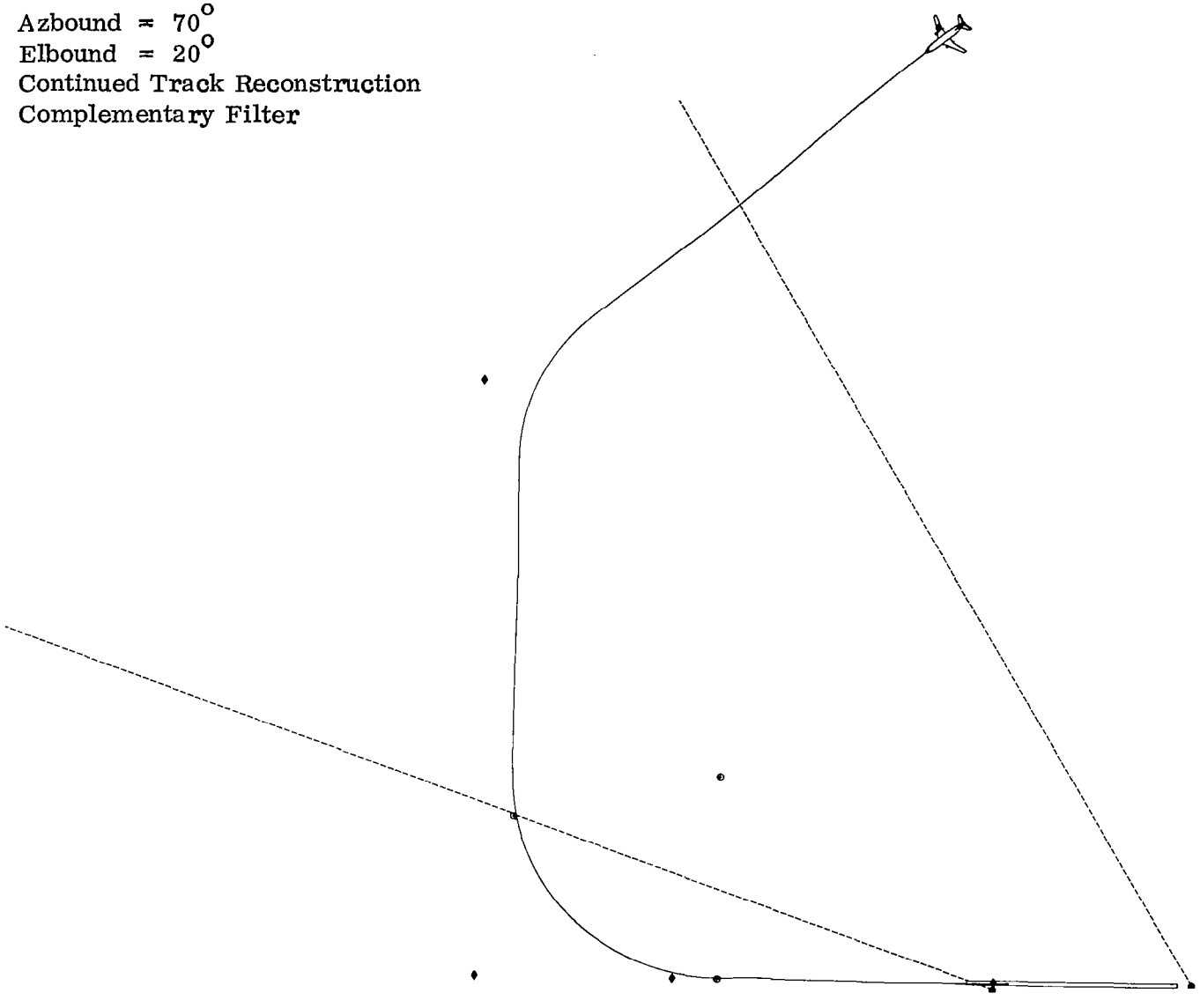

Final Distance = 1.72 Nautical Miles

Aircraft Ground Track

Fig. 11(a) CASE 9

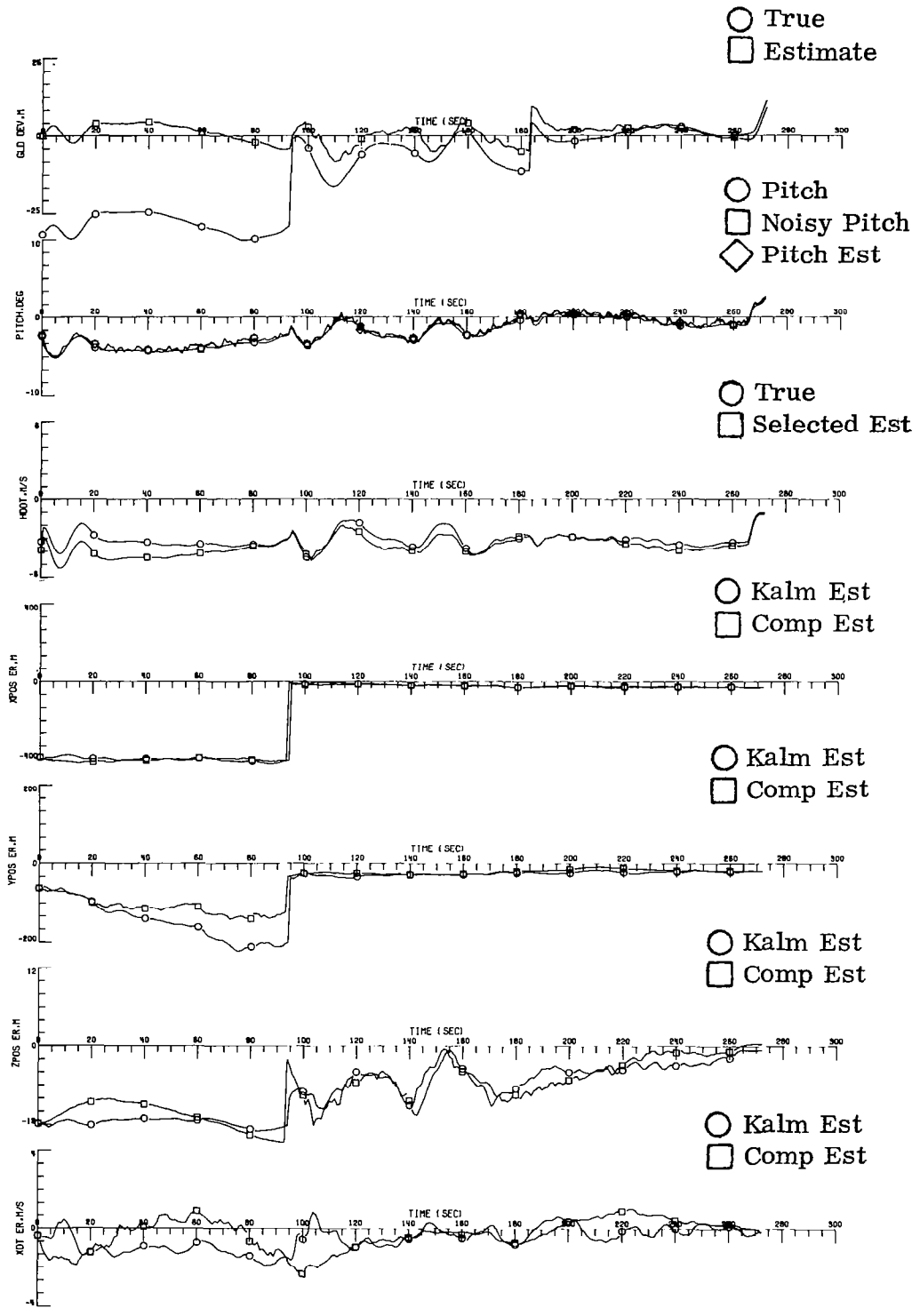

Fig. 11(b) CASE 9

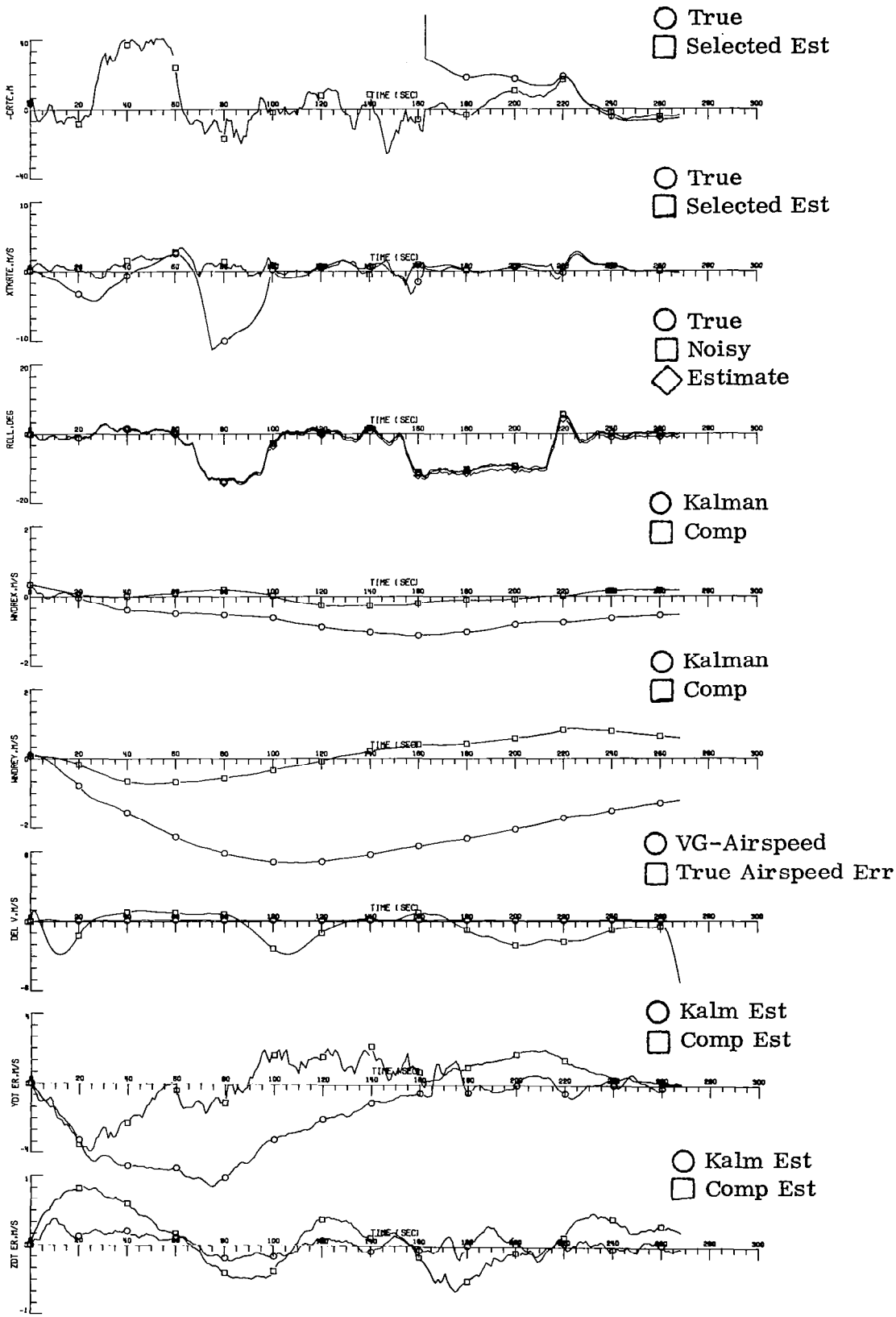

Fig. 11(c) CASE 9

Azbound = 70^{o}
Elbound = 8^{o}
Continued Track Reconstruction
Complementary Filter

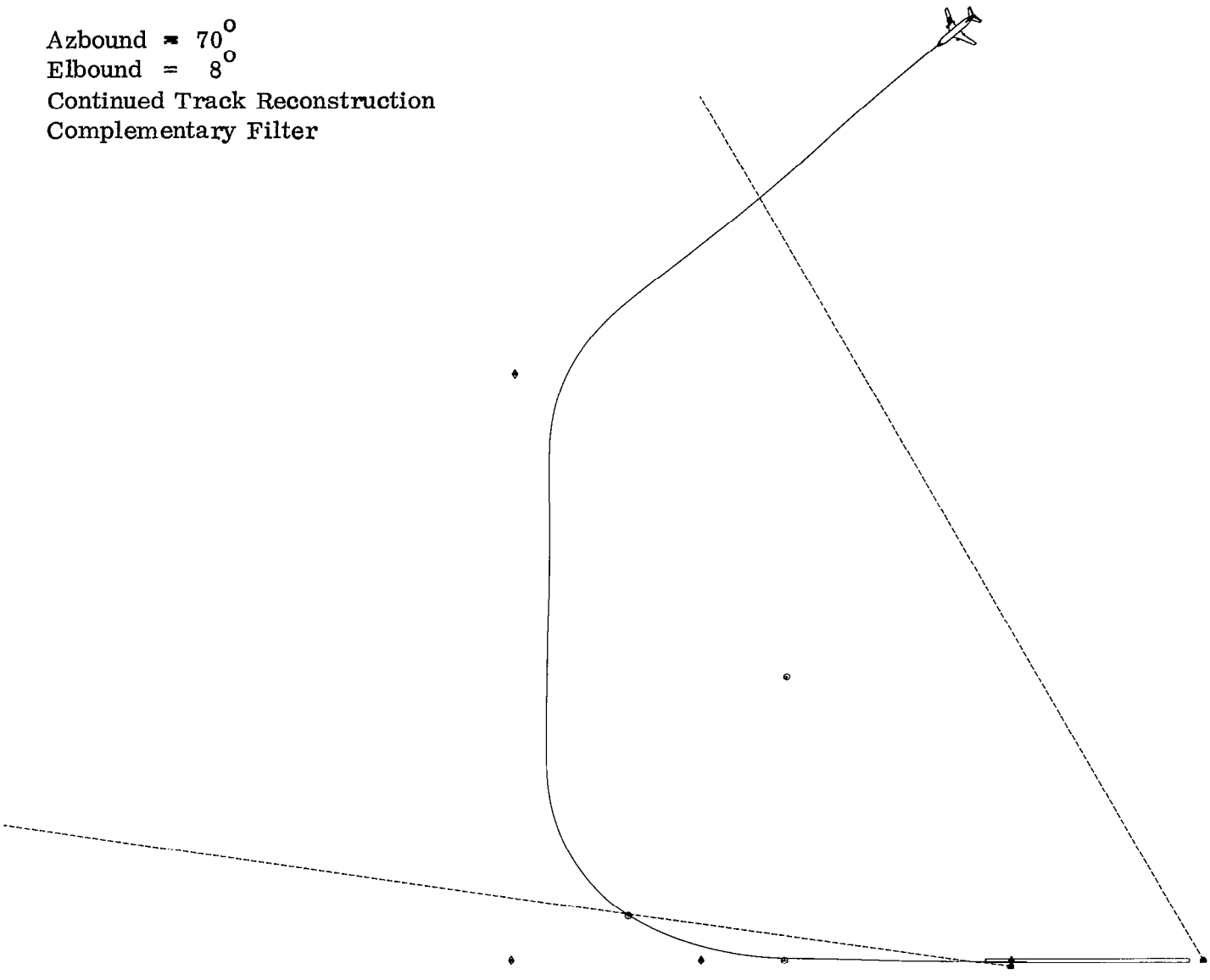

Final Distance = 1.47 Nautical Miles

Aircraft Ground Track

Fig. 12(a) CASE 10

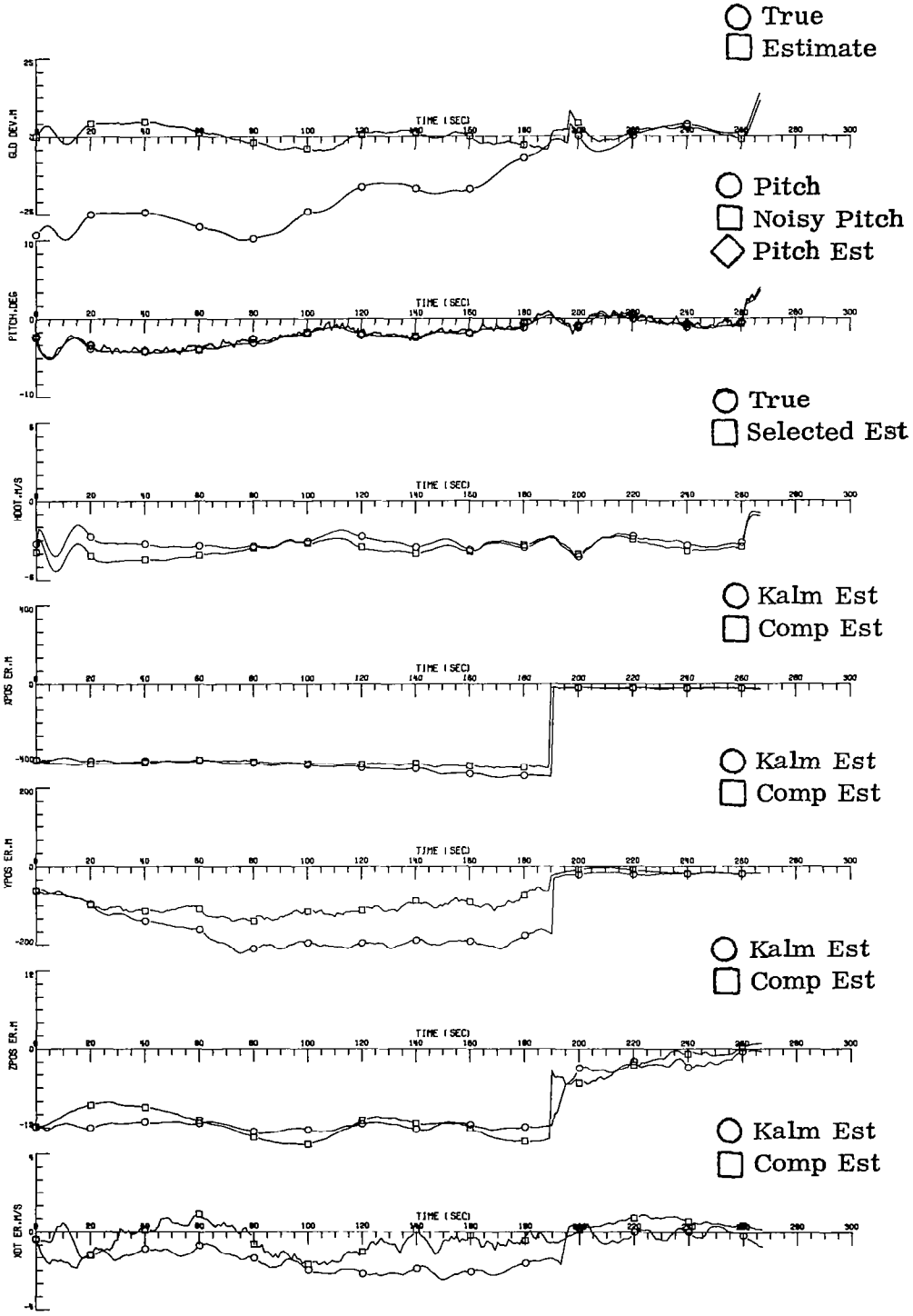

Fig. 12(b) CASE 10

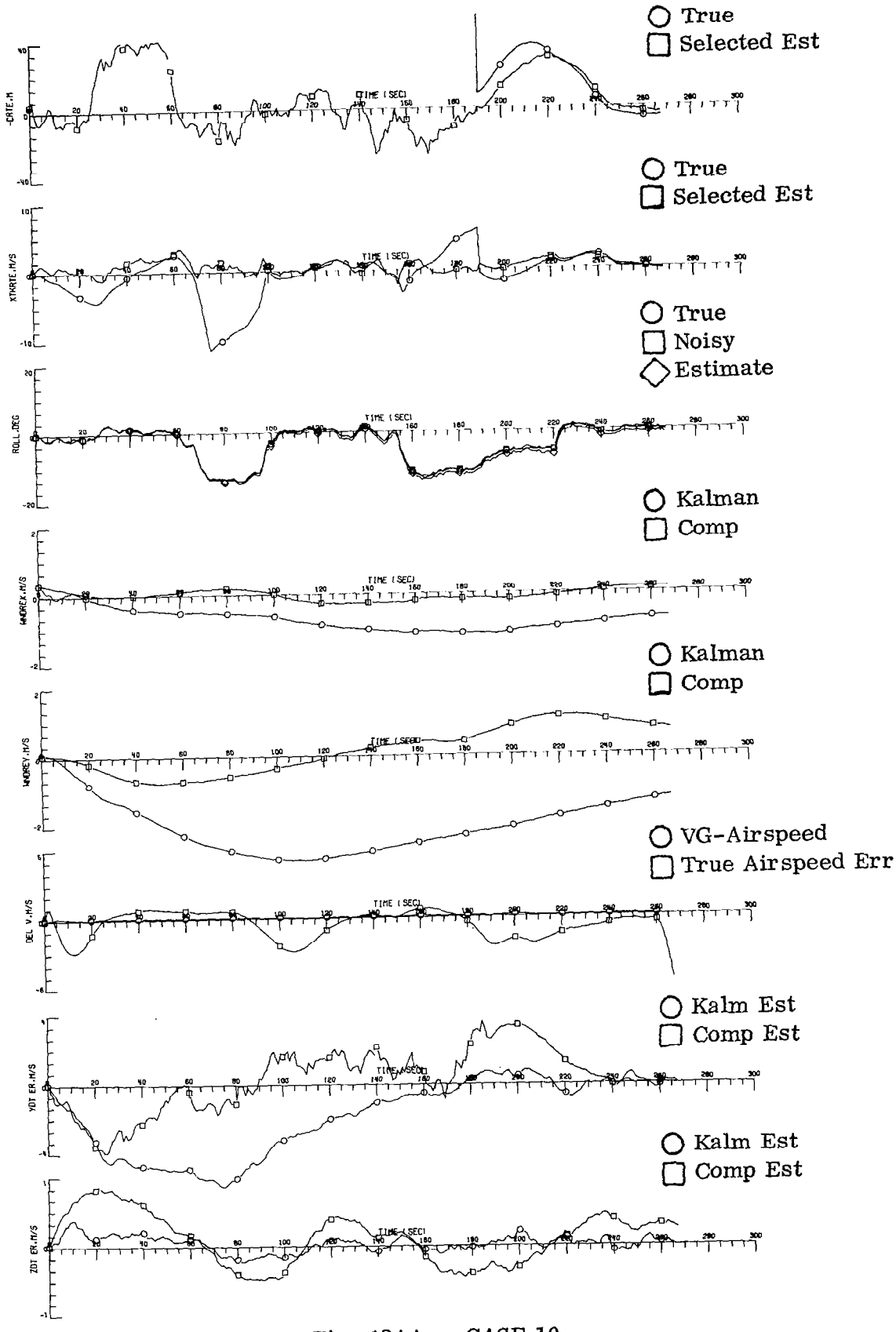

Fig. 12(c) CASE 10

TABLE III

INPUT DATA FOR WAYPOINT CONSTRUCTION

CASE 11 & 12

N = 3

I	$\lambda(I)$ DEG	$\delta(I)$ DEG	h(I) m	$v_D(I)$ m/sec	IC
1	-77.0268144	40.26663483	897.59	74.594	0
2	-77.0683161	40.23380727	452.04	69.450	1
3	-77.1453838	40.29759451	0.	64.305	0

Azbound = 70^{o}
Elbound = 80^{o}
Continued Track Reconstruction
Complementary Filter

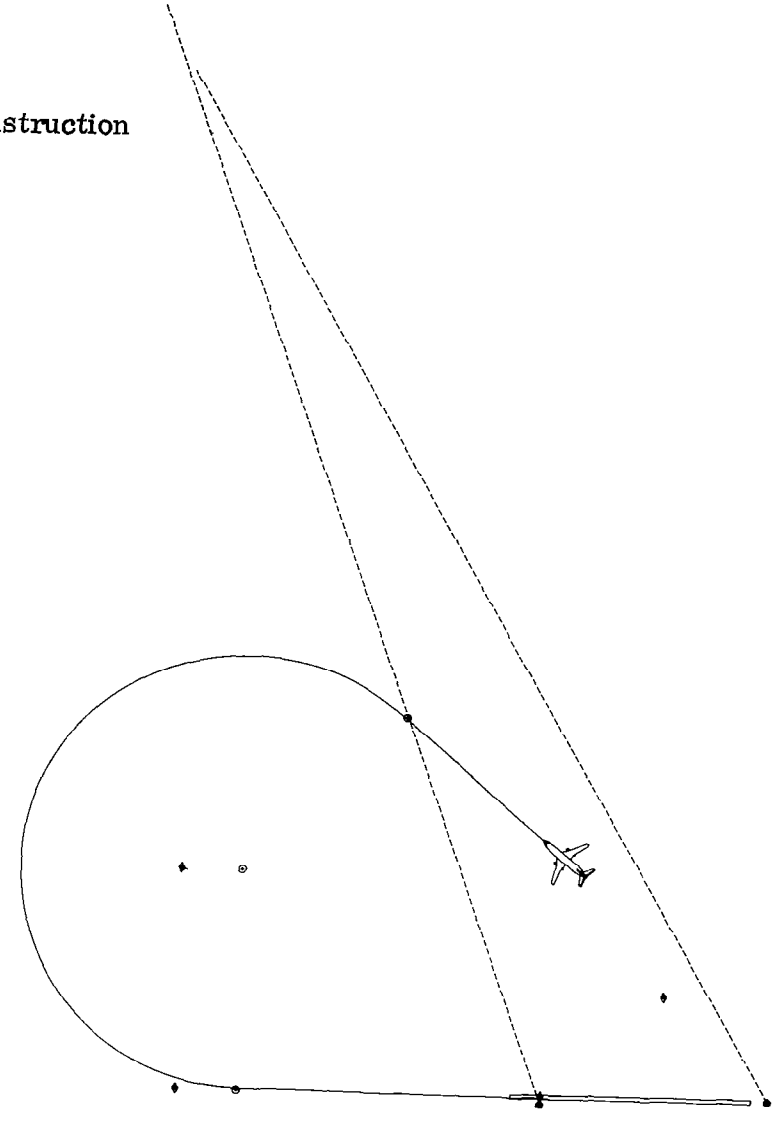

Final Distance = 1.67 Nautical Miles

Aircraft Ground Track

Fig. 13(a) CASE 11

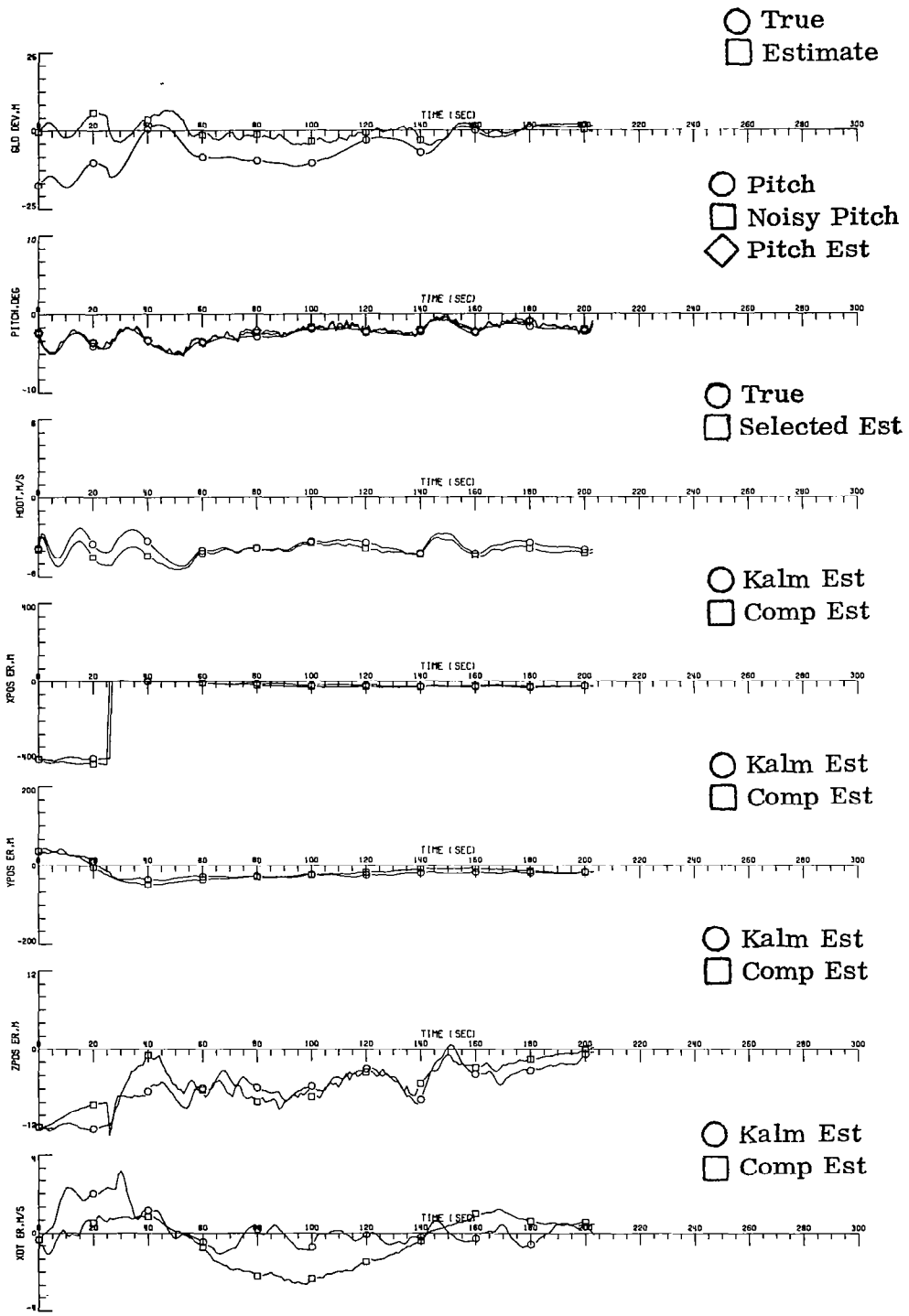

Fig. 13(b) CASE 11

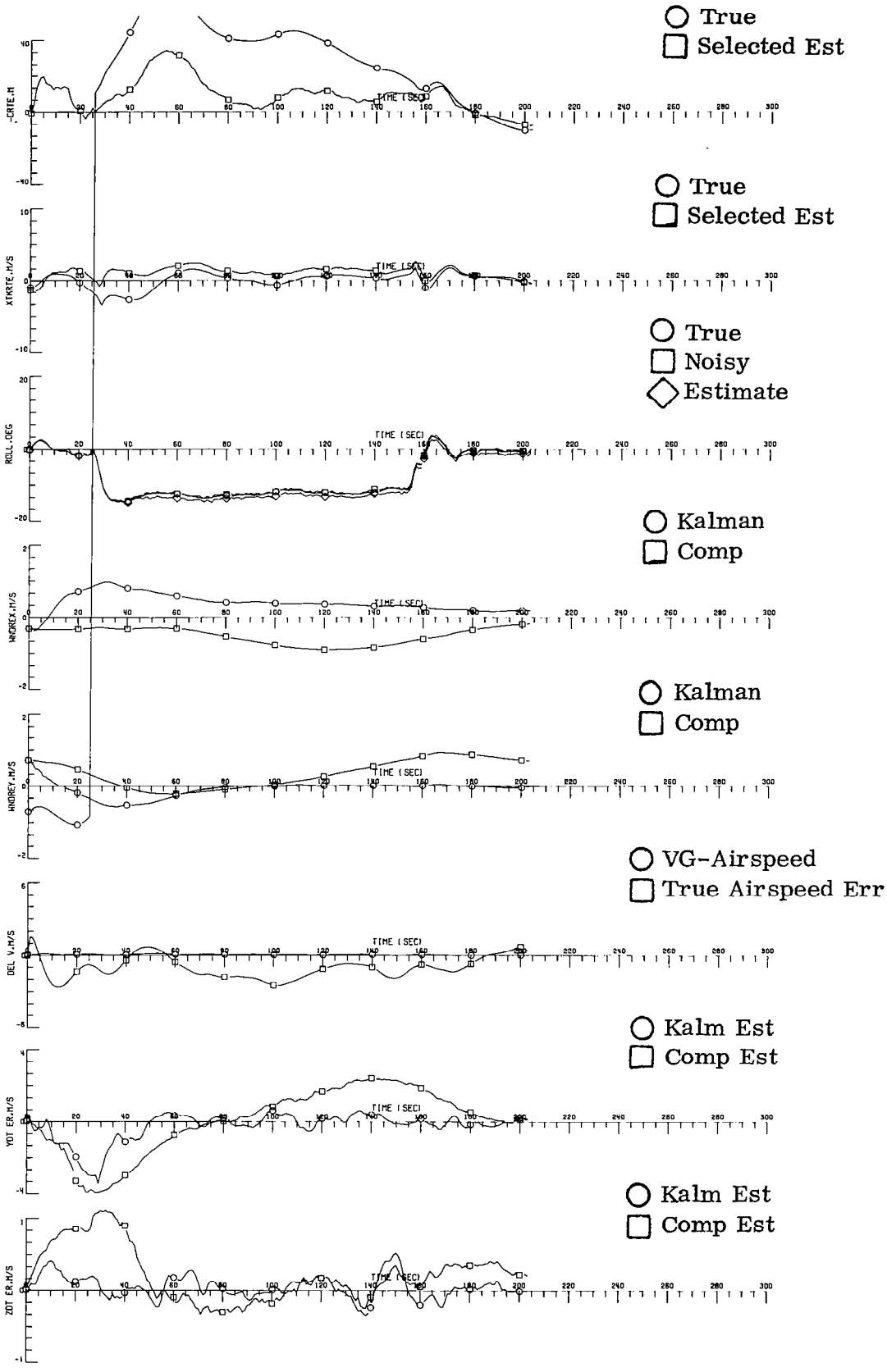

Fig. 13(c) CASE 11

Azbound = 70^{o}
Elbound = 30^{o}
Continued Track Reconstruction
Complementary Filter

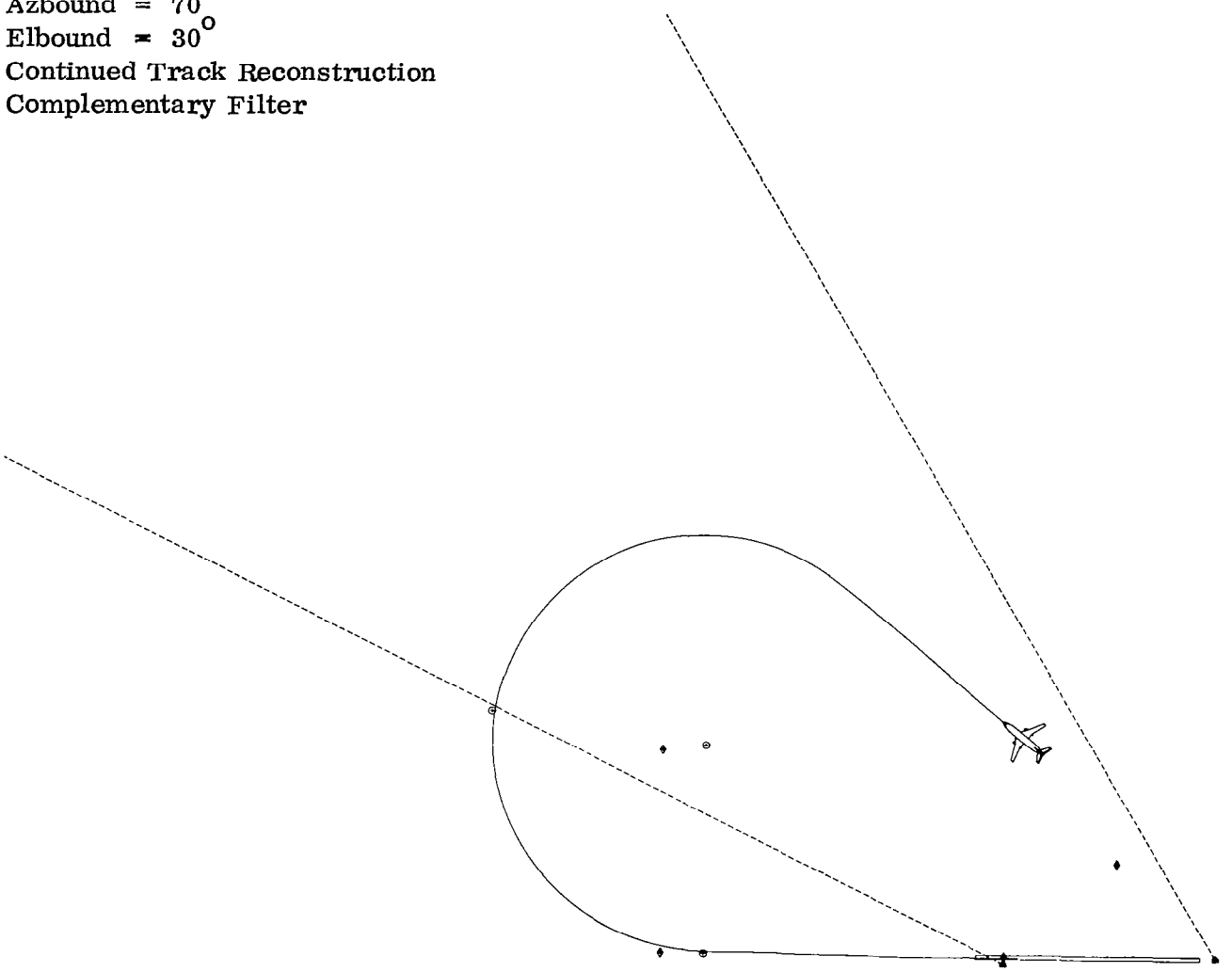

Final Distance = 1.75 Nautical Miles

Aircraft Ground Track

Fig. 14(a) CASE 12

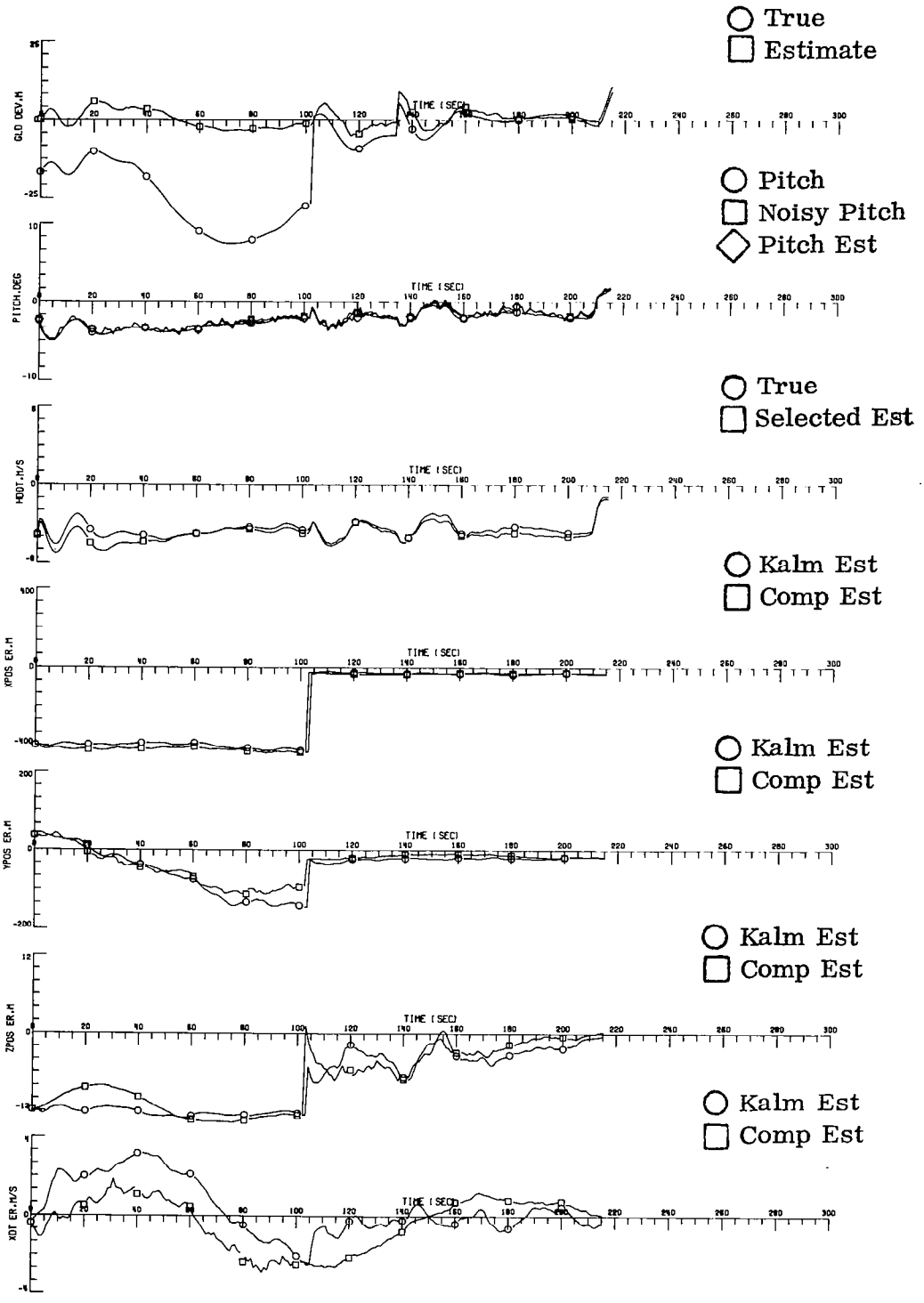

Fig. 14(b) CASE 12

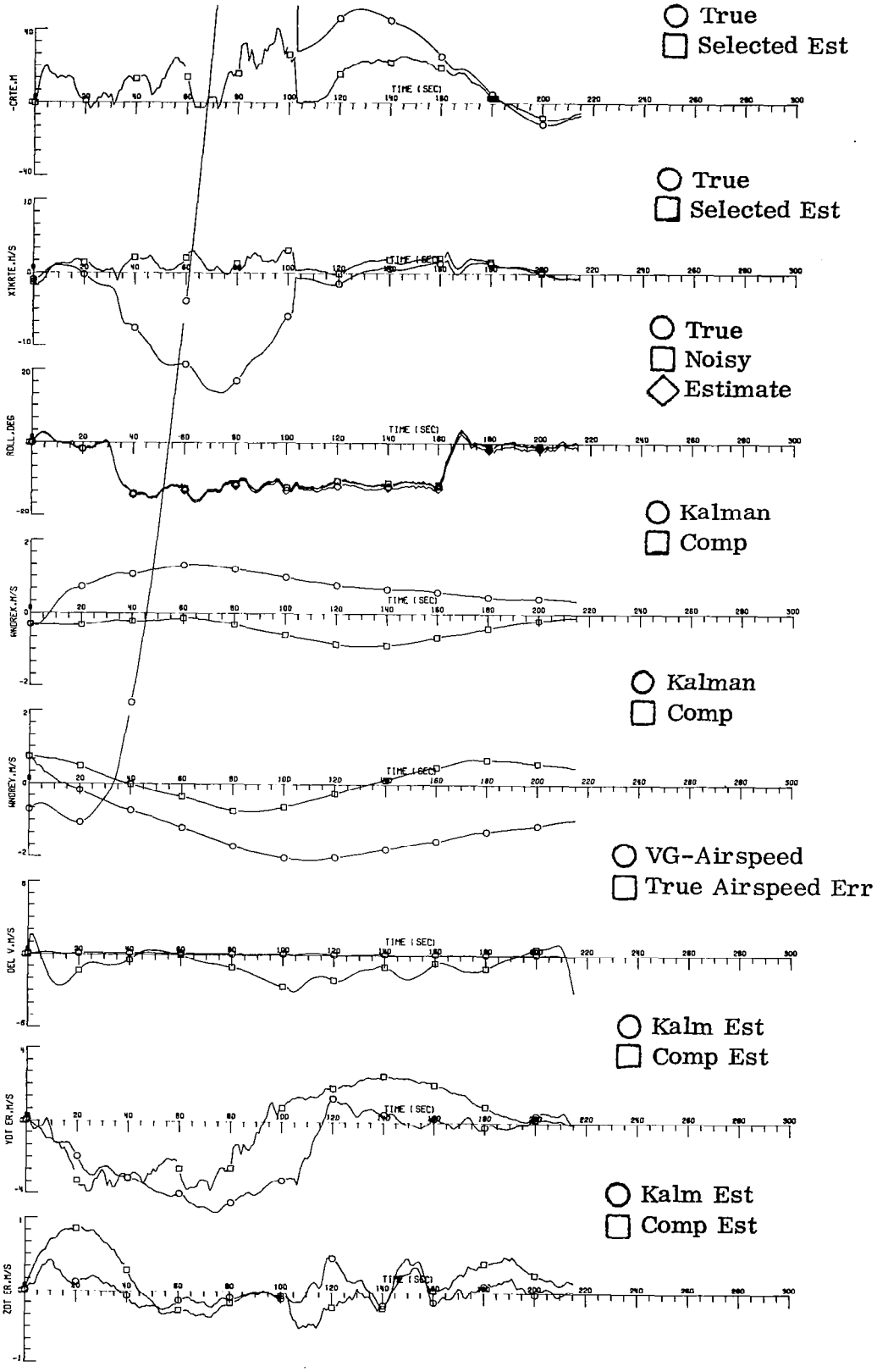

Fig. 14(c) CASE 12

APPENDIX I

Uniform Waypoint Path Construction

This appendix derives the equations for constructing a desired path, consisting of straight lines (great circles) connected by arcs of circles of a fixed radius. The resulting continuous path is located on the surface of a rotating, spherical earth. The connecting turn circles may be less than or greater than 180^{o} in arc length, and are limited only to be less than 360^{o}. The required input data consist of the latitude and longitude of a sequence of waypoints, the radius of each turn circle and the sign of the turn, the desired altitude and airspeed at each waypoint, an integer code designating whether each waypoint is regular waypoint, or the center of the turn, an integer variable indicating whether the initial point is the start of a straight line segment or on a turn, and the integer total number of waypoints. Given N waypoints there are only N-2 turns.

A. Initial Data

Let N be the number of waypoints (N must be at least three). At each waypoint we must supply the following:

For I = 1, N

λ (I) = longitude in degrees

δ (I) = latitude in degrees

h (I) = height above the sphere in meters (2.1)

v_D(I) = desired airspeed in meters/sec

IC (I) = 0 if waypoint is regular

1 if waypoint is center of turn

For I = 1, N-2

R_T(I) = radius of turn

SNDP (I) = sign of turn (2.2)

1 for clockwise, -1 for counter clockwise

For the first waypoint

ITURN = 0 means the initialization starts on a straight line segment (2.3)

ITURN = 1 means the initialization starts in a turn. This is used only on reconstruction, if the update is to take place on a turn.

B. Vector Representation of Each Waypoint

The vector representation of each waypoint is in the earth fixed system. Converting the angle data into radians, the waypoint unit vectors are given by

$$\text{For I} = 1, \text{N}$$

$$\hat{WR}(I) = \begin{Bmatrix} \sin \delta (I) \\ -\cos \delta (I) \sin \lambda (I) \\ \cos \delta (I) \cos \lambda (I) \end{Bmatrix} \tag{2.4}$$

C. The Unit Normal Vectors

Between each consecutive pair of waypoints construct a plane. If IC (I) = 0 and IC (I+1) = 0, then the plane is the plane containing the two vectors, and the unit normal to that plane is given by

$$\hat{WN}(I) = \frac{\hat{WR}(I) \times \hat{WR}(I+1)}{\left|\hat{WR}(I) \times \hat{WR}(I+1)\right|} \tag{2.5}$$

If IC (I) = 0, and IC (I+1) = 1, then we are going from a normal point to a circle, and we construct the plane which contains the first waypoint and is tangent to turn circle of the given radius, R_T. Since there are two tangent planes from a point to a circle, the sign of the turn removes the ambiguity. In a manner simular to Eq. (2.5) we first form the plane from the regular waypoint to the center of the turn. The unit normal to that plane is given by

$$\hat{XN} = \frac{\hat{WR}(I) \times \hat{WR}(I+1)}{\left|\hat{WR}(I) \times \hat{WR}(I+1)\right|} \tag{2.6}$$

To obtain the unit normal to the plane tangent to the turn, we must rotate the unit normal, $\hat{XN}$, about the waypoint vector $\hat{WN}$ (I) through the angle, A, formed by the plane between $\hat{WR}$ (I) and $\hat{WR}$ (I+1), and the plane between $\hat{WR}$ (I) and the tangent waypoint at the circle, $\hat{PI}$ (2I - 1), (see Fig. I1).

To obtain the angle A, we have from spherical trigonometry

$$\sin \beta = \hat{WR}(I) \times \hat{WR}(I+1) \tag{2.7a}$$

$$\cos \beta = \hat{WR}(I) \cdot \hat{WR}(I+1) \tag{2.7b}$$

$$\sin \alpha = \sin (R_T(I) / r_E \tag{2.7c}$$

$$\cos \alpha = \sqrt{1 - \sin^2 \alpha}$$

If ITURN = 1, and we are in the turn, then $\hat{WR}$ (I) is $\hat{PI}$ (2I-1), and we set

$$\begin{aligned} \sin \beta &= \sin \alpha \\ \cos \beta &= \cos \alpha \\ \cos A &= 0 \\ \sin A &= 1 \end{aligned} \tag{2.7d}$$

Otherwise we have

$$\begin{aligned} \sin A &= \sin \alpha / \cos \beta \\ \cos A &= \sqrt{1 - \sin^2 A} \end{aligned} \tag{2.7e}$$

The desired equation for $\hat{WN}$ (I) is given by

$$\hat{WN}(I) = \cos A \, \hat{XN} + \sin A \, \text{sign} (\Delta\psi (I)) \, \hat{WR}(I) \times \hat{XN} \tag{2.8}$$

If IC (I) = 1 and IC (I+1) = 0, then we require the plane containing the outgoing tangent point, PI (2I) and WR (I+1). Again we form the plane

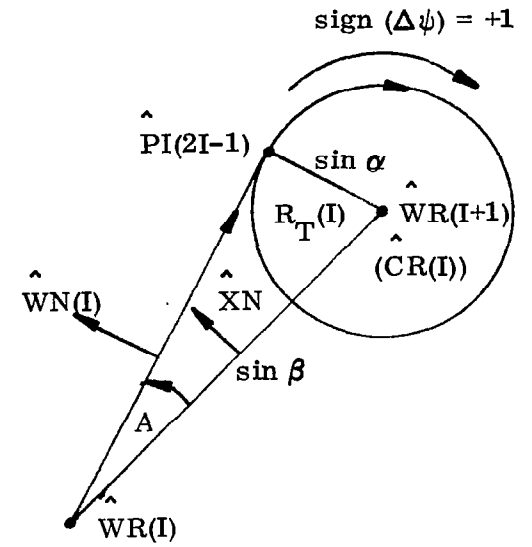

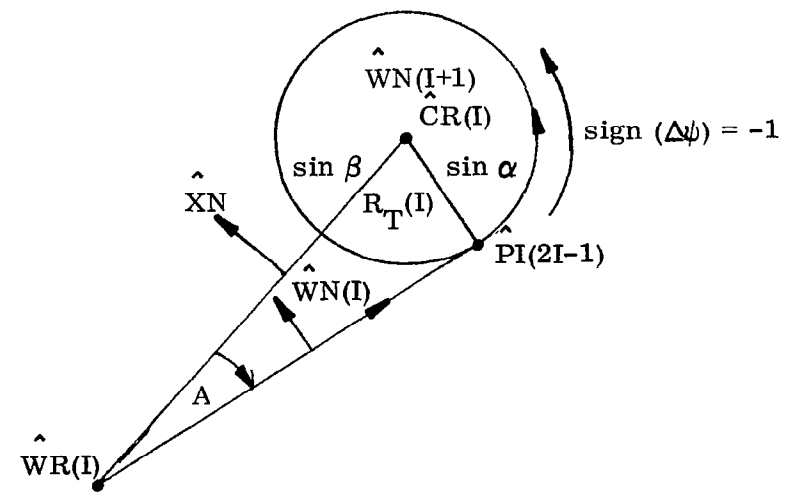

UNIT NORMAL IC(I) = 0, IC(I+1) = 1

Figure I1

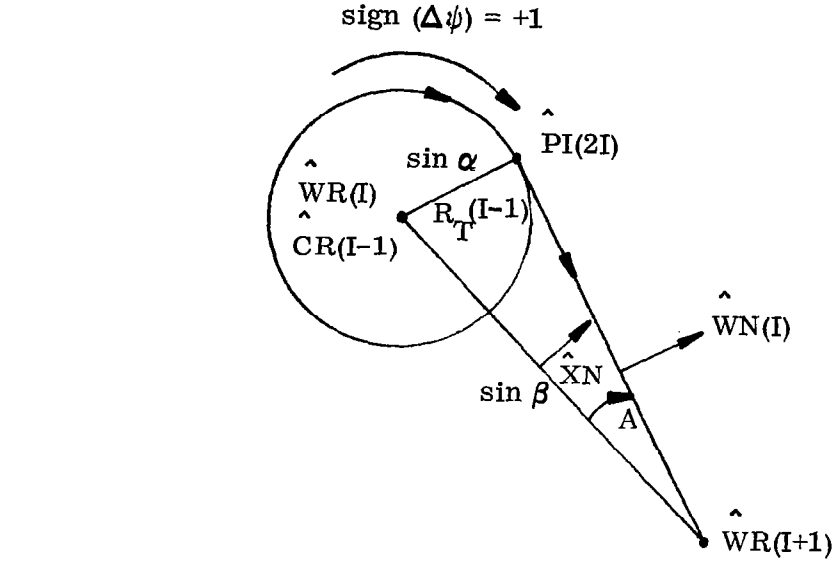

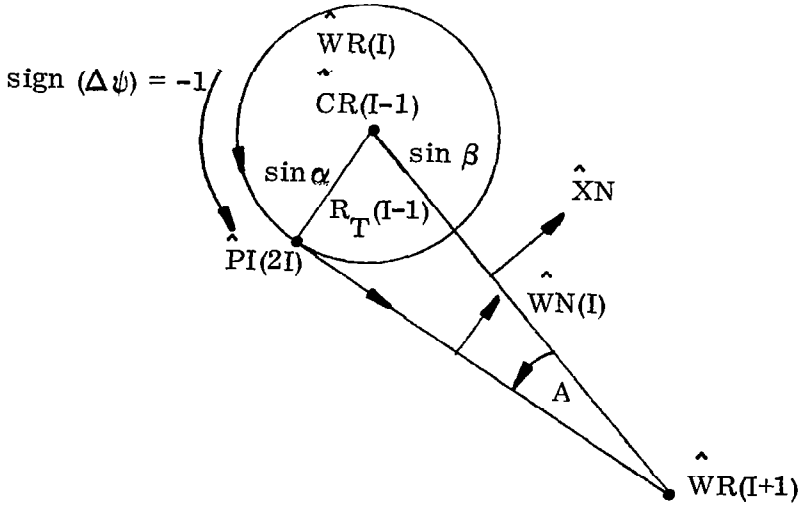

UNIT NORMAL IC(I) = 1, IC(I+1) = 0

Figure I2

containing $\hat{WR}$ (I) and $\hat{WR}$ (I+1), construct the unit normal $\hat{XN}$ and rotate $\hat{XN}$ about $\hat{WR}$ (I+1), through the negative of the angle A. (See Fig. I2).

For this case we retain Eq. (2.6), Eq.'s (2.7a) and (2.7b). However,

$$\sin \alpha = \sin (R_T (I-1)/r_E) \tag{2.9a}$$

$$\cos \alpha = \sqrt{1 - \sin^2 \alpha} \tag{2.9b}$$

$$\sin A = - \frac{\sin \alpha}{\cos \beta} \tag{2.9c}$$

$$\cos A = \sqrt{1 - \sin^2 A} \tag{2.9d}$$

and the desired unit normal is given by

$$\hat{WN} (I) = \cos A \, \hat{XN} + \sin A \, \text{sign} (\Delta\psi (I-1)) \, \hat{WR} (I+1) \times \hat{XN} \tag{2.10}$$

The reason for using R_T (I-1), and $\Delta\psi$ (I-1) is that we are on the outgoing leg and the turn circle we refer to is behind us not ahead.

One more precaution is required. In the event N is 3 and we have chosen to construct a path starting in the turn, then we are no longer free to choose a radius because the outgoing unit normal must be parallel to the runway unit normal. Consequently, if IC (I) = 1, and IC (I+1) = 0, and N = 3, we are compelled to compute the outgoing normal to be parallel to the runway normal and we must compute the radius of the turn to be consistent with this outgoing unit normal.

For this case, if IC (I) = 1 and IC (N) = 0, the unit normal to the runway is given by

$$\hat{WN} = \cos \psi_R \, \hat{N} - \sin \psi_R \, \hat{WR} (N) \times \hat{N} \tag{2.11}$$

where

$$\hat{N} = \begin{Bmatrix} \cos \delta (N) \\ \sin \delta (N) \sin \lambda (N) \\ -\sin \delta (N) \cos \lambda (N) \end{Bmatrix} \tag{2.11a}$$

and ψ_R is the runway azimuth in radians

If IC (I) = 1 and IC (I+1) = 1, then the required path must be a great circle tangent to two circles. To obtain the unit normal to this common plane we require $R_T(I)$, R_T (I+1), $\hat{WR}$ (I) , $\hat{WR}$ (I+1), sign ($\Delta\psi$ (I)) and sign ($\Delta\psi$(I+1). The unit normal is given by

$$\hat{WN}\ (I) = a_1\ \hat{WR}\ (I+1) + a_2\ \hat{WR}\ (I) + a_3\ \hat{WR}\ (I) \times \hat{WR}\ (I+1) \qquad (2.12)$$

where

$$\begin{aligned} a_1 &= (\cos\beta \sin\alpha_1 - \sin\alpha_2) / \sin^2\beta \\ a_2 &= (\cos\beta \sin\alpha_2 - \sin\alpha_1) / \sin^2\beta \\ a_3 &= (\cos\alpha_1 \cos\alpha_2 \sin\gamma) / \sin^2\beta \end{aligned} \qquad (2.12a)$$

$$\begin{aligned} \sin\beta &= \hat{WR}\ (I) \times \hat{WR}\ (I+1) \\ \cos\beta &= (1 - \sin^2\beta)^{\frac{1}{2}} \end{aligned} \qquad (2.12b)$$

$$\begin{aligned} \sin\alpha_1 &= \sin (R_T(I) / r_E) \\ \sin\alpha_2 &= \sin (R_T(I+1) / r_E) \\ \sin\gamma &= \left|\hat{PI}\ (2I) \times \hat{PI}\ (2I+1)\right| \\ \cos\gamma &= (\cos\beta - \sin\alpha_1 \sin\alpha_2) / (\cos\alpha_1 \cos\alpha_2) \\ \sin\gamma &= (1 - \cos^2\gamma)^{\frac{1}{2}} \end{aligned} \qquad (2.12c)$$

See Fig. (I3).

This exhausts all the possible unit normals for any pair of consecutive way points.

D. Center of Turn Unit Vector

The unit vector to the center of turn is defined in one of two ways. Either , the center is itself a waypoint, or else it may be computed given the incoming and outgoing unit normals, $\hat{WN}$ (I), and $\hat{WN}$ (I+1), the radius of the turn, R_T (I), and the sign of the turn, sign ($\Delta\psi$ (I)).

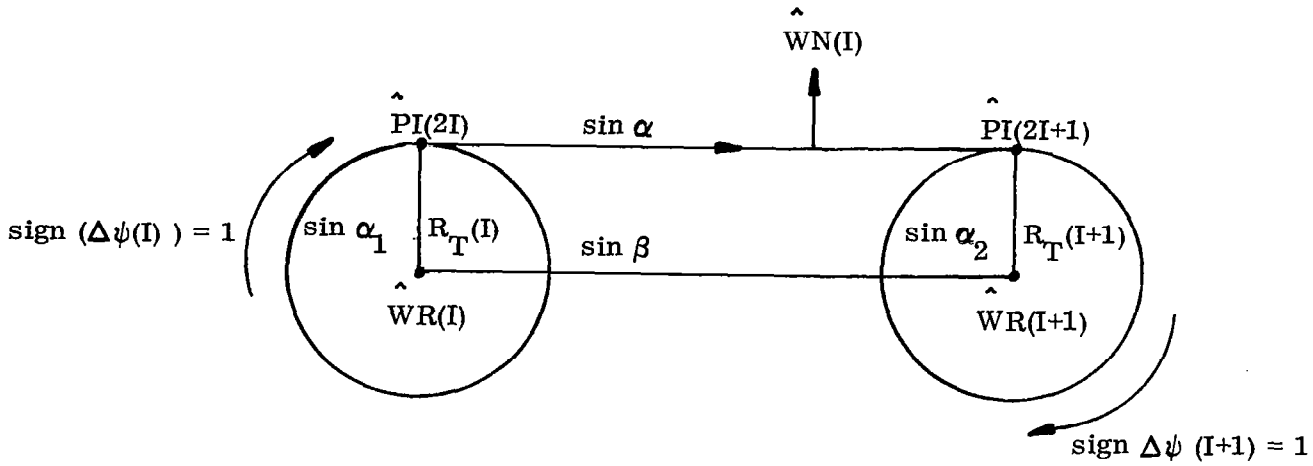

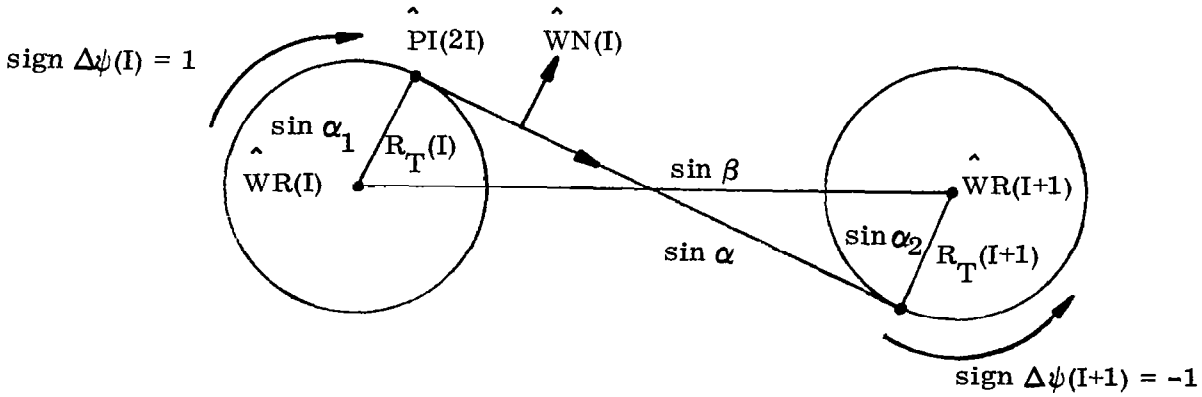

UNIT NORMAL IC(I) = 1, IC(I+1) = 1

Figure I3.

If IC (I+1) = 1, we have

$$\hat{CR}(I) = \hat{WR}(I+1) \tag{2.13}$$

If IC (I+1) = 0, we have

$$\hat{CR}(I) = a_1 \hat{WR}(I+1) + a_2 (\hat{WN}(I) + \hat{WN}(I+1)) \tag{2.14}$$

where

$$a_1 = \left(1. - \frac{2 \sin^2 \alpha}{1. + \hat{WN}(I) \cdot \hat{WN}(I+1)}\right)^{\frac{1}{2}}$$

$$a_2 = - \frac{\sin \alpha \quad \text{sign}(\Delta\psi(I))}{1. + \hat{WN}(I) \cdot \hat{WN}(I+1)} \tag{2.14a}$$

$$\sin \alpha = \sin (RT(I)/r_E$$

E. Turn Angle

The unit vector to the center of the turn, $\hat{CR}(I)$, and the incoming normal, $\hat{WN}(I)$ determine a plane which contains the unit vector, $\hat{PI}(2I-1)$, which is at intersection of start of the turn and the incoming great circle. We define a unit vector $\hat{YN}$, which lies in the $\hat{CR}(I)$, $\hat{WN}(I)$ plane and which is perpendicular to $\hat{CR}(I)$.

$$\hat{YN} = \frac{\text{sign } \Delta\psi}{\cos \alpha} \hat{WN}(I) + \frac{\sin \alpha}{\cos \alpha} \hat{CR}(I) \tag{2.15}$$

where

$$\sin \alpha = \sin (RT(I) / r_E \tag{2.15a}$$

We define, the turn angle, $\Delta\psi(I)$, or the angle through which we must rotate $\hat{YN}$, about the unit vector, $-\hat{CR}(I)$, in order that the rotated unit vector, $\hat{YN}'$, will lie in the plane containing the unit center of the turn, $\hat{CR}(I)$, and the outgoing normal, $\hat{WR}(I+1)$. (See Fig. I4).

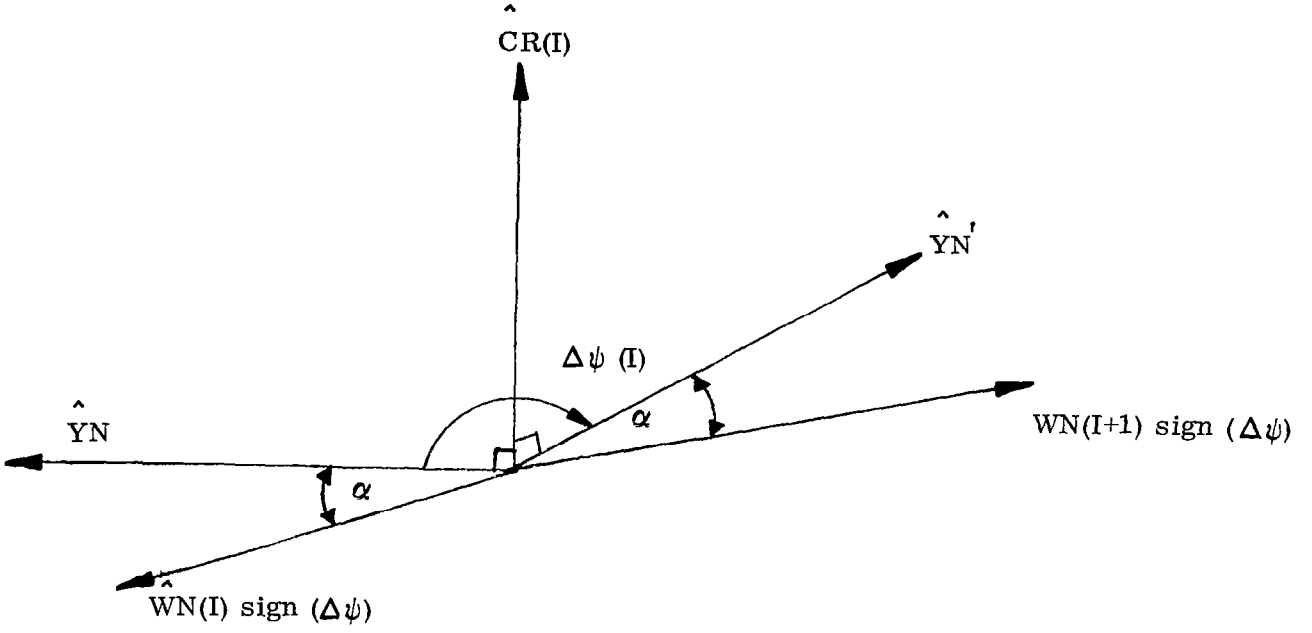

Figure I4. Turn Angle $\Delta\psi$ (I)

$$\hat{YN}' = \cos(\Delta\psi(I))\ \hat{YN} - \sin(\Delta\psi)\ \hat{CR}(I) \times \hat{YN} \tag{2.16}$$

We have

$$\cos(\Delta\psi(I)) = \hat{YN} \cdot \hat{YN}' = \frac{\hat{WN}(I) \cdot \hat{WN}(I+1) - \sin^2\alpha}{\cos^2\alpha} \tag{2.16a}$$

$$\sin(\Delta\psi(I)) = -\hat{CR}(I) \times \hat{YN} \cdot \hat{YN}' = -\frac{\hat{CR}(I) \times \hat{WN}(I) \cdot \hat{WN}(I+1)}{\cos^2\alpha} \tag{2.16b}$$

It follows that the turn angle is given by

$$\Delta\psi = \tan^{-1} \frac{-\hat{CR}(I) \times \hat{WN}(I) \cdot \hat{WN}(I+1)}{\hat{WN}(I) \cdot \hat{WN}(I+1) - \sin^2\alpha} \tag{2.16c}$$

It is necessary to use the four quadrant definition of the arc tangent, and since the numerical routines that compute this function turn all angles over 180^o into their negative complement, it is necessary to test for angles over 180^o.

The recommended test is

$$\text{sign}(\Delta\psi(I))\ \tan^{-1} \frac{-\hat{CR}(I) \times \hat{WN}(I) \cdot \hat{WN}(I+1)}{\hat{WN}(I) \cdot \hat{WN}(I+1) - \sin^2\alpha} \geq 0. \tag{2.16d}$$

Thus if the product of the sign $(\Delta\psi)$ and the $\tan^{-1}(\Delta\psi)$ proves to be negative, we set

$$\Delta\psi(I) = \tan^{-1}(\Delta\psi) + \text{sign}(\Delta\psi)(2\pi) \tag{2.16e}$$

F. End of Segment Unit Vector

The terminal unit vector at end of each great circle, $\hat{PI}(2I-1)$, is used in the guidance equations to determine the distance to go to the end of the segment. The required unit vector lies in the plane of the center of the turn, $\hat{CR}(I)$ and the incoming normal, $\hat{WN}(I)$.

We have

$$\hat{PI}(2I-1) = \frac{1}{\cos\alpha}\hat{CR}(I) + \frac{\sin\alpha}{\cos\alpha}\,\text{sign}\,(\Delta\psi(I))\,\hat{WN}(I) \tag{2.17}$$

where

$$\sin\alpha = \sin(R_T(I)/r_E)$$

$$\cos\alpha = (1 - \sin^2\alpha)^{\frac{1}{2}} \tag{2.17a}$$

In the event that the initial coordinate is on the turn circle, as in the case of trajectory reconstruction and ITURN = 1, we have

$$\hat{PI}(1) = \hat{WR}(1) \tag{2.17b}$$

The start of the next great circle segment on the outgoing leg is given by

$$\hat{PI}(2I) = \frac{1}{\cos\alpha}\hat{CR}(I) + \frac{\sin\alpha}{\cos\alpha}\,\text{sign}\,\Delta\psi\,\hat{WN}(I+1) \tag{2.17c}$$

G. The Unit Vector Normal to the Turn Circle

In the turn, the guidance equations require the unit vector normal to the turn circle at the end of the middle of the turn, and at the end of the full turn. The first unit vector is obtained by rotating $\hat{YN}$ about $\hat{CR}(I)$ through the angle, $\Delta\psi(I)/2$.

$$\hat{GN}(2I-1) = a_1\hat{WN}(I) + a_2\hat{CR}(I) + a_3\hat{CR}(I) \times \hat{WN}(I) \tag{2.18}$$

$$a_1 = \cos\left(\frac{\Delta\psi}{2}\right)\frac{\text{sign}\,(\Delta\psi(I))}{\cos\alpha}$$

$$a_2 = \cos\left(\frac{\Delta\psi}{2}\right)\frac{\sin\alpha}{\cos\alpha} \tag{2.18a}$$

$$a_3 = -\sin\left(\frac{\Delta\psi}{2}\right)\frac{\text{sign}\,(\Delta\psi(I))}{\cos\alpha}$$

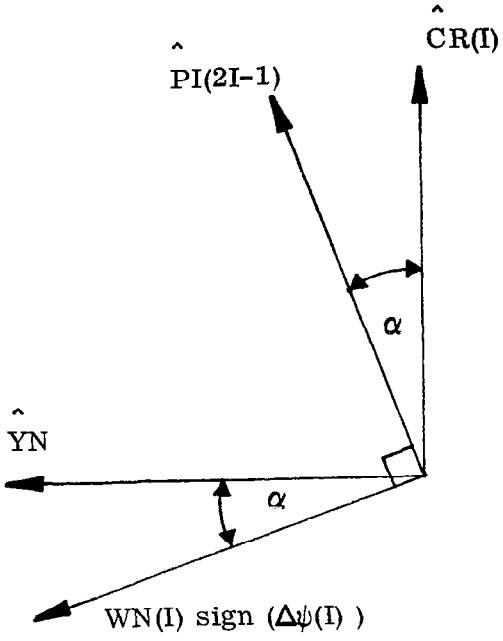

Figure I5a

Incoming End of Segment

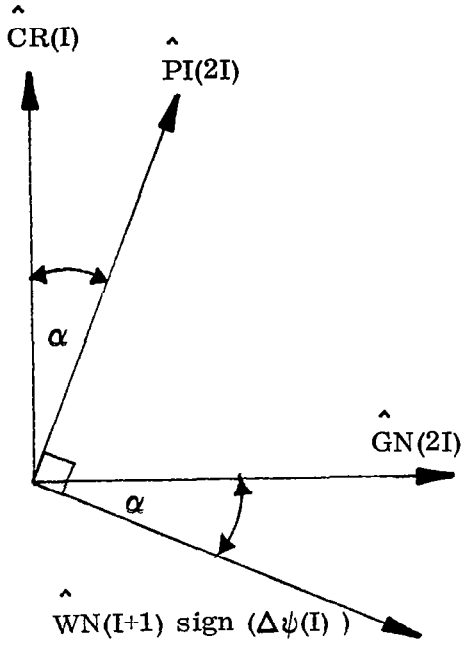

Figure I5b

Outgoing End of Segment

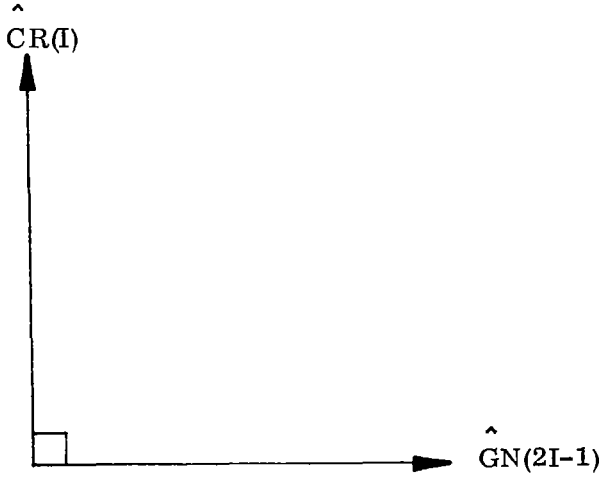

Figure I5c

Middle of Turn Normal to Circle

To obtain the normal to the turn circle at the end of turn, we have

$$\hat{GN}(2I) = \hat{YN}' = \frac{\sin \alpha}{\cos \alpha} \hat{CR}(I) + \frac{\text{sign } (\Delta\psi(I))}{\cos \alpha} \hat{WN}(I+1) \qquad (2.18b)$$

(See Fig. I5)

H. Altitude and Airspeed Gradients

To determine the gradients in altitude and airspeed it is necessary to obtain the length of the arc segments between the vectors at which the altitude and airspeed values are specified. There are three types of segments.

1) The segment covered by the distance, along the surface of the earth, between the initial waypoint, $\hat{WR}(1)$, and the first incoming tangent, $\hat{PI}(1)$, plus the distance along the turn circle to the middle of the turn, terminating at GN(1).

2) All internal segments consisting of the distance along the second half of each turn, plus the distance between the outgoing tangent, $\hat{PI}(2I)$ and the next incoming tangent ($\hat{PI}(2I+1)$, (along the surface of the earth) plus the first half of the next turn.

3) The final segment covered by the second half of the last turn plus the distance along the surface of the earth from the last tangent $\hat{PI}(2(N-1))$ to the final waypoint $\hat{WR}(N)$.

Let the distance along each great circle be DW(I).

$$DW(1) = \sin^{-1} (| \hat{WR}(1) \times \hat{PI}(1) |) \; r_E \qquad (2.19a)$$

Let $I = 1, N-3 \quad (N > 3)$

$I = I+1$

$$DW(J) = \sin^{-1} (| \hat{PI}(2I) \times \hat{PI}(2I+1) |) \; r_E \qquad (2.19b)$$

The final, DW(N-1), is given by

$$DW(N-1) = \sin^{-1} (\hat{PI}(2\ (N-1)\ ) \times \hat{WR}(N)\ )\ r_E \tag{2.19c}$$

Let the distance along each half turn be XARC(I), we have

$$I = 1,\ N-2$$

$$XARC(I) = \frac{\Delta\psi(I)}{2}\ R_T(I) \tag{2.19d}$$

Let the gradient in altitude be GRAD(I), then

$$GRAD(1) = \frac{h(2) - h(1)}{DW(1) + XARC(1)} \tag{2.19e}$$

Let $I = 1,\ N-3 \qquad N > 3$

$J = I+1$

$$GRAD(J) = \frac{h(J+1) - h(J)}{XARC(I) + XARC(J) + DW(J)} \tag{2.19f}$$

$$GRAD(N-1) = \frac{H(N) - h(N-1)}{XARC(N-2) + DW(N-1)} \tag{2.19g}$$

Let the gradient in airspeed be DVG(I) , then

$$DVG(1) = \frac{v_D(2) - v_D(1)}{DW(1) + XARC(1)} \tag{2.19h}$$

Let $I = 1,\ N-3 \qquad N > 3$

$J = I+1$

$$DVG(J) = \frac{v_D(J+1) - v_D(J)}{XARC(I) + XARC(J) + DW(J)} \tag{2.19i}$$

$$DVG(N-1) = \frac{v_D(N) - v_D(N-1)}{XARC(N-2) + DW(N-1)} \tag{2.19j}$$

(See Fig. I6)

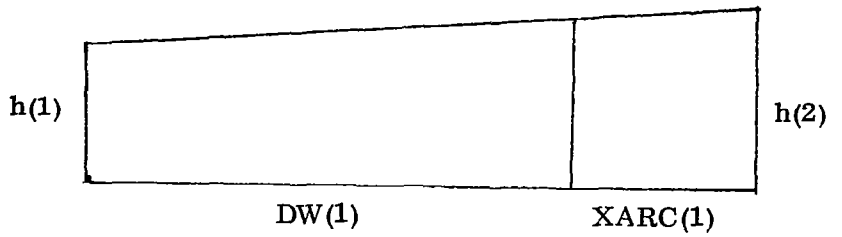

I6a. GRADIENT IN ALTITUDE 1ST SEGMENT

I = 1, N-3 (N > 3)
J = I+1

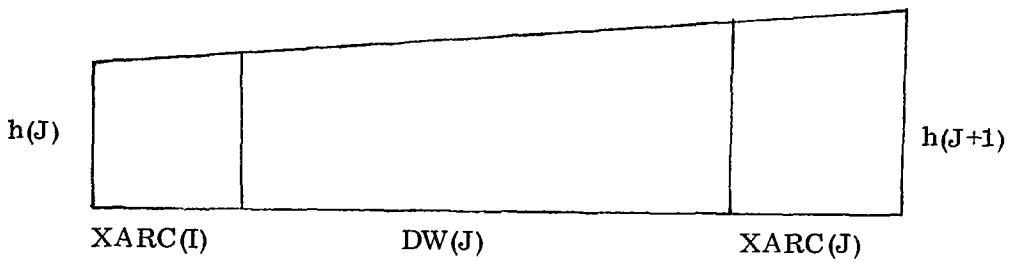

I6b. GRADIENT IN ALTITUDE INTERNAL SEGMENT

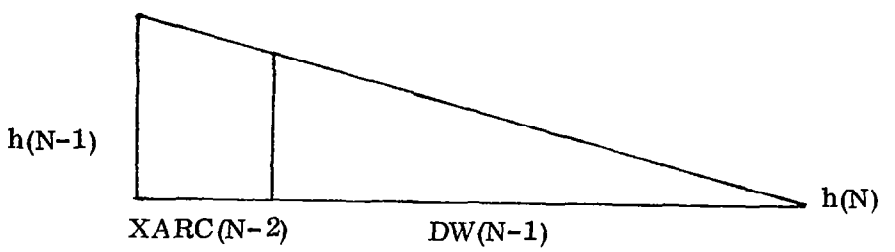

I6c. GRADIENT IN ALTITUDE LAST SEGMENT

Figure I6

In the event ITURN = 1 and IMOD = 2, we are initiating the sequence in the turn, we set

$$DW(1) = 0. \tag{2.19k}$$

Furthermore, in order not to cause an abrupt change in desired gradient, we set

$$h(2) = h(1) + GRX \ XARC(1) \tag{2.19l}$$

In this way we insure that

$$GRAD(1) = GRX \tag{2.19m}$$

In the event ITURN = 1 and IMOD = 0, we are initiating the sequence in the turn, however, since we are in the second half of the turn, the next waypoint is some distance away and we are in no danger of causing an abrupt change in altitude gradient. In this case we set

$$\begin{aligned} h(2) &= h(1) \\ DW(1) &= 0. \\ XARC(1) &= \Delta\psi(1) \ r_E \end{aligned} \tag{2.19n}$$

I. Waypoint Guidance Array

The initial input contains N waypoints. The final path contains 3N-4 waypoints. These points subtend 3N-5 segments; N-1 of which are arcs of great circles and 2(N-2) comprise N-2 pairs of half turns. Each segment contains guidance data which are constant over that segment. These data are conveniently arranged in 3N-5 guidance arrays which are computed initially at the beginning of each flight and called up sequentially, as required,

at the start of each segment. The elements for each of the 3N-5 segments are listed below for both the great circle arcs and the half turns.

Let II go from 1 to 3N-5

J = Integer part of II/3 + 1

K = 2J - 1

If MODULO (II, 3) = 2 then L = J

If MODULO (II, 3) = 0 then L = J-1

Array for great circles:

$$
\begin{aligned}
WP(1) &= \hat{WN}(J,1) \\
WP(2) &= \hat{WN}(J,2) \\
WP(3) &= \hat{WN}(J,3) \\
WP(4) &= \hat{PI}(K,1) \\
WP(5) &= \hat{PI}(K,2) \\
WP(6) &= \hat{PI}(K,3)
\end{aligned}
\qquad (2.20)
$$

If II = 3N-5

$$
\left(
\begin{aligned}
WP(4) &= \hat{WR}(N,1) \\
WP(5) &= \hat{WR}(N,2) \\
WP(6) &= \hat{WR}(N,3)
\end{aligned}
\right)
\qquad (2.20a)
$$

$$
\begin{aligned}
WP(7) &= \text{sign } (\Delta\psi(J)) \\
WP(8) &= \hat{CR}(J,1) \\
WP(9) &= \hat{CR}(J,2) \\
WP(10) &= \hat{CR}(J,3) \\
WP(11) &= DW(J) \\
WP(12) &= R_T(J) \\
WP(13) &= 0. \\
WP(14) &= \sin(\tan^{-1}(GRAD(J)))
\end{aligned}
\qquad (2.20b)
$$

If $\Pi = 1$

$$\begin{pmatrix} HEND = H(1) \\ VEND = v_D(1) \end{pmatrix} \tag{2.20c}$$

If $\Pi > 1$, but $< 3N-5$

$$\begin{aligned} HEND &= HEND + GRAD(J)\ (r_E \sin^{-1}(|\hat{PI}(2J-2) \times \hat{PI}(2J-1)|)) \\ VEND &+ VEND + DVD(J)\ (r_E \sin^{-1}(|\hat{PI}(2J-2) \times \hat{PI}(2J-1)|)) \end{aligned} \tag{2.20d}$$

If $\Pi = 3N-5$

$$\begin{pmatrix} HEND = H(N) \\ VEND = v_D(N) \end{pmatrix} \tag{2.20e}$$

$$\begin{aligned} WP(15) &= HEND \\ WP(16) &= GRAD(J) \\ WP(17) &= VEND \\ WP(18) &= DVD(J) \\ WP(19) &= J \\ WP(20) &= |\Delta\psi(J)/2| \end{aligned} \tag{2.20f}$$

ARRAY FOR HALF TURNS

If MODULO $(\Pi, 3) = 2$, then $L = J$

$$\begin{aligned} WP(1) &= \hat{GN}(2L-1, 1) \\ WP(2) &= \hat{GN}(2L-1, 2) \\ WP(3) &= \hat{GN}(2L-1, 3) \end{aligned} \tag{2.21a}$$

If MODULO $(\Pi, 3) = 0$, then $L = J-1$

$$\begin{aligned} WP(1) &= \hat{GN}(2L, 1) \\ WP(2) &= \hat{GN}(2L, 2) \\ WP(3) &= \hat{GN}(2L, 3) \end{aligned} \tag{2.21b}$$

$$
\begin{aligned}
WP(4) &= 0 \\
WP(5) &= 0 \\
WP(6) &= 0 \\
WP(7) &= \text{sign}\,(\Delta\psi(L)) \\
WP(8) &= CR(L,1) \\
WP(9) &= CR(L,2) \\
WP(10) &= CR(L,3) \\
WP(11) &= |\Delta\psi(L)/2| \\
WP(12) &= R_T(L) \\
WP(13) &= 0. \\
WP(14) &= \sin(\tan^{-1}(GRAD(J)))
\end{aligned}
\qquad (2.21b)\ \text{(Cont'd.)}
$$

$$
HEND = HEND + GRAD(J)\,(R_T(L)\,|\Delta\psi(L)/2|)
$$

$$
VEND = VEND + DVD(J)\,(R_T(L)\,|\Delta\psi(L)/2|)
$$

$$
\begin{aligned}
WP(15) &= HEND \\
WP(16) &= GRAD(J) \\
WP(17) &= VEND \\
WP(18) &= DVD(J) \\
WP(19) &= J \\
WP(20) &= |\Delta\psi(L)/2|
\end{aligned}
\qquad (2.21c)
$$